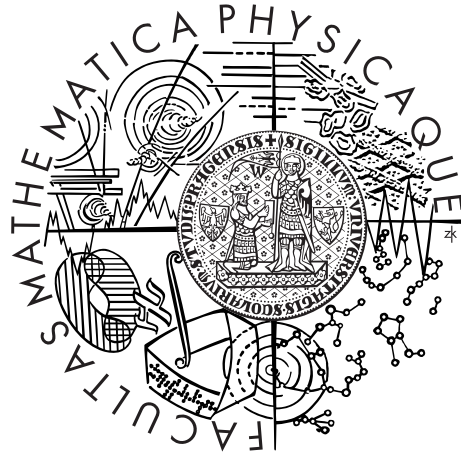Charles University in Prague Faculty of Mathematics and Physics

DOCTORAL THESIS

Artem Ryabov

Stochastic dynamics and energetics of biomolecular systems

Department of Macromolecular Physics

Supervisor: prof. RNDr. Petr Chvosta, CSc.

Study programme: Physics

Specialization: Biophysics, Chemical and Macromolecular Physics

Prague 2014

Preface

The thesis comprises two topics from nonequilibrium statistical physics I was particularly interested in during my PhD studies (2010-2014) at the Department of Macromolecular Physics of the Faculty of Mathematics and Physics of Charles University in Prague. The both problems are complex enough to exhibit a rather nontrivial physics, yet still simple enough so they could be confronted with paper and pencil. The first model originated from biophysics as a model for ion transport through narrow channels in cell membranes. The second model belongs to a newly emerging field of stochastic thermodynamics, where a Brownian particle diffusing in an optical trap has become a paradigm for both theory and experiment.

Before going deeper with a discussion, I would like to thank many people whose support served as a vital propelling force driving me through my studies. First of all, I would like to thank prof. RNDr. Petr Chvosta, CSc. for his guidance and for many stimulating debates. I thank RNDr. Viktor Holubec, Ph.D. and Ján Šomvársky, CSc., my colleagues at the department, for various enlightening discussions. I am deeply indebted to co-workers from the group of statistical physics at Universität Osbanrück for their kind hospitality during my stays there and for their help with numerics. My work would be impossible without permanent support from my family, friends and, of course, Dagmar, whose tolerance and encouragement were indispensable to the completion of this thesis.

In Prague, June 25, 2014   Artem Ryabov

I declare that I carried out this doctoral thesis independently, and only with the cited sources, literature and other professional sources.

I understand that my work relates to the rights and obligations under the Act No. 121/2000 Coll., the Copyright Act, as amended, in particular the fact that the Charles University in Prague has the right to conclude a license agreement on the use of this work as a school work pursuant to Section 60 paragraph 1 of the Copyright Act.

In Prague date ....   Artem Ryabov

Název práce: Stochastická dynamika a energetika biomolekulárních systémů

Autor: Artem Ryabov

Katedra: Katedra makromolekulární fyziky

Vedoucí disertační práce: prof. RNDr. Petr Chvosta, CSc., Katedra makromolekulární fyziky

Abstrakt: Obsahem práce jsou přesně řešitelné modely nerovnovážné statistické fyziky. Nejprve je studována prostorově omezená jedno-dimenzionální difúze částic s interakcí typu vyloučeného objemu. Diskutovány jsou otevřené systémy s absorpčními hranicemi a tedy s proměnným počtem částic. Dynamika jedné vybrané částice a doba jejího záchytu absorpčními hranicemi jsou odvozeny z přesného výrazu pro hustotu pravděpodobnosti pro polohu částice. Hlavními důsledky interakce jsou změny dynamických exponentů, výrazné zpomalení difúzní dynamiky a změny časových škál popisujících proces absorpce ve srovnání s referenčním souborem neinteragujících částic. Druhá část práce je zaměřena na stochastickou termodynamiku malých systémů. V této části je zformulován a přesně vyřešen experimentálně relevantní model Brownova pohybu v anharmonickém časově závislém potenciálu. Potenciál je složen ze dvou komponent, časově závislé harmonické části a časově nezávislé logaritmické bariéry v počátku souřadnic. Cílem je vypočítat hustotu pravděpodobnosti pro práci vykonanou na částici vnější silou. Pro jisté časové závislosti potenciálu se podařilo nalézt přesný výraz pro charakteristickou funkci této hustoty. Asymptotická analýza tohoto výsledku vede k explicitním formulím popisujícím hustotu v oblastech extrémních hodnot práce.

Klíčová slova: prostorově omezená difúze, dynamika interagujících částic, doba prvního dosažení, stochastická termodynamika, přesně řešitelné modely

Title: Stochastic dynamics and energetics of biomolecular systems

Author: Artem Ryabov

Department: Department of Macromolecular Physics

Supervisor: prof. RNDr. Petr Chvosta, CSc., Department of Macromolecular Physics

Abstract: The thesis comprises exactly solvable models from non-equilibrium statistical physics. First, we focus on a single-file diffusion, the diffusion of particles in narrow channel where particles cannot pass each other. After a brief review, we discuss open single-file systems with absorbing boundaries. Emphasis is put on an interplay of absorption process at the boundaries and inter-particle entropic repulsion and how these two aspects affect the dynamics of a given tagged particle. A starting point of the discussions is the exact distribution for the particle displacement derived by order-statistics arguments. The second part of the thesis is devoted to stochastic thermodynamics. In particular, we present an exactly solvable model, which describes a Brownian particle diffusing in a time-dependent anharmonic potential. The potential has a harmonic component with a time-dependent force constant and a time-independent repulsive logarithmic barrier at the origin. For a particular choice of the driving protocol, the exact work characteristic function is obtained. An asymptotic analysis of the resulting expression yields the tail behavior of the work distribution for small and large work values.

Keywords: single-file diffusion, first-passage properties, stochastic thermodynamics, work distribution, exactly solvable models

Contents

Introduction

The present thesis is thematically divided into two parts: the stochastic *dynamics* of particles and the stochastic *energetics*. Let us now address both of them, respectively.

Single-file diffusion

In various situations stochastic motion of particles takes place in confined spaces. The confinement can be of a rather different nature, depending on system in question. Examples range from macroscopic systems to processes in nano-world, including traffic flow dynamics [1], customers waiting in tandem queues [2] (a well known situation when just after waiting to be served in one queue a person is immediately sent to another), movement of pedestrians in a pedestrian zone [3] or ants following trails [4] (the two very similar phenomena where confinement is not static since trails may evolve in time). On micro- and nano-meter scales, we encounter numerous systems which are of great interest in modern biophysics and chemistry like propagation of bacteria through confined spaces [5] and a broad spectrum of processes involved in intracellular transport [6, 7] (see below).

In the thesis we focus on Brownian motion taking place under, in a sense, the most extreme case of the external confinement. We assume that Brownian particles move in narrow channels, the channels being so narrow that their diameter is comparable with the diameter of Brownian particles. The second important ingredient of the model is the interparticle interaction. We consider only the hard-core interaction between the particles (also known as the excluded-volume or steric interaction), which means that the volume occupied by a single particles is inaccessible to other particles. As a consequence, the Brownian motion of particles will be restricted to a one-dimensional domain (infinite line, half-line, or finite interval) and, during the diffusion, the neighboring particles are not allowed to pass each other.

Diffusion in such conditions is known as the single-file diffusion (SFD). The concept of SFD has been originally introduced in 1955 in biophysics to explain anomalous properties of transport of ions through molecular-sized channels in membranes [8]. Since that time many systems has been discovered where SFD is the basic mechanism of mass transport. For example, the processes from cell biology like motion of proteins on double-stranded DNA [9,10] and sliding of ribosomes along messenger RNA (transcription of genetic information) [6]. Further examples of SFD comprise one-dimensional conductors [11, 12], polymers translocating by reptation [13], diffusion in zeolites (important catalysts and molecular sieves) [14–18], and inside nanotubes [19]. Recently several artificial systems, where the motion of colloids is constrained to one dimension, has been realized experimentally in order to test the basic properties of molecules involved in SFD [20–26].

In mathematical literature SFD has been introduced in 1965 by Harris [27] who derived the basic law which nowadays is considered to be the hallmark of SFD. Harris has shown that the mean squared displacement of a given marked particle (a tagged particle or a tracer) grows with time as $t^{1/2}$ in contrast to the linear time-dependence observed for a single noninteracting Brownian particle. The slowdown of the diffusion emerges from the hindering of the motion of a tagged particle caused by collisions with its nearest neighbors. From a general perspective, this result illustrates that in low-dimensional *nonequilibrium* systems even the simplest interactions (like the hard-core one) can lead to rich physical behavior [28–32]. Of course, this is in sharp contrast to what is known from the equilibrium statistical physics, where classical one-dimensional systems nowadays serve mainly as pedagogical tools.

In the thesis we address the motion of the tracer in the single-file system with absorbing boundaries. The emphasis is on an interplay between the hard-core inter-particle interaction and the absorption process. Exact probability density functions (PDFs) for a position of the tracer diffusing under different conditions are derived. Starting from these exact PDFs, the dynamics and the first-passage properties of the tracer are discussed for different geometries and initial conditions.

Stochastic energetics

Above, we have focused our attention on the stochastic dynamics of particles. The dynamics, however, represents only one part of the whole physical picture. An equally important part concerns with energy transformations in small nonequilibrium systems. A theoretical framework which has been designed to study energy flows in systems governed by stochastic evolution equations (in our case by the Langevin equation [33]) is known as the *stochastic energetics* [34] (or the *stochastic thermodynamics* [35], we will use the both terms interchangeably).

The Langevin equation for a Brownian particle immersed in a fluid is, in itself, consistent with well established laws of the classical thermodynamics. The equation contains the damping term (dissipation) and the noise term (fluctuations) which physically originate from the same source (interaction with the molecules of the surrounding liquid) and hence the two terms are not independent. They are connected by the Einstein's (fluctuation-dissipation) relation for the diffusion coefficient. As a result, for any time-independent confining potential, the system described by the Langevin equation will eventually reach a Gibbsian canonical equilibrium state. Thus the consistency with the well established results of equilibrium statistical mechanics is achieved.

Stochastic energetics, introduced by Sekimoto [36, 37], goes far beyond above considerations. Its main goal is to provide a direct link from the stochastic dynamical equations to the thermodynamic description of the nonequilibrium process. Within the framework of the stochastic energetics, the quantities known from the classical thermodynamics, like work, heat and entropy, are identified along individual stochastic trajectories of the system. Thus defined (generalized) thermodynamic formalism holds for small systems, where fluctuations are inseparable from the dynamics, and for arbitrarily far-from-equilibrium processes. One of the advantages of the stochastic energetics (as compared e.g. to a more fundamental thermostated Hamiltonian dynamics) is that the analysis based on the Langevin equation (or on the Markovian master equation for discrete-state systems [35]) has proven to be particularly suitable for description of experiments on small systems (see Chap. 4 for details).

The paradigmatic system in the field of stochastic energetics is the Brownian particle diffusing in a confining external potential, which can be realized e.g. by the optical trap. Although the properties of the PDF for the position of the particle are relatively well understood [33], PDFs that characterize energetic quantities remain less explored. In the thesis we investigate a distribution of work performed on the Brownian particle diffusing in a time-dependent asymmetric potential well. The potential consists of a harmonic component with a time-dependent force constant and of a time-independent logarithmic barrier at the origin. The model is exactly solvable. The exact result for the characteristic function of the work allows us to extract essential properties of the work PDF, e.g., all its moments and the both tails. In particular, the results could be of interest for experimental determination of free energies using the Jarzynski equality (as discussed in detail in Chap. 4), where the tail of the work PDF for large negative values of work has two properties: 1) it corresponds to rare events which are almost never observed in experiments; 2) it significantly contributes to the value of the exponential average occurring in the Jarzynski equality (cf. Eq. (4.7)) and thus also to the value of

the estimated free energy.

Thesis organization

The first part of the thesis (Chaps. 1, 2 and 3) is devoted to the single-file diffusion. Classical approaches and new directions in the theory of tracer dynamics are reviewed in Chap. 1. We would like to emphasize that the focus here is *on the properties of a tagged particle.* Which means that collective phenomena like nonequilibrium phase transitions and other intriguing topics are left without comment (we refer to Refs. [28–32] for more details).

In Chap. 2 we discuss the dynamics and the first-passage properties of the tracer in a semi-infinite system with a single absorbing boundary for two qualitatively different initial conditions. First, we consider the system with (initially) finite number of particles (Sec. 2.2), and, second, the system in the thermodynamic limit where the number of particle is infinite, but the initial mean density is constant (Sec. 2.3). In the both cases the first-passage properties (survival probabilities, PDFs for times of absorption) and the tracer dynamics (time-dependence of PDFs and their moments for both the unconditioned dynamics and the dynamics conditioned on nonabsorption) are deduced from the exact PDF of the tracer position. The latter is constructed using the mapping between the SFD system and the corresponding system of noninteracting particles (which is a direct generalization of ideas for a system without absorption as reviewed in Chap. 1).

Chap. 3 generalizes the analysis of Chap. 2 to the case of a finite interval with two types of boundary conditions: (i) both boundaries are absorbing (Sec. 3.2); (ii) one boundary is absorbing and the second boundary is reflecting (Sec. 3.3). The focus is on the first-passage properties and on their scaling behavior for large system size and for large initial number of particles. Sec. 3.2.3 accounts for possibility of random interval length.

The second part of the thesis (Chaps. 4 and 5) is devoted to the stochastic thermodynamics. In Chap. 4 we first define (stochastic) work and heat, and second, we review the two most widely known fluctuation theorems (the Crooks theorem and the Jarzynski equality) and their roles in determination of free-energy landscapes of macromolecules.

Chap. 5 addresses a nontrivial model for which the work characteristic function can be obtained exactly. Using the Lie-algebraic approach, the task to solve the Fokker-Planck equation for the joint PDF of work and position is reduced to the solution of a Riccati equation and to the evaluation of two quadratures (Sec. 5.2). PDF for particle position is derived in a closed form for any external driving (Sec. 5.3). On the other hand, it is only for a specific driving protocol that the Riccati equation is solved exactly in terms of elementary functions (Sec. 5.4) yielding desired information about work PDF including all its moments and the both its tails (Secs. 5.4, 5.5).

The thesis is concluded by a brief summarizing chapter (unnumbered). Notice that full-length concluding sections discussing main physical features of individual models are presented at the ends of Chaps. 2, 3, and 5, see Secs. 2.4, 3.4, and 5.5, respectively.

1. Basics of single-file diffusion

The simple hard-core interaction does not affect collective properties of the system. These are quantities that are symmetric with respect to any permutation of the particles. However, in one dimension, the interaction has a prominent effect on the diffusion of a single marked particle – a tagged particle or a tracer. The present chapter studies basic dynamical features of the tracer dynamics under different conditions.

The chapter is organized as follows. Sec. 1.1 is introductory, it comprises definitions of basic concepts and the clarification of relation between the positions of interacting particles and order statistics of positions of noninteracting ones. The physical consequences of the interparticle interactions are reviewed is Secs. 1.2, 1.3, and 1.4. Namely, Sec. 1.2 is devoted to the subdiffusion of the tracer in an infinite homogeneous system. Sec. 1.3 contrasts the findings of Sec. 1.2 with the case of finite number of diffusing particles. The second topic treated in Sec. 1.3 concerns different dynamical regimes distinguished by different time-dependence of tracer's mean squared displacement. In Sec. 1.4 we recall asymptotic properties of the single-file diffusion front. The chapter is concluded by Sec. 1.5, where a few alternative approaches to SFD are pointed out.

1.1 Brownian motion with hard-core interaction

1.1.1 "Collisions" of two particles

From the point of view of the classical mechanics an elastic collision of two particles is an encounter at which the total energy of the particles as well as their total momentum are conserved. A result of such an impact in the case of two identical (same masses) particles moving in one dimension is that after the encounter the particles just *interchange their velocities* as compared to their states before the collision. Let us now discuss how one can define the elastic collision for identical particles performing an overdamped Brownian motion, i.e., for the particles that possess *no well defined velocities*. We offer two (equivalent) solutions to this at a first glance ill-posed problem. The first one, and we can call it "the probabilistic approach" (sometimes referred to as "a heuristic approach" [38]), is due to Harris [27]. It is based on the equivalence of the positions of interacting particles and order statistics build on the positions of noninteracting ones. The second one, which we can call "the analytical approach", stems from the definition of the reflecting boundary conditions for the diffusion equation. As we shall see throughout the thesis, the first approach provides us a quick and intuitive way to the most important quantities – exact probability density functions for individual particles, while the second yields a straightforward way to answer the frequently asked question: "Are you sure that your probabilistic reasoning is correct?"[1]

Probabilistic approach

Consider two identical (same mobilities) Brownian particles diffusing on a line. Their positions at time t are given by $\mathbf{X}_{1:2}(t)$ (the left one) and $\mathbf{X}_{2:2}(t)$ (the right one). We assume that except at the instants of their collisions the two particles are mutually independent. We suppose that due to the mutual interaction the particles cannot pass

---

[1]Actually, the original approach of the present author to the single-file diffusion was the analytical one, cf. Refs. [39,40]. It was only after completing analytical derivations that the full power and beauty of the probabilistic interpretation has been recognized [41,42]. In chapters of the present thesis devoted to SFD mainly the probabilistic reasoning is used. The alternative analytical route to the results is always outlined but not strictly followed.
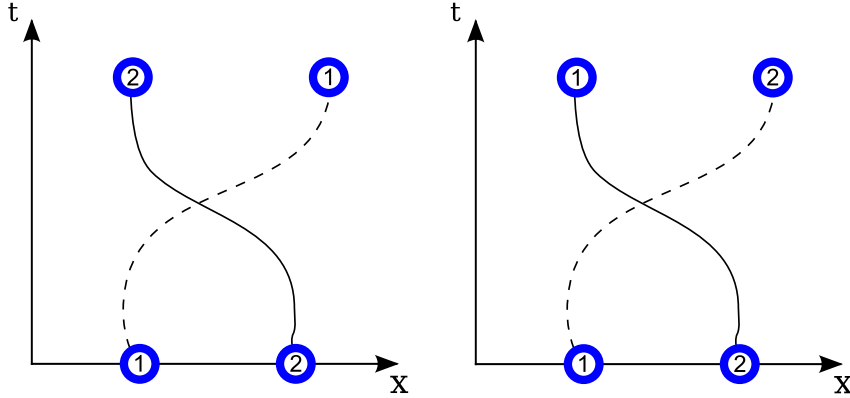
Figure 1.1: Schematic illustration of space-time trajectories of two particles. The left panel: noninteracting particles pass freely through each other, their labels remain attached to individual trajectories. The right panel: interacting particles collide when they encounter hence the ordering of the labels is preserved. Except for the particle labeling, the two sets of trajectories are statistically equivalent.

each other, thus the initial ordering, $\mathbf{X}_{1:2}(0) < \mathbf{X}_{2:2}(0)$, is preserved for all times. As long as the two particles are identical we can follow Harris [27] and relate the motion of interacting particles to order statistics of positions of independent noninteracting ones. To this end, let $\mathbf{X}_1(t)$ and $\mathbf{X}_2(t)$ be positions of the two identical noninteracting Brownian particles, then we can set

$$
\begin{aligned}
\mathbf{X}_{1:2}(t) &= \min\left\{\mathbf{X}_1(t), \mathbf{X}_2(t)\right\}, \\
\mathbf{X}_{2:2}(t) &= \max\left\{\mathbf{X}_1(t), \mathbf{X}_2(t)\right\}.
\end{aligned}
\tag{1.1}
$$

The two equations embodies nothing but the very basic fact that, *except for the particle labeling, the space-time trajectories of two identical hard-core interacting particles are equivalent to the space-time trajectories of the noninteracting ones*, cf. Fig. 1.1. In other words, any collision event can be equivalently described as follows. We can imagine that instead of the mutual reflection the two approaching particles pass freely through each other and, just after they pass each other, we exchange their labels. Thus we can generate the dynamics of interacting particles simply by exchanging the labels of noninteracting ones. Notice that this picture is in agreement with the classical description of one-dimensional elastic collisions and, at the same time, it makes no reference to the particle velocities which presently do not exist.

The correspondence between the interacting and the noninteracting pictures is behind the fact that the single-file model is exactly solvable and that many important quantities (PDFs of individual particles, their mean squared displacements, and others), could be derived by analytical methods.

Analytical approach

Let us now formulate the SFD problem as the initial-boundary value problem for the two-particle Smoluchowski equation. For the two identical particles the equation reads [33]

$$
\frac{\partial}{\partial t} p(x_1, x_2, t) = \sum_{i=1}^{2} \left[D \frac{\partial^2}{\partial x_i^2} - \frac{\partial}{\partial x_i} \mathcal{F}(x_i, t) \right] p(x_1, x_2, t),
\tag{1.2}
$$

where D stands for the diffusion coefficient of each of the particles and $\mathcal{F}(x, t)$ is the external force acting on the particles. The above diffusion equation contains no evidence of interaction yet. In order to incorporate the hard-core interaction, it is
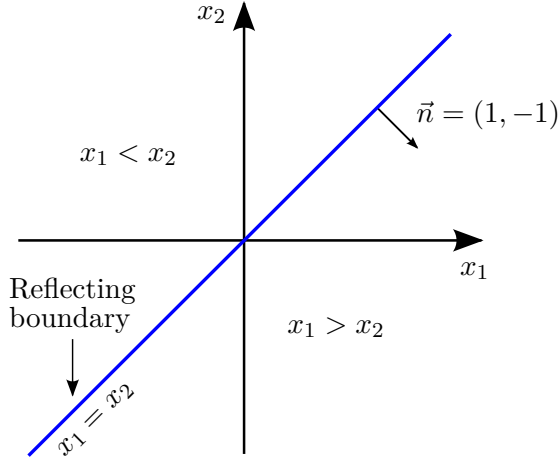
Figure 1.2: The two-particle SFD is equivalent to the single-particle diffusion in 2d plane with the reflecting line $x_1 = x_2$. The (unnormalized) projection of the current vector $\vec{J} = (J_1, J_2)$ onto the direction perpendicular to the reflecting boundary, $\vec{J} \cdot \vec{n} = J_1 - J_2$, vanishes at the reflecting boundary which yields the non-crossing boundary condition (1.4).

convenient to map the two-particle diffusion in one dimension onto the diffusion of a single "representative particle" in two dimensions. In the latter picture, the coordinates of individual particles x_1, x_2 correspond to the vector components of the position of the representative particle. The hard-core interaction of two diffusing particles means that the representative particle is not allowed to cross the line $x_1 = x_2$ where the collisions occur. Thus the hard-core interaction can be incorporated as the reflecting boundary condition imposed along the line $x_1 = x_2$.

The perfectly reflecting boundary condition requires [33] that the component of the probability current which is perpendicular to the boundary vanishes at the boundary. In the present case, the components of the probability current parallel with the coordinate axes are given by

$$J_i(x_1, x_2, t) = \left[-D\frac{\partial}{\partial x_i} + \mathcal{F}(x_i, t) \right] p(x_1, x_2, t), \qquad i = 1, 2. \tag{1.3}$$

Then the boundary condition that represents the hard-core interaction, *the non-crossing boundary condition*, reads

$$(J_1(x_1, x_2, t) - J_2(x_1, x_2, t))|_{x_1 = x_2} = 0, \tag{1.4}$$

see Fig. 1.2 for more details. Explicitly, the above requirement reads

$$D\left(\frac{\partial}{\partial x_2} - \frac{\partial}{\partial x_1} \right) p(x_1, x_2, t) \bigg|_{x_1 = x_2} = [\mathcal{F}(x_2, t) - \mathcal{F}(x_1, t)] p(x_1, x_2, t) \bigg|_{x_1 = x_2}. \tag{1.5}$$

Thus the hard-core interaction splits the two-dimensional state space in two half-planes. Within which of the two half-planes ($x_1 < x_2$, or $x_1 > x_2$) the representative particle moves is dictated by the initial condition. For instance if we set

$$p(x_1, x_2, 0) = \delta(x_1 - y_1)\delta(x_2 - y_2), \qquad y_1 < y_2, \tag{1.6}$$

then the particle ordering at any time t is in agreement with that in Eqs. (1.1).

Notice that also this second approach to SFD maps the many particle problem with interaction onto the single-particle one. As we discuss below, for identical particles

(same D and $\mathcal{F}$ for all particles) the two approaches are equivalent. In contrast to the probabilistic approach, the analytical formulation can be easily extended to the case of *nonidentical* particles (unique D_i, and/or $\mathcal{F}_i$ for each particle). However, this advantage is rather formal since for a general N, $N > 2$, little is known about the exact solution of the Smoluchowski equation when the interacting particles are different (see Sec. 1.5 for the review of the progress in this direction, and Refs. [43–46] for a discussion of some particular two-particle cases).

1.1.2 Propagator for general N

Having prepared the two approaches to the two-particle SFD, let us now formulate, solve and interpret the general N-particle problem. We assume that N interacting particles which are acted upon by the same external force $\mathcal{F}$ are diffusing in one dimension, each with the diffusion coefficient D. The evolution of the joint PDF of particles positions is governed by the Smoluchowski equation

$$\frac{\partial}{\partial t} p(\vec{x}, t|\vec{y}, t_0) = \sum_{i=1}^{N} \left[D \frac{\partial^2}{\partial x_i^2} - \frac{\partial}{\partial x_i} \mathcal{F}(x_i, t) \right] p(\vec{x}, t|\vec{y}, t_0), \qquad t > t_0. \qquad (1.7)$$

Initially, at time t_0, the particles are located at positions specified by the components of the vector $\vec{y}$, $\vec{y} = (y_1, y_2, \ldots, y_N)$. Hence the initial condition to the above equation is given by

$$p(\vec{x}, t_0|\vec{y}, t_0) = \delta(x_1 - y_1)\delta(x_2 - y_2)\ldots\delta(x_N - y_N), \qquad (1.8)$$

Due to the hard-core interaction, the initial ordering of the particles:

$$y_1 < y_2 < \ldots < y_N, \qquad (1.9)$$

is conserved for all times. This is ensured by $(N-1)$ non-crossing boundary conditions (cf. Eq. (1.4))

$$D\left(\frac{\partial}{\partial x_{i+1}} - \frac{\partial}{\partial x_i} \right) p(\vec{x}, t|\vec{y}, t_0)\bigg|_{x_i = x_{i+1}} = [\mathcal{F}(x_{i+1}, t) - \mathcal{F}(x_i, t)]\, p(\vec{x}, t|\vec{y}, t_0)\bigg|_{x_i = x_{i+1}}, \qquad (1.10)$$

$i = 1, 2, \ldots, N-1$.

Let us assume that $f(x, t|y, t_0)$ is the propagator (the Green function) for the corresponding problem with $N = 1$. That is, $f(x, t|y, t_0)$ satisfies the single-particle Smoluchowski equation

$$\frac{\partial}{\partial t} f(x, t|y, t_0) = \left[D \frac{\partial^2}{\partial x^2} - \frac{\partial}{\partial x} \mathcal{F}(x, t) \right] f(x, t|y, t_0), \qquad (1.11)$$

subject to the initial condition

$$f(x, t_0|y, t_0) = \delta(x - y). \qquad (1.12)$$

Then, as it has been demonstrated in Ref. [39], the propagator for the N-particle SFD problem, has a structure of the *permanent* [47] (which is similar to the determinant but not containing the minus signs). It reads

$$p(\vec{x}, t|\vec{y}, t_0) = \sum_{\sigma \in S_N} \prod_{j=1}^{N} f(x_{\sigma(j)}, t|y_j, t_0) \qquad (1.13)$$

if components of the vector $\vec{x} = (x_1, x_2, \ldots, x_N)$ satisfy

$$x_1 < x_2 < \ldots < x_N, \qquad (1.14)$$

and it vanishes, if at least one of the above inequalities is violated. In Eq. (1.13) the summation is taken over all $N!$ permutations σ of particle labels at time t (of course, equivalently, we can sum over all permutations of the initial positions). Notice that the normalization of the propagator $p(\vec{x}, t | \vec{y}, t_0)$ follows from the normalization of the PDF $f(x, t | y, t_0)$. Since $f(x, t | y, t_0)$ is normalized to one in the one-dimensional space, any summand in Eq. (1.13) is normalized to one in the *unrestricted N*-dimensional space. There are $N!$ such summands in Eq. (1.13), at the same time, the hard-core interaction, as expressed through the non-crossing boundary conditions, reduces the total volume of the N-particle state-space by the factor $1/N!$, which implies the required normalization of $p(\vec{x}, t | \vec{y}, t_0)$ and causes that $p(\vec{x}, t | \vec{y}, t_0)$ is different from zero only when $\vec{x}$ lies in the N-dimensional wedge determined by inequalities (1.14) (the so called Weyl chamber of the symmetric group S_N [48, 49]).

Formula (1.13) expresses the exact solution of the many-particle problem with the hard-core interaction through a simpler object, which is the single-particle probability density. The special case of the above propagator for the unbiased ($\mathcal{F} = 0$) SFD model has been found by Rödenbeck et al. [50] employing the reflection principle, and by Lizana and Ambjörnsson [51, 52] using the Bethe Ansatz.

The permanent-like expression (1.13) possesses an interpretation in terms of non-interacting particles which is perfectly consistent with the probabilistic picture behind Eqs. (1.1). Let $\mathbf{X}_i(t)$ be the position of the ith noninteracting particle distributed with the PDF $f(x_i, t | y_i, t_0)$, $i = 1, 2$. Hence $\mathbf{X}_i(t_0) = y_i$, $y_1 < y_2$, and for a moment we consider again that $N = 2$. Then the propagator

$$p(x_1, x_2, t | y_1, y_2, t_0) = f(x_1, t | y_1, t_0) f(x_2, t | y_2, t_0) + f(x_2, t | y_1, t_0) f(x_1, t | y_2, t_0), \quad (1.15)$$

which is different from zero only for $x_1 < x_2$, is nothing but the simultaneous PDF of random positions $\mathbf{X}_{1:2}(t)$, $\mathbf{X}_{2:2}(t)$ of two interacting particles (as defined by Eqs. (1.1)) conditioned on the initial state: $\mathbf{X}_{1:2}(t_0) = y_1$, $\mathbf{X}_{2:2}(t_0) = y_2$. In other words, the propagator $p(x_1, x_2, t | y_1, y_2, t_0)$ accounts for all 2! possibilities, how the two noninteracting particles can be ordered: either $\{\mathbf{X}_{1:2}(t), \mathbf{X}_{2:2}(t)\} = \{\mathbf{X}_1(t), \mathbf{X}_2(t)\}$ if $\mathbf{X}_1(t) < \mathbf{X}_2(t)$ (the first term on the right-hand side), or $\{\mathbf{X}_{1:2}(t), \mathbf{X}_{2:2}(t)\} = \{\mathbf{X}_2(t), \mathbf{X}_1(t)\}$ when $\mathbf{X}_1(t) > \mathbf{X}_2(t)$ (the second term with permuted x_1, x_2), cf. Fig. (1.1).

The correspondence between the interacting particles and the noninteracting ones based on definitions (1.1), can be extended to a general N [27]. To this end, at specified time t, *we identify the position of the nth interacting particle, say* $\mathbf{X}_{n:N}(t)$*, with the position of the nth leftmost particle among the noninteracting ones.* In statistics, the thus defined random variable $\mathbf{X}_{n:N}(t)$ is known as *the nth order statistic* [53] (it is the nth smallest one of independent random variables $\mathbf{X}_1(t), \ldots, \mathbf{X}_N(t)$). Thus e.g. the first order statistic $\mathbf{X}_{1:N}(t)$ is the position of the leftmost interacting particle and it is identified with the position of the leftmost noninteracting one:

$$\mathbf{X}_{1:N}(t) = \min\{\mathbf{X}_1(t), \ldots, \mathbf{X}_N(t)\}, \quad (1.16)$$

and similarly for any n. Then, similarly as in $N = 2$ case, the simultaneous PDF of positions of all N interacting particles (the simultaneous PDF of values of all N order statistics) conditioned on the initial positions is given exactly by the N-particle propagator (1.13).

1.1.3 PDF of a tagged particle

The noninteracting particles which has been used to construct the positions of the interacting ones are assumed to be identical as for their physical properties (same D and $\mathcal{F}$). This assumption is necessary for the permanent (1.13) to be the exact propagator

for the interacting particles. A rather complicated structure of the propagator (sum of products) can be reduced to a simple product-like expression if we add a further assumption regarding the initial conditions.

Let us assume that the initial position of any noninteracting particle, $\mathbf{X}_i(t_0)$, $i = 1, \ldots, N$, is drawn from the PDF $f(y, t_0)$. This choice of the initial condition implies that all noninteracting particles are identical as for all their statistical properties. That is, not only each particle diffuses with the same D and it is acted upon by the same force $\mathcal{F}$, but also *the initial condition is, in a statistical sense, the same for all particles* (in contrast to the previous case described by PDFs $f(x, t|y_i, t_0)$ which differ by initial deterministic positions). A remarkable simplification follows from this assumption in the corresponding interacting case. We get the result in two steps. First, the PDF for the position of any noninteracting particle at time t is the same and it is given by $f(x, t)$, which follows from $f(x, t_0)$ via the integration:

$$f(x, t) = \int \mathrm{d}y f(x, t|y, t_0) f(y, t_0). \tag{1.17}$$

Second, the PDFs $f(x_i, t)$ replace the conditioned PDFs $f(x_i, t|y_j, t_0)$ in Eq. (1.13). Consequently, the sum on the right-hand side of Eq. (1.13) contains $N!$ *identical summands* and the simultaneous PDF for positions $\mathbf{X}_{1:N}(t), \ldots, \mathbf{X}_{N:N}(t)$, of interacting particles reads

$$p(\vec{x}, t) = N! \prod_{j=1}^{N} f(x_j, t), \tag{1.18}$$

when the vector $\vec{x}$ lies in the wedge (1.14) and it vanishes otherwise. In particular, for $t = t_0$ we obtain the initial simultaneous PDF in the factorized form

$$p(\vec{x}, t_0) = N! \prod_{j=1}^{N} f(x_j, t_0). \tag{1.19}$$

Such initial condition can be thought to describe e.g. the Gibbs equilibrium state as it will be discussed in Chap. 2, cf. Eq. (2.36). In particular, the factorized form of Eq. (1.18) may evoke an impression that the positions of interacting particles are not correlated. This is not the case, the interparticle correlations appear due to the fact that $\vec{x}$ is restricted to the wedge (1.14).

Of course, one can follow a different line of reasoning, assuming first that the initial condition is given by Eq. (1.19), and, second, evolving the initial condition by the propagator (1.13). The result will be again given by Eq. (1.18). That is, for this specific initial condition the simultaneous PDF factorizes for all times t, $t \geq t_0$ [40].

The basic advantage of the factorized simultaneous PDF is that it yields an analytically tractable expression for the marginal PDF $p_{n:N}(x, t)$ for the position $\mathbf{X}_{n:N}(t)$ of the nth interacting particle:

$$p_{n:N}(x, t) = \frac{N!}{(n-1)!(N-n)!} f(x, t) \left[\int_0^x \mathrm{d}x' f(x', t) \right]^{n-1} \left[1 - \int_0^x \mathrm{d}x' f(x', t) \right]^{N-n}. \tag{1.20}$$

The interpretation of the right-hand side in terms of N statistically identical noninteracting particles, whose positions are distributed with the PDF $f(x, t)$, is rather straightforward. The expression $p_{n:N}(x, t)\mathrm{d}x$ equals the probability that there is a single particle in $(x, x + \mathrm{d}x)$ ($f(x, t)\mathrm{d}x$) and, simultaneously, there are $(n-1)$ noninteracting particles to the left of x (with the probability $[\int_0^x \mathrm{d}x' f(x', t)]^{n-1}$), and the remaining $(N-n)$ particles are to the right of x (with the probability $[1 - \int_0^x \mathrm{d}x' f(x', t)]^{N-n}$). The combinatorial prefactor accounts for all possible permutations of labels.

In Chaps. 2, 3 we will derive the generalization of the above marginal PDF for the SFD model with one (Eq. (2.39)) and two (Eq. (3.13)) absorbing boundaries.

1.2 SFD in homogeneous system with constant density

Let us now turn to the key feature of the single-file dynamics – the subdiffusive behavior of the tagged particle. Consider an infinite line occupied by particles with constant density ρ. Particles are distributed randomly. This means that empty intervals between adjacent particles are exponentially distributed random variables with mean value $1/\rho$. At the initial time we choose a single particle (a tracer) and we follow its motion (alternatively, we can insert a single particle into the system). Clearly, the space available for the tracer diffusion is effectively reduced by the presence of other particles. This hindrance results in a slowdown of diffusive spreading of tracer PDF, as compared to the free diffusion. In the long-time limit, we observe a subdiffusive motion. Despite this anomalous behavior, the tracer PDF is still given by a Gaussian density but now the mean squared displacement (MSD) grows as $t^{1/2}$:

$$p_{\mathrm{T}}(x,t) \sim \frac{1}{\sqrt{2\pi \left\langle \mathbf{X}_{\mathrm{T}}^2(t) \right\rangle}}\, \mathrm{e}^{-x^2/2\left\langle \mathbf{X}_{\mathrm{T}}^2(t)\right\rangle}, \quad \left\langle \mathbf{X}_{\mathrm{T}}^2(t) \right\rangle = \frac{2}{\rho}\sqrt{\frac{Dt}{\pi}}, \quad \text{as } t \to \infty. \quad (1.21)$$

This is one of the most highlighting results of the theory of the single-file diffusion which has already been confirmed in various experiments, e.g. in NMR studies of diffusion in zeolites [14–18], and in experiments on colloids confined in narrow channels [20–26].

From a general perspective, the SFD model belongs to the class of interacting models like phantom polymer chains [54, 55] or certain fluctuating interfaces [56]. The characteristic feature of all these models is that a tagged particle (or a tagged segment) undergoes a non-Markovian diffusion described by Gaussian PDF with associated mean squared displacement proportional to $t^{1/2}$. Such stochastic process is usually said to be of a fractional Brownian motion type [52, 57–59] rather than that of a continuous-time random walk type. Since for the latter the corresponding PDF is not Gaussian but it typically exhibits a sharp cusp around the initial position, see Ref. [60] for a numerical comparison. An approximative mapping (so called harmonization) between the long-time dynamics of SFD system and that of the Rouse polymer chain can be found in Refs. [61–63]. Further, in Ref. [58] a general phenomenological description for all these processes has been developed leading to a fractional Langevin equation. Let us now build some intuition with the way how the subdiffusion arises in the SFD system.

1.2.1 Heuristic arguments

The time-dependence of the tracer displacement can be intuitively understood as follows [32, 64]. Consider a one-dimensional *lattice*. Each lattice site is either occupied by a particle or vacant, multiple occupation of sites is forbidden. On a nearly full lattice, any particle is almost always surrounded by occupied sites and therefore it rarely moves. On the other hand, the concentration of *vacancies* on such a lattice is vanishingly small. Hence the vacancies rarely meet and we can approximate their dynamics by *independent* random walks. The crucial observation is that we can draw a certain conclusions about the tracer dynamics by considering the dynamics of almost freely diffusing vacancies. Indeed, a tracer will hop to the neighboring site only if that site contains a vacancy. Hence the displacement of the tracer is given by

$$\mathbf{X}_{\mathrm{T}}(t) = \mathbf{N}_{\mathrm{R}\to\mathrm{L}}(t) - \mathbf{N}_{\mathrm{L}\to\mathrm{R}}(t), \quad (1.22)$$

where $\mathbf{N}_{\mathrm{R}\to\mathrm{L}}(t)$ is the number of vacancies that were initially to the right of the tracer and are now on the left, and vice versa for $\mathbf{N}_{\mathrm{L}\to\mathrm{R}}(t)$. Since the densities of the vacancies to the right and to the left of the tracer are equal, we expect that $\langle \mathbf{N}_{\mathrm{R}\to\mathrm{L}}(t)\rangle = \langle \mathbf{N}_{\mathrm{L}\to\mathrm{R}}(t)\rangle$. Thus the average tracer displacement, $\langle \mathbf{X}_{\mathrm{T}}(t)\rangle$, is zero. From the diffusive

motion of the vacancies it follows that $\langle \mathbf{N}_{\text{R}\to\text{L}}(t) \rangle = \langle \mathbf{N}_{\text{L}\to\text{R}}(t) \rangle \sim t^{1/2}$. Hence the difference on the right-hand side of Eq. (1.22) scales as $\sqrt{t^{1/2}}$ and the mean squared displacement of the tracer position grows as $t^{1/2}$. We recall that for the classical symmetric random walk both the number of left steps, $\mathbf{N}_{\text{L}}(t)$, and the number of right steps, $\mathbf{N}_{\text{R}}(t)$, behave as $\langle \mathbf{N}_{\text{L}}(t) \rangle = \langle \mathbf{N}_{\text{R}}(t) \rangle \sim t$. Then the particle position determined by the difference $\mathbf{X}(t) = \mathbf{N}_{\text{R}}(t) - \mathbf{N}_{\text{L}}(t)$ scales as $t^{1/2}$ and hence the mean squared displacement of the particle increases as t.

1.2.2 Derivation of tracer PDF

The most elegant derivation of the basic result (1.21) is due to Levitt [65, 66] (but see also Refs. [67–69]). The main ideas behind Levitt's construction of the tracer PDF $p_{\text{T}}(x,t)$ are (A) the trajectories of interacting particles are statistically equivalent to the trajectories of noninteracting ones; (B) the PDF $p_{\text{T}}(x,t)$ is proportional to the probability $A_0(x,t)$ that, for the reference system of noninteracting particles, the number of particles to the left of the tracer (and hence to the right of it) has not changed as compared to the initial configuration.

Let us assume that initially the tracer is located at the origin of coordinates $x = 0$. We follow its dynamics up to time t and we ask for the probability that at this time the tracer is located in $(x, x + \mathrm{d}x)$. An important quantity that will be used in construction of the tracer PDF is the mean number of noninteracting particles that initially were to the left of the tracer (i.e., to the left of $x = 0$) and, at time t are located to the right of x. It is given by the double integral

$$\nu_{\text{L}\to\text{R}}(x,t) = \rho \int_x^\infty \mathrm{d}x' \int_{-\infty}^0 \mathrm{d}y \, \frac{1}{\sqrt{4\pi Dt}} \, \mathrm{e}^{-(x'-y)^2/4Dt}. \tag{1.23}$$

And vice versa, the mean number of particles that initially were to the right of the tracer and, at time t are to the left of x reads

$$\nu_{\text{R}\to\text{L}}(x,t) = \rho \int_{-\infty}^x \mathrm{d}x' \int_0^\infty \mathrm{d}y \, \frac{1}{\sqrt{4\pi Dt}} \, \mathrm{e}^{-(x'-y)^2/4Dt}. \tag{1.24}$$

The above two quantities are merely mean values. A more complete description is provided by the corresponding probabilities. Since the reference particles are independent, the probability distribution for the overall number of crossings from left to right is the Poisson distribution with the mean value $\nu_{\text{L}\to\text{R}}(x,t)$ (and similarly for $\nu_{\text{R}\to\text{L}}(x,t)$). From the two Poisson distributions we can infer the probability that there were equal number of crossings from left to right as from right to left. The latter probability is given by the sum over all possible events which are compatible with the required condition:

$$A_0(x,t) = \sum_{k=0}^\infty \frac{[\nu_{\text{L}\to\text{R}}\nu_{\text{R}\to\text{L}}]^k}{k! \, k!} \, \mathrm{e}^{-(\nu_{\text{L}\to\text{R}}+\nu_{\text{R}\to\text{L}})}, \tag{1.25}$$

or, expressed using the modified Bessel function:

$$A_0(x,t) = \mathrm{I}_0(2\sqrt{\nu_{\text{L}\to\text{R}}\nu_{\text{R}\to\text{L}}}) \, \mathrm{e}^{-(\nu_{\text{L}\to\text{R}}+\nu_{\text{R}\to\text{L}})}. \tag{1.26}$$

The tracer PDF $p_{\text{T}}(x,t)$ can be recovered from the noninteracting picture as follows. The probability that, at time t, the tracer is located in infinitesimal interval $(x, x + \mathrm{d}x)$ is given by the product of the probability that there is a noninteracting particle in $(x, x + \mathrm{d}x)$ which is $(\rho\mathrm{d}x)$, and the probability $A_0(x,t)$ that there were equal number of trajectory crossings. Therefore, we have

$$p_{\text{T}}(x,t) = \rho A_0(x,t). \tag{1.27}$$

Let us now turn to the long-time properties of the PDF (1.27). All integrals in Eqs. (1.23), (1.24), can be evaluated analytically. This yields

$$\nu_{\mathrm{L}\to\mathrm{R}}(x,t) = \rho \left[\sqrt{\frac{Dt}{\pi}}\, e^{-x^2/4Dt} - \frac{x}{2}\left(1 - \mathrm{erf}\left(\frac{x}{\sqrt{4Dt}}\right)\right)\right], \qquad (1.28)$$

$$\nu_{\mathrm{R}\to\mathrm{L}}(x,t) = \rho \left[\sqrt{\frac{Dt}{\pi}}\, e^{-x^2/4Dt} + \frac{x}{2}\left(1 + \mathrm{erf}\left(\frac{x}{\sqrt{4Dt}}\right)\right)\right]. \qquad (1.29)$$

The both above expression increase with time. Therefore, in the long-time limit, $x \ll \sqrt{4Dt}$, we can use the asymptotic representation of the Bessel function, $\mathrm{I}_0(2z) \sim e^{2z}/\sqrt{4\pi z}$, for $z \to \infty$, to get

$$p_{\mathrm{T}}(x,t) \sim \rho(4\pi)^{-1/2}(\nu_{\mathrm{L}\to\mathrm{R}}\nu_{\mathrm{R}\to\mathrm{L}})^{-1/4}e^{-\left(\sqrt{\nu_{\mathrm{L}\to\mathrm{R}}}-\sqrt{\nu_{\mathrm{R}\to\mathrm{L}}}\right)^2}, \qquad t \to \infty. \qquad (1.30)$$

Further, we approximate the error functions in Eqs. (1.28), (1.29) by their small-argument asymptotic behavior $\mathrm{erf}(z) \sim 2z/\sqrt{\pi}$ and, after some algebra, we obtain

$$(\sqrt{\nu_{\mathrm{L}\to\mathrm{R}}} - \sqrt{\nu_{\mathrm{R}\to\mathrm{L}}})^2 \sim x^2\frac{\rho}{4}\sqrt{\frac{\pi}{Dt}}, \qquad (1.31)$$

$$(\nu_{\mathrm{L}\to\mathrm{R}}\nu_{\mathrm{R}\to\mathrm{L}})^{-1/2} \sim \frac{1}{\rho}\sqrt{\frac{\pi}{Dt}}. \qquad (1.32)$$

Returning to Eq. (1.27), the asymptotic tracer PDF is Gaussian:

$$p_{\mathrm{T}}(x,t) \sim \frac{1}{\sqrt{4\pi\mathcal{D}_{1/2}\sqrt{t}}}e^{-x^2/4\mathcal{D}_{1/2}\sqrt{t}}, \qquad t \to \infty, \qquad (1.33)$$

where we have defined the generalized diffusion coefficient

$$\mathcal{D}_{1/2} = \frac{1}{\rho}\sqrt{\frac{D}{\pi}}, \qquad (1.34)$$

which enters the subdiffusive law for the mean squared displacement

$$\left\langle \mathbf{X}_{\mathrm{T}}^2(t)\right\rangle \sim 2\mathcal{D}_{1/2}\sqrt{t}. \qquad (1.35)$$

Notice that the main ideas behind the above derivation of the Gaussian PDF (1.33), are essentially the same as those behind heuristic arguments based on Eq. (1.22). The only difference is that in the heuristic approach the freely diffusing entities are vacancies, whereas now the freely diffusing entities are noninteracting particles.

1.3 Comparison with SFD of N particles

Harris's classical result concerning $t^{1/2}$ MSD growth and the Gaussian PDF (1.21) are derived under following conditions: the system is homogeneous with a constant density of particles, and, increasing time, the subdiffusive regime is the last one which occurs in the overall dynamical description. We now wish to comment on further details of the SFD model including finite-time behavior and the dynamics of the system with finite number of particles.

1.3.1 Entropic repulsive forces

First, let us consider the long-time dynamics of the system with zero density, namely, an infinite line containing N interacting particles. The dynamics of such a system has been studied in a great detail by Aslangul [43, 70].

In Ref. [43] the two-particle problem on a lattice has been solved exactly. In the continuum limit, the two particles undergo a Brownian motion with a hard-core interaction and the problem can be solved by a transition to the center of mass coordinate system. Then the difference coordinate behaves like a Brownian particle and the original hard-core interaction manifests itself as a perfectly reflecting wall for this particle at the origin. Under these conditions, the Brownian particle exhibits an anomalous drift away from the boundary, its average position increases as $t^{1/2}$, whereas the second moment has a normal diffusive spreading. Thus for two interacting particles the following overall picture emerges. The interaction induces a repulsive drift of entropic origin. The drift is anomalous with a vanishing velocity, the average distance between the particles grows at large times as $t^{1/2}$, whereas the second moment of the position of each particle grows linearly with time. Let $\mathbf{X}_{1:2}(t)$, $\mathbf{X}_{2:2}(t)$ be respectively the position of the left and of the right particle, then we have [43]

$$-\langle \mathbf{X}_{1:2}(t) \rangle = \langle \mathbf{X}_{2:2}(t) \rangle \sim \sqrt{\frac{2Dt}{\pi}}, \qquad \langle \mathbf{X}_{1:2}^2(t) \rangle = \langle \mathbf{X}_{2:2}^2(t) \rangle \sim 2Dt. \qquad (1.36)$$

In Ref. [70] similar issues have been clarified for N interacting particles. Aslangul has assumed that, at the initial time the particles form a compact point-like cluster located at the origin. In $t \to \infty$ limit, the mean position of the nth particle ($n = 1, \ldots, N$), and its second moment evolve with time according to

$$\langle \mathbf{X}_{n:N}(t) \rangle \sim V_{n:N}\sqrt{t}, \qquad \langle \mathbf{X}_{n:N}^2(t) \rangle \sim 2D_{n:N}t. \qquad (1.37)$$

Hence the dynamical exponents are exactly the same as for two particles (1.36). Both the particle order and the total number of particles enters the result through the order-dependent transport coefficients $V_{n:N}$, $D_{n,N}$. The task of deriving exact expressions for $V_{n:N}$, $D_{n,N}$ is elusive [70], yet, for two special cases the asymptotic behavior can be given. For the particles located at the edges of the dispersing cluster the asymptotic behavior of the transport coefficients is given by $-V_{1:N} = V_{N:N} \propto [\log(N)]^{1/2}$, $D_{1:N} = D_{N:N} \propto [\log(N)]^{-1/2}$. For the central particle, we have $D_{c:N} \propto 1/N$, $c = (N+1)/2$.

Thus, when the total number of particles is finite, the mutual interactions induce an anomalous entropic drift but the diffusion is not anomalous in the long-time limit. On the other hand, notice that in the limit of $N \to \infty$, both $D_{N:N}$ and $D_{c:N}$ vanishes. This indicates a possible lowering of the dynamical exponent and the onset of a subdiffusive regime observed in the finite density situation. The middle particle is surrounded by infinitely many others and its diffusion constant vanishes as $1/N$. For the two edge particles, the logarithmic decrease of $D_{N:N}$ comes from the fact that these particles still face a free semi-infinite space to wander in (see Ref. [70] for a further discussion).

1.3.2 Three dynamical regimes

Let us consider a finite interval of the length L with N diffusing particles, and we put $\rho = N/L$. A thorough analysis of tracer dynamics in a finite interval with reflecting boundary conditions has been given by Lizana and Ambjörnsson in Refs. [51, 52]. Authors used Bethe Ansatz to derive the exact tracer PDF. In the present section we will paraphrase their results concerning different dynamical regimes for the dynamics of the

middle particle. Recently, the results have been reproduced by the scaling method in Ref. [71].

The precise setting is the following. At the initial time $t = 0$ there are N interacting particles of the diameter Δ randomly distributed in the interval of the length L. We will follow the diffusion of the central particle located initially approximately near the center of the interval (the tracer). The dynamics of the tracer is rather complex. The exact analysis based on Bethe Ansatz has revealed three dynamical regimes: (A) short times, (B) intermediate times, and (C) long times.

(A) *Short times.* For time t much smaller than the collision time t_{coll},

$$t_{\text{coll}} = \frac{1}{\rho^2 D}, \tag{1.38}$$

the tracer "does not feel" other particles and, consequently, it undergoes a free diffusion. In this regime, the tracer PDF is Gaussian with the MSD given by

$$\left\langle [\mathbf{X}_{\text{T}}(t) - \mathbf{X}_{\text{T}}(0)]^2 \right\rangle = 2Dt, \qquad t \ll t_{\text{coll}}. \tag{1.39}$$

(B) *Intermediate times.* For times t much larger than the collision time t_{coll} but still smaller than the equilibrium time t_{eq},

$$t_{\text{eq}} = \frac{L^2}{D}, \tag{1.40}$$

the tracer diffusion is anomalous, the tracer PDF is given by a Gaussian function with the mean squared displacement

$$\left\langle [\mathbf{X}_{\text{T}}(t) - \mathbf{X}_{\text{T}}(0)]^2 \right\rangle = \frac{1 - \rho\Delta}{\rho} \sqrt{\frac{4Dt}{\pi}}, \qquad t_{\text{coll}} \ll t \ll t_{\text{eq}}. \tag{1.41}$$

The generalized diffusion coefficient predicted by Eq. (1.41) is in conformity with that obtained for infinite systems with point particles ($\Delta = 0$, cf. Eqs. (1.33 - 1.35)) and also with that for the SFD on a lattice [72, 73]. The latter correspondence is obtained when both the particle diameter Δ and the lattice spacing equals to one.

(C) *Long times.* In the long-time limit, $t \gg t_{\text{eq}}$, the tracer PDF approaches an equilibrium probability density function and its MSD saturates on a constant value. We have

$$\left\langle [\mathbf{X}_{\text{T}}(t) - \mathbf{X}_{\text{T}}(0)]^2 \right\rangle \propto \frac{L^2}{N}, \qquad t \gg t_{\text{eq}}. \tag{1.42}$$

Only regimes (A) and (B) are found in the infinite system with constant particle density (discussed in Sec. 1.2), where t_{eq} diverges. Notably, in the setting discussed by Aslangul (cf. Sec. 1.3) the regime (C) is replaced by the normal diffusion and the regime (A) should be absent since the particles initially form a compact point-like cluster. In a finite interval with periodic boundary conditions the regime (C) is also different. For a periodic system at long times, all particles become highly correlated – they behave as a single effective particle and undergo a normal diffusion with the renormalized diffusion coefficient D/N [74]. A different (even superdiffusive) MSD behavior in regime (B) is reported in Ref. [75] where effects induced by the choice of initial conditions are discussed by means of Monte Carlo simulations.

1.4 Single-file diffusion front

In the finite-N case studied by Aslangul the particle near the boundary of the cluster is repelled by a finite number of its neighbors. This repulsion induces an anomalous

drift proportional to $t^{1/2}$. An important question is in order. What if the edge particle has *infinite* number of others to its left (say)? How strong is the entropic repulsion in this case? To obtain the answer let us turn to the study of statistical properties of the single-file diffusion front. Namely, in the present section we consider SFD on an infinite line. Initially the negative half-line is occupied by (infinitely many) particles distributed with the mean density ρ. There are no particles on the positive half-line. We are interested in the motion of the right-most particle.

The evolution of the density of particles $\rho(x, t)$ is governed by the diffusion equation with the step initial condition: $\rho(x, 0) = \rho$ for $x < 0$ and $\rho(x, 0) = 0$ otherwise. The density profile at time t is given by the complementary error function:

$$\rho(x, t) = \frac{\rho}{2} \operatorname{erfc}\left(\frac{x}{\sqrt{4Dt}}\right), \tag{1.43}$$

from which we obtain the mean number of particles located to the right of x:

$$\nu(x, t) = \int_x^\infty \mathrm{d}x' \rho(x', t). \tag{1.44}$$

Let us number the particles from right to left. Hence the rightmost particle is labeled by $n = 1$. How can we construct the PDF $p_n(x, t)$ of the nth interacting particle? Again we provide an answer by a proper construction based on the reference noninteracting picture. The sought probability that the nth interacting particle is in $(x, x + \mathrm{d}x)$ equals to the probability that there is a noninteracting particle in $(x, x + \mathrm{d}x)$, i.e., $\rho(x, t)\mathrm{d}x$, times the probability that there are $(n-1)$ particles to the right of x. Since the reference noninteracting particles are statistically independent, the latter probability is given by the Poisson distribution with the mean value $\nu(x, t)$. Altogether, we get

$$p_n(x, t) = \rho(x, t) \frac{[\nu(x, t)]^{n-1}}{(n - 1)!} \mathrm{e}^{-\nu(x,t)}. \tag{1.45}$$

Let us now focus on statistical properties of the right-most particle (sometimes called as the single-file diffusion front, or just a diffusion front). Its cumulative distribution function, $F_1(x, t) = \int_{-\infty}^x \mathrm{d}x' p_1(x', t)$, equals

$$F_1(x, t) = \exp[-\nu(x, t)]. \tag{1.46}$$

In the long-time limit $F_1(x, t)$ converges to Gumbel distribution:

$$F_1(x, t) \sim \exp\left[-\exp\left(-\frac{x}{b(t)} + a(t)\right)\right], \quad t \to \infty, \tag{1.47}$$

with parameters

$$b(t) = \sqrt{\frac{2Dt}{\log(2Dt)}}, \quad a(t) = \log\left(\frac{2\rho Dt}{\sqrt{2\pi}\log(2Dt)}\right). \tag{1.48}$$

For the proof of the convergence we refer to the proof of Theorem 3 in Ref. [76] (Arratia in Ref. [76] has used λ instead of our ρ and has worked with a standard Brownian motion for which $D = 1/2$).

Gumbel distribution (1.47) gives us asymptotic behavior of all moments of the front position. The asymptotic mean position assumes the form

$$\langle \mathbf{X}_1(t) \rangle \sim \sqrt{\frac{2Dt}{\log(2Dt)}} \left[\gamma + \log\left(\frac{2\rho Dt}{\sqrt{2\pi}\log(2Dt)}\right)\right], \quad t \to \infty. \tag{1.49}$$

17

where γ stands for Euler's constant, $\gamma \approx 0.5772156649$. For the variance we obtain

$$\left\langle [\mathbf{X}_1(t) - \langle \mathbf{X}_1(t) \rangle]^2 \right\rangle \sim \frac{\pi^2}{6} \frac{2Dt}{\log(2Dt)}, \qquad t \to \infty. \tag{1.50}$$

Thus an anomalous entropic drift produced by infinite number of particles scales with time faster than $t^{1/2}$-law observed in Aslangul's finite-N setting. Interestingly enough, an effective one-sided restriction of particle's motion results in a slowdown of its diffusion. The asymptotic variance (1.50) grows with time slower than that in the case of the normal diffusion (i.e., slower than t) but still faster than in the case of $t^{1/2}$ subdiffusion.

Finally, a few remarks are in order. First, Gumbel distribution $\exp(-\exp(-x))$ is one of the three possible limiting distributions for extreme order statistics. The three distributions with brief comments on the related theory are presented in App. A. Second, there exists a recent work [77] concerning diffusion front.[2] Third, in Refs. [78, 79] fluctuations of the current through the origin has been studied for the simple symmetric exclusion process with a similar initial condition as that of the present section. For the asymmetric simple exclusion process the similar initial conditions have been discussed in Refs. [80–88], in particular in connection to random matrix theory.

1.5   Further reading

Let us now mention a few selected directions of research which has not been covered in the preceding text.

(1) Recently SFD of *nonidentical* particles (different diffusion constants) has attracted a considerable attention. In this case the correspondence between the interacting particles and the noninteracting ones breaks down and the model is no-longer integrable. Various approximative [89] and numerical methods have been developed including scaling arguments [90] and the harmonization technique [45, 62] which approximates the SFD system by the particles interconnected by harmonic springs (the Rouse model). With the aid of this mapping, in Ref. [63] a force-response relation for tracer has been studied. Rigorously, a convergence to a fractional Brownian motion, a law of large numbers and a central limit theorem has been proven in Ref. [91].

(2) Several studies are devoted to SFD in one dimension with *more general interparticle interactions than just the hard-core one* [92–98]. For instance, typical $t^{1/2}$ subdiffusive behavior is reported also for inelastically colliding particles [99, 100]. What if the interaction is long-ranged? This important generalization has been studied in seminal work [92] with the following conclusion: provided that the correlation length between the particles is finite the tracer MSD grows asymptotically as $t^{1/2}$ and the generalized diffusion coefficient is related to the compressibility of the system. These predictions were tested experimentally for colloidal particles [21, 22] and for charged millimetric steel balls [95, 96]. Hydrodynamic interactions, yet another effect, are screened significantly in one dimension; cf. Ref. [23] for both experimental and theoretical study, and Ref. [98] for extensive numerical analysis.

Above examples may evoke an impression that $t^{1/2}$ scaling of the MSD must be observed in any one-dimensional diffusive system regardless the form of interparticle interaction. Of course this is not the case. A notable counterexample where long-ranged interactions modify the subdiffusive regime is provided by Brownian particles interacting by the logarithmic potential (Dyson's Brownian motion). In this case the

---

[2]Notice that Sabhapandit's expression for the cumulative distribution function of the front position (Eq. (7) in Ref. [77]) differs from $F_1(x, t)$ in Eq. (1.46) by a nontrivial multiplicative factor. Probabilistic interpretation of Eq. (7) in Ref. [77] remains unclear to the present author (actually, $F_1(x, t)$ corresponds to the right-hand side of Eq. (5) in Ref. [77]).

tracer MSD grows as $\log(t)$ [101]. Other cases are listed in next paragraphs. There, deviations from typical $t^{1/2}$ subdiffusion are caused by interaction with external fields and/or with confining channel, and even by a certain type of initial conditions.

(3) Single-file dynamics *in spaces with dimension greater than one* is of considerable interest in recent years. In particular, a reduction of the confined two-dimensional single-file dynamics of discs to the one-dimensional longitudinal motion of rods has been carried out in Refs. [102–105]. When the diameter of the tube is slightly greater than the doubled diameter of the disc a crossover from the subdiffusion to a normal diffusion occurs. An accurate description of this phenomenon is still under active debate [106–108]. For particles interacting by Yukawa potential, numerical analysis of Ref. [109] reveals rather different diffusive regimes and transitions depending on the shape of the channel. The screened Coulomb potential (described through a modified Bessel function of the second kind K_0, as inspired by experiments [95,96]) leads to nontrivial properties of fluctuations in the vicinity of transitions between different equilibrium conformations of the system [110–112].

(4) Effects induced by *external fields* acting on particles have become the subject of several studies [39,61,63,113–123]. Strictly speaking, the previous point (3) also belongs to this category. A particularly hard and still unsolved problem is when the external field acts on the tagged particle only. Theoretical advances in this direction can be found in Refs. [61,63,120,121]. The external field acting on all particles can model, for example, entropic forces stemming from inhomogenities of real channels [124]. SFD in random potentials have been studied both theoretically [122,125] and experimentally [123]. Channels with random walls have been considered in Ref. [126]. Diffusion of magnetic dipoles in modulated channels is discussed in Refs. [113–115].

(5) *Initial conditions* may imply two unexpected effects on the dynamics of the tracer. First, the power law initial distribution results in t^α subdiffusion, where α is neither 1 nor 1/2 [71,117,127]. Second, the initial condition determines the value of the generalized diffusion coefficient [128], which is a long-memory effect unobserved in the normal diffusion (where the diffusion coefficient is determined by Einstein's relation).

(6) In some studies the *dynamics of individual particles is not normal Brownian motion*. Instead, the particles may follow e.g. the deterministic dynamics [129–132] or some kind of an anomalous kinetics [127,133–135]. An outstanding result valid for all these systems is the so called Percus diffusion formula [117,129]. The formula relates MSD of the tracer in a system with interaction with motion of a single particle in the absence of interaction: $\left\langle [\mathbf{X}_{\mathrm{T}}(t) - \mathbf{X}_{\mathrm{T}}(0)]^2 \right\rangle \sim \left\langle |\mathbf{X}(t) - \mathbf{X}(0)| \right\rangle / \rho$. It is valid for an infinite homogeneous system with constant density of particles and in Ref. [117] it has been derived for a rather broad class of anomalous processes including e.g. the continuous-time random walk and the fractional Brownian motion. Thus for instance if for a free diffusion $\left\langle [\mathbf{X}(t) - \mathbf{X}(0)]^2 \right\rangle \propto t^\alpha$ then for the tracer motion $\left\langle [\mathbf{X}_{\mathrm{T}}(t) - \mathbf{X}_{\mathrm{T}}(0)]^2 \right\rangle \propto t^{\alpha/2}$.

(7) The *first-passage* time density for a tracer in a homogeneous system has been discussed in Ref. [59]. An open single-file system (the interval with at least one absorbing boundary) has been studied numerically for a biased SFD [136], for an unbiased SFD [50] (briefly discussed as a particular example), and analytically for an unbiased diffusion in Refs. [40–42]. The latter works form a basis of the following Chaps. 2, 3. A closely related problem of orders statistics of first-passage times for independent random walkers [137–147] will be discussed in a more detail in Chap. 2.

Last but not least, in the above brief review we have restricted ourselves mainly to the physically-oriented literature. Rigorous (mathematical) results concerning the dynamics of the tracer can be found in the following references. Besides the seminal works of Harris [27] and Spitzer [148], central limit theorems for a tagged particle are discussed in Refs. [76,91,149], and reviewed in Ref. [150].

2. SFD in a semi-infinite system with absorbing boundary
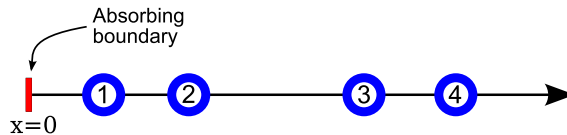
2.1 Definition of the model

Figure 2.1: Schematic illustration of the possible initial configuration of $N = 4$ particles and their labeling.

Consider diffusion of hard-core interacting Brownian particles in a semi-infinite one-dimensional interval with the absorbing boundary at the origin. Initially, N particles are distributed along the half-line $(0, \infty)$. During the time evolution, each particle diffuses with the same diffusion constant D. The particles cannot enter the interval from the outside and they are allowed to leave it only through the boundary at the origin. The boundary is perfectly absorbing, i.e., if any particle hits the origin it is absorbed with the probability one. At initial time $t = 0$, let us label the particles according to ordering of their positions from the left to the right, cf. Fig. 2.1. We have

$$0 < \mathbf{X}_{1:N}(0) < \mathbf{X}_{2:N}(0) < \ldots < \mathbf{X}_{N:N}(0) < \infty, \qquad (2.1)$$

where the random variable $\mathbf{X}_{n:N}(0)$ denotes the position of the nth particle at $t = 0$. The hard-core interaction guarantees that the initial ordering of particles is conserved over time. Notice that the particle No. 1 is the first one that might be absorbed. It is only after this event happens that the particle No. 2 can approach the origin and be absorbed. Let us denote as $\mathbf{T}_{n:N}$ the random time of the absorption of the nth particle. The particle ordering implies the corresponding ordering of absorption times:

$$0 < \mathbf{T}_{1:N} < \mathbf{T}_{2:N} < \ldots < \mathbf{T}_{N:N} < \infty. \qquad (2.2)$$

The last inequality, $\mathbf{T}_{N:N} < \infty$, means that the rightmost particle (and hence any particle) is eventually absorbed with the probability one. At the same time, the mean value $\langle \mathbf{T}_{N:N} \rangle$ is infinite, as will be shown in the following.

The second setting discussed in the present chapter is the semi-infinite system which is initially occupied by an *infinite* number of particles – the system is initially in equilibrium with the constant mean density ρ. In such a system each tagged particle possesses an infinite number of right neighbors and the two above sets of inequalities now read[1]

$$0 < \mathbf{X}_1(0) < \mathbf{X}_2(0) < \ldots < \mathbf{X}_n(0) < \ldots, \qquad (2.3)$$

$$0 < \mathbf{T}_1 < \mathbf{T}_2 < \ldots < \mathbf{T}_n < \ldots, \qquad (2.4)$$

where the random variable $\mathbf{X}_n(0)$ denotes the initial position of the nth tracer and $\mathbf{T}_n$ stands for the corresponding absorption time.

---

[1] Notice that the notation $\mathbf{X}_n(t)$ has been used in the introductory Chap. 1 for noninteracting particles. Hence it seems to be more plausible to denote the position of the nth tracer and its absorption time as $\mathbf{X}_{n:\infty}(t)$, $\mathbf{T}_{n:\infty}$, respectively. However, we have decided not to include the symbol "∞" into the notation. The precise meaning should be always clear from the context and we believe that no confusion may arise. From now on the position of a generic noninteracting particle and its absorption time will be denoted by unindexed random variables $\mathbf{X}(t)$, $\mathbf{T}$, respectively.

In both above settings (the finite-N case and the system in the thermodynamic limit) we are primarily interested in the dynamics of the tracer, in the dynamics of the tracer *conditioned on nonabsorption* and in the characterization of absorption times. The present chapter is based on works [40, 42].

2.2   Finite number of interacting particles

2.2.1   Single diffusing particle

Brownian motion absorbed at the origin

All properties of interacting particles can be constructed form the elements describing a corresponding system of noninteracting particles. Thus, let us for a moment take $N\!=\!1$ and summarize basic formulas for a single particle.

Suppose that at initial time $t = 0$ the particle is located at the position y, $y > 0$. The PDF of the particle's position at time t conditioned on its initial position is determined by solving the diffusion equation[2]

$$\frac{\partial}{\partial t} f(x, t \,|\, y, 0) = D \frac{\partial^2}{\partial x^2} f(x, t \,|\, y, 0) \tag{2.5}$$

subject to the absorbing boundary condition at the origin,

$$f(0, t \,|\, y, 0) = 0, \tag{2.6}$$

and to the initial condition

$$f(x, 0 \,|\, y, 0) = \delta(x - y). \tag{2.7}$$

This problem is readily solved by the method of images [151]. The result reads

$$f(x, t \,|\, y, 0) = \frac{1}{\sqrt{4\pi D t}} \left[\mathrm{e}^{-(x-y)^2/4Dt} - \mathrm{e}^{-(x+y)^2/4Dt} \right]. \tag{2.8}$$

Having this Green function, the time evolution of an arbitrary initial PDF, say $f(x)$, is given by

$$f(x, t) = \langle f(x, t \,|\, \mathbf{X}(0), 0) \rangle = \int_0^\infty \mathrm{d}y \, f(x, t \,|\, y, 0) f(y). \tag{2.9}$$

As for the initial PDF $f(x)$, in the following analysis we only assume that all its moments exist. For the sake of illustrations, we take the particular initial condition

$$f(x) = \frac{\mathrm{e}^{-x/L}}{L}, \quad L > 0, \quad x \geq 0. \tag{2.10}$$

The spatial integral of the PDF (2.9) over the interval $(0, +\infty)$ equals the *survival probability*, that is, the probability that the particle has not been absorbed by time t. If we denote by $\mathbf{T}$ the time of absorption, we can write

$$S(t) = \mathrm{Prob}\,\{\mathbf{T} > t\} = \int_0^\infty \mathrm{d}x \, f(x, t) = \left\langle \mathrm{erf}\!\left(\frac{\mathbf{X}(0)}{\sqrt{4Dt}} \right) \right\rangle, \tag{2.11}$$

where the last expression stands for the average of the error function with respect to initial PDF $f(x)$. The time-evolution of the survival probability is linked to the

---

[2]Everywhere in Chaps. 2, 3 all PDFs that have originated in the one-dimensional single-particle problem are denoted by the letter "f". Contrary to this, PDFs that occur in the many-particle problem with interaction will be designated by the letter "p".

probability current $j(x,t)$ through the origin of coordinates. The probability that the particle has already been absorbed by time t, $[1 - S(t)]$, grows with time according to

$$\frac{\mathrm{d}}{\mathrm{d}t}[1 - S(t)] = \left. D\frac{\partial}{\partial x}f(x,t)\right|_{x=0} = -j(0,t). \tag{2.12}$$

At time $t = 0$, the survival probability equals to one. The long-time behavior of $S(t)$ may be derived by inserting the power series representation of the error function into Eq. (2.11). The main asymptotic term decays as the power law:

$$S(t) \sim \frac{\langle \mathbf{X}(0)\rangle}{\sqrt{\pi D}}\, t^{-1/2}, \qquad t \to \infty. \tag{2.13}$$

The prefactor depends on the diffusion constant and on the mean initial position of the particle.

The survival probability $S(t)$ yields the complete probabilistic description of the absorption process. The same information can be obtained from a complementary quantity. Namely, from the PDF for the time of absorption $\phi(t)$. It is defined by the equation $\mathrm{Prob}\{\mathbf{T} < t\} = \int_0^t \mathrm{d}t'\,\phi(t')$, and hence it is directly related to the survival probability:

$$1 - S(t) = \int_0^t \mathrm{d}t'\,\phi(t'), \qquad \phi(t) = -\frac{\mathrm{d}}{\mathrm{d}t}S(t). \tag{2.14}$$

The long-time asymptotic behavior of $\phi(t)$ is given by

$$\phi(t) \sim \frac{\langle \mathbf{X}(0)\rangle}{\sqrt{4\pi D}}\, t^{-3/2}, \qquad t \to \infty. \tag{2.15}$$

The mean time to absorption (or *the mean exit time*)

$$\langle \mathbf{T}\rangle = \int_0^\infty \mathrm{d}t\, t\phi(t) \tag{2.16}$$

and all higher moments of the PDF $\phi(t)$ diverge. On the other hand, the particle will certainly leave the interval since the survival probability $S(t)$ tends to zero, cf. Eq. (2.13).

Brownian motion conditioned on nonabsorption

According to the above results, the mean escape time of the particle is infinite, nevertheless, the particle eventually escapes from the interval with the probability one. At a given time t, starting with an ensemble of all possible particle trajectories, it is interesting to restrict the attention on the subensemble of those paths which have not hit the boundary up to time t. The subensemble is described by the conditional probability density function, the condition being the nonabsorption up to time t. The conditional PDF reads

$$f(x, Dt \,|\, \mathbf{T} > t) = \frac{f(x,t)}{S(t)}. \tag{2.17}$$

The power series representation of the PDF $f(x, Dt \,|\, \mathbf{T} > t)$ is given in Eq. (B.9). It follows that

$$f(x, Dt \,|\, \mathbf{T} > t) = \frac{x}{2Dt}\,\mathrm{e}^{-x^2/4Dt}\left[1 + O\left(t^{-1}\right)\right], \tag{2.18}$$

where "$O\left(t^{-1}\right)$" stands for all terms of the series (B.9) that tend to zero at least as t^{-1} when $t \to \infty$. Therefore, in the long-time limit, the conditioned PDF (2.17) assumes the asymptotic form

$$f(x, Dt \,|\, \mathbf{T} > t) \sim \frac{x}{2Dt}\,\mathrm{e}^{-x^2/4Dt}, \qquad t \to \infty. \tag{2.19}$$

22

Notice that this asymptotic representation is non-negative and it is normalized to one on $x \in [0, +\infty)$. The distribution with the PDF (2.19) is known as the Rayleigh distribution. The asymptotic PDF (2.19) is independent of the initial condition $f(x)$. In the long-time limit there remains just one length scale associated with the dynamics – the diffusion length $\sqrt{2Dt}$. All other length scales which have been introduced by the initial condition are already forgotten.

The first and the second moment of the asymptotic PDF (2.19) read

$$\langle \mathbf{X}(t) \rangle_{\mathbf{T}>t} \sim \sqrt{\pi Dt}, \qquad (2.20)$$

$$\left\langle \mathbf{X}^2(t) \right\rangle_{\mathbf{T}>t} \sim 4Dt, \qquad (2.21)$$

respectively. The mean position of the surviving trajectories should be compared with the corresponding result for the unconditioned dynamics, that is, with $\langle \mathbf{X}(t) \rangle = \langle \mathbf{X}(0) \rangle$. Provided a trajectory has avoided absorption by time t, the particle is typically found far from the origin and its position grows as $t^{1/2}$. One can say that the conditioning implies an effective force which drags the particle away from the absorbing boundary. The first-order correction to the asymptotic result (2.20) vanishes as $t^{-1/2}$ and it depends on the initial condition. Using Eq. (B.9), we get

$$\langle \mathbf{X}(t) \rangle_{\mathbf{T}>t} = \sqrt{\pi Dt} \left[1 + \frac{1}{12} \frac{\langle \mathbf{X}^3(0) \rangle}{\langle \mathbf{X}(0) \rangle} \frac{1}{Dt} + O\left(t^{-2} \right) \right]. \qquad (2.22)$$

The same holds true also for the first correction to the second moment (2.21).

The single-particle stochastic dynamics conditioned on nonabsorption has been explored extensively in probability theory. A comprehensive bibliography survey is available in Ref. [152]. Usually, the conditioning suggests itself in the frame of biological, demographic, ecological and epidemiological models, where the absorbed diffusion process models the populations undergoing extinction. By the conditioning on nonabsorption, the focus is shifted on the properties of long-surviving paths of the process. One specific consequence of the conditioning on nonextinction is the deceleration of the instantaneous mortality rates (mortality rate plateaus) [153]. It should be noted that, under certain conditions, the conditioned process converges towards a time-invariant distribution, the so called quasistationary distribution. The study of quasistationary distributions began with the seminal work of Yaglom on subcritical Galton-Watson processes [154], for a further discussion see e.g. Refs. [155–158] and references therein. Independently, conditional distributions occur in conformational statistics of polymer chains interacting with surfaces [159–162]. For instance a three-dimensional analogue of the asymptotic PDF (2.19) describes the end-to-end distance of the polymer grafted by one end to the reflecting wall [159].

2.2.2 Mapping on single-particle diffusion in N dimensions

Let us now return to diffusion of interacting particles. The dynamics of N interacting particles possesses a noteworthy geometric interpretation. It resides in mapping of the N interacting diffusing particles onto a single "representative particle" diffusing in N dimensions (cf. Sec. 1.1, for the situation without absorption).

At $t = 0$ there are N particles inside the interval $(0, \infty)$. Until the absorption of the particle No. 1, the situation corresponds to the diffusion of a single representative particle in the N-dimensional wedge domain[3]

$$\{ \vec{x}_N : 0 < x_1 < x_2 < \ldots < x_{N-1} < x_N < \infty \} \qquad (2.23)$$

---

[3]The vector notation used: $\vec{x}_{N-k} = (x_{k+1}, \ldots, x_N)$, $k = 0, 1, \ldots, (N-1)$.

bounded by $(N-1)$ reflecting hyperplanes

$$\left\{\vec{x}_N : 0 < x_1 < ... < x_n = x_{n+1} < ... < x_N < \infty\right\}, \tag{2.24}$$

$n = 1, ..., (N-1)$, which represent the non-crossing conditions, and by the absorbing hyperplane

$$\left\{\vec{x}_N : x_1 = 0, 0 < x_2 < ... < x_{N-1} < x_N < \infty\right\}, \tag{2.25}$$

which accounts for the possibility of the absorption of the leftmost particle. The diffusion within this wedge is characterized by the PDF $p^{(N)}(\vec{x}_N, t)$ and it is governed by the N-dimensional diffusion equation

$$\frac{\partial}{\partial t}p^{(N)}(\vec{x}_N, t) = D\sum_{j=1}^{N}\frac{\partial^2}{\partial x_j^2}p^{(N)}(\vec{x}_N, t). \tag{2.26}$$

The non-crossing boundary conditions that describe reflections of the representative particle on $(N-1)$ reflecting hyperplanes read

$$\left(\frac{\partial}{\partial x_j} - \frac{\partial}{\partial x_{j+1}}\right)p^{(N)}(\vec{x}_N, t)\Big|_{x_j=x_{j+1}} = 0, \tag{2.27}$$

$j = 1, \ldots, N-1$. The conditions guarantee the zero probability currents in the directions perpendicular to reflecting hyperplanes. The exit of the left-most particle from the pore corresponds to "sticking" of the representative particle to the absorbing hyperplane and it is incorporated by the absorbing boundary condition

$$p^{(N)}(\vec{x}_N, t)\Big|_{x_1=0} = 0. \tag{2.28}$$

Absorption of the leftmost particle in the original picture reduces the dimension of the space available for diffusion of the representative particle. After the absorption of particle No. 1, the representative particle diffuses within the $(N-1)$-dimensional wedge domain

$$\left\{\vec{x}_{N-1} : 0 < x_2 < ... < x_{N-1} < x_N < \infty\right\} \tag{2.29}$$

bounded by $(N-2)$ reflecting hyperplanes

$$\left\{\vec{x}_{N-1} : 0 < x_2 < ... < x_n = x_{n+1} < ... < x_N < \infty\right\}, \tag{2.30}$$

$n = 2, ..., (N-1)$, and by the absorbing hyperplane

$$\left\{\vec{x}_{N-1} : x_2 = 0, 0 < x_3 < ... < x_{N-1} < x_N < \infty\right\}. \tag{2.31}$$

The diffusion within this domain is described by the PDF $p^{(N-1)}(\vec{x}_{N-1}, t)$. This PDF varies in time due to the following *three* reasons: (A) diffusion of $(N-1)$ interacting particles, (B) a possible absorption of the particle No. 2 if it hits the absorbing boundary, (C) the absorption of the particle No. 1 while the remaining particles are situated in the infinitesimal domain $(\vec{x}_{N-1}, \vec{x}_{N-1} + \mathrm{d}\vec{x}_{N-1})$. We thus arrive at the *inhomogeneous* generalized diffusion equation with a source term on its right-hand side:

$$\frac{\partial}{\partial t}p^{(N-1)}(\vec{x}_{N-1}, t) = D\sum_{j=2}^{N}\frac{\partial^2}{\partial x_j^2}p^{(N-1)}(\vec{x}_{N-1}, t) + D\frac{\partial}{\partial x_1}p^{(N)}(\vec{x}_N, t)\Big|_{x_1=0}. \tag{2.32}$$

The last term on the right-hand side represents the probability current which accounts for the above point (C).[4] The hard-core interaction of $(N-1)$ particles is again incorporated through non-crossing boundary conditions on the reflecting hyperplanes:

$$\left(\frac{\partial}{\partial x_j} - \frac{\partial}{\partial x_{j+1}}\right)p^{(N-1)}(\vec{x}_{N-1}, t)\Big|_{x_j=x_{j+1}} = 0, \tag{2.33}$$

---

[4]The idea behind the last term on the right-hand side of Eq. (2.32) is essentially the same as that behind equation (2.12).
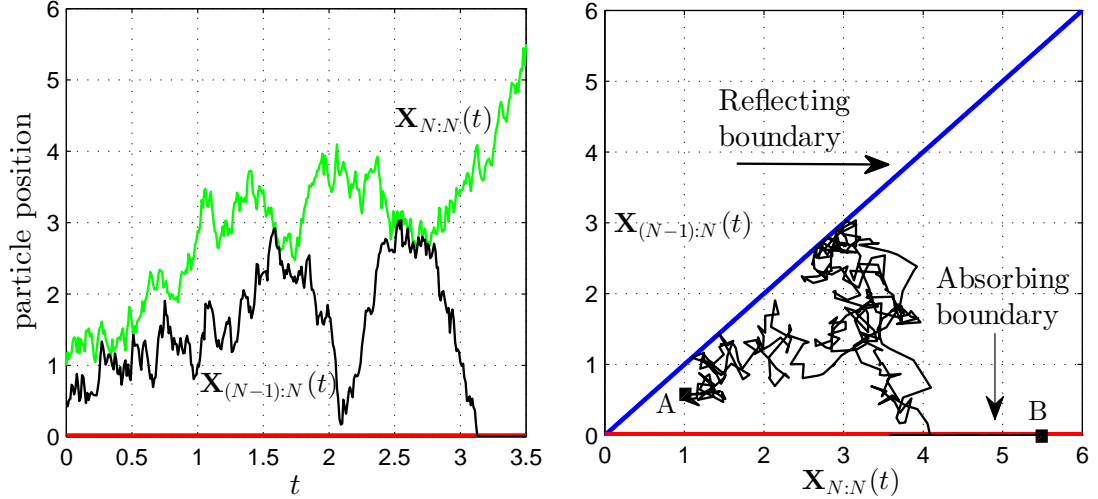
Figure 2.2: Mapping of the two-particle SFD onto the diffusion of one representative particle in the 2D wedge domain. The left panel shows the space-time trajectories of two interacting particles diffusing in the interval $(0, \infty)$. The red line $x = 0$ represents the absorbing boundary. Whenever the particles collide, their trajectories are mutually reflected. One such event occurs roughly at time $t \approx 1.6$. The particle No. $(N-1)$ leaves the pore approximately at $t \approx 3.2$. At that moment, the coordinate of the rightmost particle is roughly $x \approx 4.1$. The right panel shows the 2D diffusion of the representative particle within the wedge domain bounded by the reflecting boundary (the blue line) and by the absorbing boundary (the red line). The point $A = [1, 0.5]$ denotes the initial position of the representative particle. Whenever the trajectory hits the blue line it is reflected. The reflection corresponds to collisions of the two interacting particles. At the point $\approx [4.1, 0]$, the trajectory of the representative particle sticks to the absorbing boundary. This event represents the exit of the second rightmost particle from the interval at $t \approx 3.2$. Afterwards, the representative particle continues to diffuse along the line $x = 0$. Its final position at time $t = 3.5$ is shown by the point $B \approx [5.5, 0]$.

$j = 2, \ldots N - 1$. The absorbing boundary condition describing the possible escape of the particle No. 2 (the reason (B)) reads

$$p^{(N-1)}(\vec{x}_{N-1}, t)\Big|_{x_2=0} = 0. \tag{2.34}$$

Notice that the initial condition supplementing Eq. (2.32) is simply $p^{(N-1)}(\vec{x}_{N-1}, 0) = 0$. This follows from the assumption that, at $t = 0$, there are N particles inside the interval and hence the $(N-1)$-dimensional wedge (2.29) is empty.

Eventually, after the absorption of $(N-2)$ particles, there are two last particles left inside the interval. This case is illustrated in Fig. 2.2 where the corresponding representative particle diffuses in the 2D wedge domain $\{\vec{x}_2 : 0 < x_{N-1} < x_N < \infty\}$ bounded by just one reflecting boundary $\{\vec{x}_2 : 0 < x_{N-1} = x_N < \infty\}$ and by the absorbing half-line $\{\vec{x}_2 : x_{N-1} = 0, 0 < x_N < \infty\}$. Its motion is described by the PDF $p^{(2)}(\vec{x}_2, t)$. After this event, the diffusion of the representative particle is described by the PDF $p^{(1)}(x_N, t)$. The exit of the left particle corresponds to the sticking of the representative particle to the half-line $\{\vec{x}_2 : x_{N-1} = 0, 0 < x_N < \infty\}$. The exit of the last particle simply means the sticking of the representative particle to the origin. The probability of finding the representative particle at the origin at t is given by the

function $p^{(0)}(t)$. It obeys the simple evolution equation (cf. Eq. (2.12))

$$\frac{\mathrm{d}}{\mathrm{d}t} p^{(0)}(t) = D \frac{\partial}{\partial x_N} p^{(1)}(x_N, t) \Big|_{x_N = 0}, \qquad (2.35)$$

with the initial condition $p^{(0)}(0) = 0$. Further it will be denoted by $\phi_{N:N}(t)$ since $p^{(0)}(t)$ is nothing but the PDF of the time of absorption of the rightmost particle $\mathbf{T}_{N:N}$.

Summing up the above steps, we have obtained the *hierarchy of $N + 1$ coupled evolution equations* (2.26) - (2.35) that completely describe the dynamics of the system. The diffusion equation (2.26) is *closed*. Together with Eqs. (2.27), (2.28) and with the initial condition $p^{(N)}(\vec{x}_N, 0)$ it constitutes a well-defined initial-boundary value problem with a unique solution, the PDF $p^{(N)}(\vec{x}_N, t)$. Suppose that we know it. Then we insert its value at $(0, x_2, ..., x_N)$ into the source term on the right-hand side of Eq. (2.32). The inhomogeneous equation (2.32), supplemented by boundary conditions (2.33), (2.34), and by the initial condition $p^{(N-1)}(\vec{x}_{N-1}, 0) = 0$ constitutes again a closed initial-boundary value problem. Having obtained its solution, the PDF $p^{(N-1)}(\vec{x}_{N-1}, t)$, we again evaluate it at $(0, x_3, ..., x_N)$ and use as the source term in the equation for the PDF $p^{(N-2)}(\vec{x}_{N-2}, t)$, etc. The whole hierarchy is terminated by Eq. (2.35).

Finally, notice that the individual evolution equations may be generalized to cover many effects beyond SFD of hard-core interacting particles. For instance, one can easily incorporate external forces acting on particles and/or more general interparticle interactions.

2.2.3 PDF of a tagged particle

Considering a general number of particles N, the model setting must be completed by the specification of an initial state. Among all possible forms of initial distributions there exists one which leads to a considerable simplification of the subsequent analytical calculations. Even more importantly, the distribution is physically quite natural for real single-file systems. It describes the situation which emerges, e.g., after previous constitution of a steady state, or after previous autonomous relaxation towards a thermodynamic equilibrium. Namely, we assume that the initial joint PDF for the N-particle system is given by

$$p^{(N)}(\vec{x}_N, 0) = \begin{cases} N! \displaystyle\prod_{n=1}^{N} f(x_n) & \text{for } \vec{x}_N \in \mathcal{R}_N, \\[2ex] 0 & \text{for } \vec{x}_N \notin \mathcal{R}_N, \end{cases} \qquad (2.36)$$

where $\mathcal{R}_N$ denotes the N-particle phase space defined as a space of all possible configurations of N hard-core interacting particles on the semi-infinite interval $(0, \infty)$, i.e.,

$$\mathcal{R}_N = \{\vec{x}_N : 0 < x_1 < x_2 < ... < x_N < \infty\}. \qquad (2.37)$$

which is nothing but wedge domain (2.23). The symbol $\vec{x}_N \in \mathcal{R}_N$ means that the components of the vector $\vec{x}_N = (x_1, ..., x_N)$ obey all the inequalities in (2.37). If $\vec{x}_N \notin \mathcal{R}_N$, then at least one of them is violated. In general, the function $f(x)$ in Eq. (2.36) can be any PDF defined and normalized on the half-line $x \in [0, \infty)$. The normalization of the function $f(x)$ implies the proper normalization of the initial condition (2.36). This can be checked by a direct integration of the expression over the phase space $\mathcal{R}_N$.

At initial time $t = 0$, the *marginal* PDF for the position of the nth particle is obtained by integrating the function (2.36) over the coordinates of all other $(N-1)$ particles. If $p_{n:N}(x, 0)$ denotes the marginal PDF in question, then we have

$$p_{n:N}(x, 0) = \frac{N!}{(n-1)!(N-n)!} f(x) \left[\int_0^x \mathrm{d}x' \, f(x')\right]^{n-1} \left[1 - \int_0^x \mathrm{d}x' \, f(x')\right]^{N-n}, \quad (2.38)$$
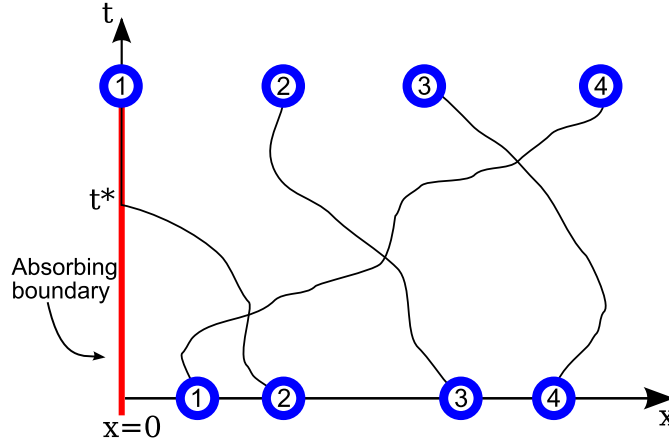
Figure 2.3: Schematic illustration of space-time trajectories of four particles. At time t* the leftmost particle hits the absorbing boundary. After this event the leftmost particle exits the interval and will never return. Equivalently we can imagine that for all times t, $t > $ t*, the absorbed particle resides in the trap located at $x = 0$.

where $(n-1)$ is the number of particles located to the left of the nth particle and $(N-n)$ gives the number of those on the right. The last expression has been written in the form which suggests two (equivalent) probabilistic interpretations. First, suppose that we have generated N points on the half-line, each of them being independently drawn from the distribution with the PDF $f(x)$. Then $p_{n:N}(x,0)$ is the PDF for the nth rightmost of them, i.e., for the nth order statistic. Second, consider the system of N identical and noninteracting particles. Let the position of each of them be described by the PDF $f(x)$. Then the PDF $p_{n:N}(x,0)$ equals the probability that there is a particle in $(x, x + \mathrm{d}x)$ and, simultaneously, there are precisely $(n-1)$ particles at arbitrary coordinates to the left of it, and the remaining $(N-n)$ particles are located at arbitrary coordinates to the right of it, cf. Eq. (1.20).

In the following, provided we need a further specification of the PDF $f(x)$, we always take $f(x)$ as defined in Eq. (2.10). This expression together with Eq. (2.36) yields a complete specification of the initial state. The state can be prepared for instance in the following way. Up to time $t = 0$ the interval is closed (reflecting boundary at the left end of the interval at $x = 0$), and each particle is pushed against the reflecting boundary by an external space-homogeneous and time-independent force (e.g. particles under the action of gravitational or electrostatic force). We assume that the N-particle system has reached the state of thermal equilibrium. At time $t = 0$ instantaneously (adiabatically) the interval becomes opened, i.e., we replace the reflecting boundary by the absorbing one, and the external field is switched off.

At arbitrary t, $t > 0$, the PDF for the position of the nth particle has a similar structure as its initial PDF (2.38). It reads

$$p_{n:N}(x,t) = \frac{N!}{(n-1)!(N-n)!} f(x,t) \left[F(x,t)\right]^{n-1} [1 - F(x,t)]^{N-n}, \qquad (2.39)$$

where the time-dependent single-particle PDF $f(x,t)$ is given in Eq. (2.9). Regardless the two replacements: $f(x) \to f(x,t)$, $\int_0^x \mathrm{d}x' f(x') \to F(x,t)$, the tracer PDF (2.39) possesses exactly the same probabilistic interpretation in terms of noninteracting particles as its initial form (2.38). Now, the term that accounts for the number of particles to the left of x, namely $[F(x,t)]^{n-1}$, *must account also for the possibility that some of $(n-1)$ particles have already been absorbed by time t*. This fact is incorporated by a proper choice of the function $F(x,t)$. It is convenient to imagine that the absorbed

particle after the instant of the absorption resides forever in the trap located at $x = 0$, see Fig. 2.3. Therefore the probability $F(x, t)$ of finding a single noninteracting particle to the left of x is given by the sum of probabilities of two disjoint events:

$$F(x, t) = [1 - S(t)] + \int_0^x \mathrm{d}x' \, f(x', t), \qquad (2.40)$$

where $[1 - S(t)]$ is the probability that the single-diffusing particle is located inside the trap, while the second term on the right-hand side of Eq. (2.40) stands for the probability that the particle is found in $(0, x)$. Notice that, in Ref. [40], the PDF (2.39) has been derived analytically by integration of the exact solution of hierarchy of diffusion equations from Sec. 2.2.2. We shall not repeat the proof here.

Finally notice that the following equality holds:

$$f(x, t) = \frac{1}{N} \sum_{n=1}^{N} p_{n:N}(x, t), \qquad (2.41)$$

which can be proved by the direct summation of the expressions (2.39). In particular the above equation tells us that the density of particles for the system of N interacting particles is the same as that for the system of N noninteracting particles. This statement holds true for any collective quantity describing the interacting particles (that is such quantity that does not change after any permutation of labels).

2.2.4 First-passage properties

Survival probabilities

The presence of absorbing boundary implies that the PDF $p_{n:N}(x, t)$ of the nth tagged particle is no longer normalized to one for $t > 0$. The spatial integral of the PDF, i.e., the survival probability $S_{n:N}(t)$ of the nth tagged particle,

$$S_{n:N}(t) = \int_0^\infty \mathrm{d}x \, p_{n:N}(x, t), \qquad (2.42)$$

can be written as the sum of powers of the single-particle survival probability $S(t)$. It reads[5]

$$S_{n:N}(t) = n \binom{N}{n} [S(t)]^{N-n+1} \sum_{k=0}^{n-1} \frac{(-1)^k}{N - n + k + 1} \binom{n-1}{k} [S(t)]^k, \qquad (2.43)$$

To gain a better insight into the escape process in question, let us first examine the difference between the survival probabilities of the adjacent particles:

$$S_{(n+1):N}(t) - S_{n:N}(t) = \binom{N}{n} [S(t)]^{N-n} [1 - S(t)]^n. \qquad (2.44)$$

The difference is simply the probability that the particle No. n has already exited the interval and, simultaneously, the particle No. $(n+1)$ is still diffusing inside the interval. At the same time, the right-hand side by itself possesses a similar interpretation in terms of noninteracting particles. It equals the probability that exactly n of the initial number

---

[5]Main steps of the underlying calculation are following. We define the auxiliary function $B(x, t)$, $F(x, t) = 1 - B(x, t)$. Then we expand the term $[F(x, t)]^{n-1}$ in the tracer PDF (2.39) according to the binomial theorem into the sum of powers of B. Properties of the auxiliary function B ($f(x, t) = -\partial B / \partial x$, $B(0, t) = S(t)$, $B(\infty, t) = 0$) allows for a direct integration of each term of the emerging sum which yields Eq. (2.43).

N of noninteracting particles have already exited the interval by time t. Thus the mass transport out of the pore is not affected by the hard-core interaction. In particular, in the statistical sense, it will take the same time until all N particles escape from the pore regardless they interact or not (previously this fact has been observed in Monte Carlo simulations in Ref. [163]).

Several other observations are worth emphasizing. For instance, it follows from Eq. (2.44) that functions $S_{n:N}(t)$ are ordered as

$$0 \leq S_{1:N}(t) \leq S_{2:N}(t) \leq ... \leq S_{N:N}(t) \leq 1, \qquad (2.45)$$

where the equalities hold at $t = 0$, when all N particles are initially inside the pore (hence $S_{n:N}(0) = 1$ for all n), and in the limit $t \to \infty$ ($S_{n:N}(\infty) = 0$ for all n, c.f. Eq. (2.48) below). Each hard-core particle acts on the adjacent ones as a stochastically moving reflecting boundary. Effectively, the collisions between the particles induce entropic repulsive forces. For example, the exit of the rightmost particle is hindered by the remaining $(N-1)$ particles which greatly increases its survival probability $S_{N:N}(t)$. On the other hand, the leftmost particle is pushed by the remaining ones towards the absorbing boundary which significantly reduces its lifetime inside the interval. Thus the survival probability $S_{1:N}(t)$ rapidly decreases towards zero. However, as a direct consequence of Eq. (2.41) we obtain

$$S(t) = \frac{1}{N} \sum_{n=1}^{N} S_{n:N}(t) \qquad (2.46)$$

which relates the arithmetic mean of tagged particles' survival probabilities to the survival probability of the single-diffusing particle. Hence $S_{N:N}(t)$ cannot exceed $NS(t)$.

Above considerations manifest themselves most pronouncedly if we consider the time-asymptotic behavior of the survival probabilities. The main asymptotic term of the sum in Eq. (2.43) is given by the summand containing the lowest power of $S(t)$. It reads

$$S_{n:N}(t) = \frac{n}{(N-n+1)} \binom{N}{n} [S(t)]^{N-n+1} + O\left([S(t)]^{N-n+2}\right). \qquad (2.47)$$

Using the asymptotic behavior (2.13), we obtain

$$S_{n:N}(t) \sim \frac{n}{(N-n+1)} \binom{N}{n} \left[\frac{\langle \mathbf{X}(0) \rangle}{\sqrt{\pi D}}\right]^{N-n+1} t^{-(N-n+1)/2}, \qquad t \to \infty. \qquad (2.48)$$

Thus each survival probability tends to zero, i.e., each particle will certainly exit the interval. The decay exponent is determined by the difference $(N-n)$ which is nothing but the number of particles located to the right of the nth one. That is, regardless the actual value of N the survival probability of the rightmost particle decays to zero as $t^{-1/2}$, that of the second rightmost as t^{-1} etc. This can be understood on physical grounds. The survival probability of the rightmost particle decays exactly with the same dynamical exponent as $S(t)$ (cf. Eq. (2.13)). Indeed, after a "long enough" time it is highly probable that all other particles have already escaped from the interval and thus the rightmost particle behaves as a freely-diffusing one. The total number of particles N just quantifies the exact meaning of "long enough" leaving the dynamical exponent intact. Similarly for the nth particle: in the long-time limit, it is highly probable that all $(n-1)$ particles, which were initially to the left of the nth one, have already been absorbed. Thus, regardless the actual value of N, the nth particle behaves as if it was the leftmost one in the system of $(N-n)$ particles.

For a finite N, the exponent of the power-law decay $t^{-(N-n+1)/2}$ quantifies the effect of entropic repulsion among the particles. Further insight can be given after taking the

large-N limit in the above expressions. Let us now consider the large-N behavior of the survival probabilities for the rightmost and for the leftmost particle, respectively.

To obtain the asymptotic survival probability for the rightmost particle we define the standardizing constant

$$a_N = \frac{(NL)^2}{\pi D}.$$ (2.49)

After the standardization, the cumulative distribution function for the time of absorption of the rightmost particle converges to the Fréchet distribution with the parameter $\alpha = 1/2$ (cf. App. A):

$$\lim_{N\to\infty} \text{Prob}\left\{\frac{\mathbf{T}_{N:N}}{a_N} < t\right\} = \exp\left(-\frac{1}{\sqrt{t}}\right).$$ (2.50)

Hence for the survival probability we obtain

$$S_{N:N}(t) \sim 1 - \exp\left(-\frac{LN}{\sqrt{\pi Dt}}\right), \quad N \gg 1.$$ (2.51)

As a consequence of the entropic repulsion, the survival probability of the rightmost particle is almost unity on the time-scales shorter than $(NL)^2$.

Defining now

$$\tilde{a}_N = \frac{\pi D L^2}{4 N^2},$$ (2.52)

the following limit

$$\lim_{N\to\infty} \text{Prob}\left\{\frac{\mathbf{T}_{1:N}}{\tilde{a}_N} < t\right\} = 1 - \exp\left(-\sqrt{t}\right).$$ (2.53)

implies the large-N asymptotic representation of the survival probability of the leftmost particle:

$$S_{1:N}(t) \sim \exp\left(-\frac{N}{L}\sqrt{\frac{4Dt}{\pi}}\right), \quad N \gg 1.$$ (2.54)

The above equation depends on the combination N/L. In fact we can set $N = L\rho$, then the above result indicates that in the thermodynamic limit we can expect the exponential decay of survival probabilities of individual particles (instead of the power-law decay in the present finite-N case). This is indeed the case as we will demonstrate in Sec. 2.3.3 (see Eq. (2.86) for $n = 1$).

PDFs of absorption times

Due to the relative simplicity of the hard-core interaction, all quantities concerning the dynamics of interacting particles possess an interpretation in term of noninteracting ones. What is the interpretation of the survival probability $S_{n:N}(t)$? Instead of providing a rather lengthy explanation of the right-hand side of Eq. (2.43) it is easier to interpret the corresponding PDF $\phi_{n:N}(t)$ for the absorption time. The PDF is related to the survival probability as follows

$$\phi_{n:N}(t) = -\frac{\text{d}}{\text{d}t} S_{n:N}(t), \qquad S_{n:N}(t) = 1 - \int_0^t \text{d}t' \, \phi_{n:N}(t').$$ (2.55)

From Eq. (2.43), we obtain

$$\phi_{n:N}(t) = \frac{N!}{(n-1)!(N-n)!} \phi(t) \left[1 - S(t)\right]^{n-1} \left[S(t)\right]^{N-n},$$ (2.56)

where $\phi(t)$ is the PDF for the absorption time of a single noninteracting particle, cf. Eq. (2.14). As we have already mentioned, the overall mass transport properties are not influences by the hard-core interaction. Therefore the absorption time of the nth tracer is statistically equivalent to the time of the nth absorption event which occurs in the system of noninteracting particles. The PDF for the latter event appears on the right-hand side of Eq. (2.56) [137, 138]. Actually, several studies which deal with the order statistics of absorption times for noninteracting particles exist, see Refs. [137–147]. In particular, the present result (2.56) clearly demonstrates that any *one-dimensional* result concerning order statistics of first-passage times of noninteracting particles to a *single* absorbing boundary can be interpreted as the first-passage problem for the interacting particles. The generalization of this relationship to the case of *two* absorbing boundaries is established in the next chapter, see Eq. (3.32).

Let us now examine the existence of the moments of the PDF $\phi_{n:N}(t)$. It follows directly from Eq. (2.56) that the long-time tail of the PDF $\phi_{n:N}(t)$ is given by

$$\phi_{n:N}(t) \sim \frac{n}{2} \binom{N}{n} \left[\frac{\langle \mathbf{X}(0) \rangle}{\sqrt{\pi D}} \right]^{N-n+1} t^{-\frac{N-n+1}{2}-1}, \qquad t \to \infty. \qquad (2.57)$$

Consequently, the mean absorption time of the nth particle,

$$\langle \mathbf{T}_{n:N} \rangle = \int_0^\infty \mathrm{d}t \, t \phi_{n:N}(t), \qquad (2.58)$$

is infinite when $(N - n) \leq 2$ (i.e., for the rightmost and for the second rightmost particle). When $(N - n) > 2$, the integral (2.58) becomes finite regardless the actual value of N. Similarly, the second moment of the absorption time $\langle \mathbf{T}_{n:N}^2 \rangle$ exists only when $(N-n) > 3$ holds (i.e., for all particles except for the three rightmost ones). Notice that a similar conclusion for the mean first-passage time of the first of N noninteracting particles has been proved in Ref. [139]. In the present interacting picture, this mean first-passage time corresponds to the mean first-passage time of the leftmost particle (which is finite when $N > 3$).

The above analysis brings us to an interesting comparison between the escape process confined by the static and by the fluctuating reflecting boundaries, respectively. Considering the semi-infinite interval with the absorbing boundary at the origin, the survival probability $S(t)$ of the single-diffusing particle decays to zero as the power law (2.13) and the mean exit time is infinite. If we add the *static* reflecting boundary on the right of the single-diffusing particle, the diffusion will be confined to an interval of a finite length. Then the survival probability decays exponentially and, consequently, the mean exit time becomes finite [151]. Consider now our SFD model with $N = 2$. Then, as for the left particle, the right one plays the role of a moving reflection boundary. That is, the left particle diffuses within a finite interval of a fluctuating length. Contrary to the case of the static boundary, the survival probability of the left particle decays as $1/t$, and its mean exit time is infinite. It is interesting that the case $N = 3$ brings us to still another behavior of the leftmost particle. For this particle, the central particle again represents a moving boundary. This boundary itself diffuses and, moreover, it feels another moving boundary to the right of it. As a result of such right-hand confinement the escape process of the leftmost particle is accelerated, its mean exit time is finite, but the variance of the exit time still diverges. For a general N, the exit time of any nth tagged particle with $(N - n) \geq 4$ possesses both a finite mean value and a finite variance.

Let us now return to the mapping which has been developed in Sec. 2.2.2 where we have discussed the analogy between the SFD problem and the diffusion of a single representative particle in the N-dimensional space. Initially, the representative particle

departs from a general interior point in the N-dimensional wedge domain. The exit of the leftmost particle has been translated to the adsorption of the representative particle onto the $(N-1)$-dimensional absorption hyperplane. Then the representative particle continues to diffuse within this hyperplane until its motion is further restricted onto the $(N-2)$-dimensional absorption hyperplane, and so on. The function $S_{n:N}(t)$ equals the probability that, at time t, the motion of the representative particle has not been restricted onto the $(N-n+1)$-dimensional hyperplane, yet. That is, it still moves in some k-dimensional wedge, where $k \geq (N-n)$. Similarly, the difference $\left[S_{(n+1):N}(t) - S_{n:N}(t)\right]$ as given in Eq. (2.44) yields the probability that, at time t, the representative particle dwells in the interior of the $(N-n)$-dimensional wedge domain. On the whole, as a byproduct, we have solved a nontrivial problem concerning the geometrically restricted N-dimensional diffusion.

2.2.5   Tracer dynamics with absorption

Let us now discuss the dynamics of individual particles with the focus on the long-time asymptotic properties. We start with the long-time asymptotic behavior of tracer PDFs (2.39). The right-most particle is special. In the long-time limit it behaves in a similar way as the single-diffusing particle. In particular, for $n = N$, the binomial theorem yields

$$p_{N:N}(x,t) = N f(x,t) \left[1 + (N-1)S(t)\left(\int_0^x \mathrm{d}x' \frac{f(x',t)}{S(t)} - 1\right) + O\left(t^{-1}\right)\right], \qquad (2.59)$$

where the remaining $(N-2)$ terms of the binomial expansion vanish at least as $[S(t)]^2$. The integral in (2.59) has been estimated in Eq. (B.10). On the whole, we obtain

$$p_{N:N}(x,t) = N f(x,t) - N(N-1)\frac{\langle \mathbf{X}(0) \rangle^2}{2\pi(Dt)^2} x\, \mathrm{e}^{-x^2/2Dt} + O\left(t^{-5/2}\right). \qquad (2.60)$$

The above expression is written in a way which shows the main asymptotic behavior,

$$p_{N:N}(x,t) \sim N f(x,t), \qquad t \to \infty, \qquad (2.61)$$

and the first correction which is given by the second term in Eq. (2.60). The correction describes the relaxation towards the main asymptotics and it is negative.

We proceed to the long-time behavior of the nth particle with $n = 1, \ldots, (N-1)$. We start again with Eq. (2.39) and rearrange it into the form

$$p_{n:N}(x,t) = n\binom{N}{n}[S(t)]^{N-n} f(x,t)$$
$$\times \left[1 - S(t) + \int_0^x \mathrm{d}x' f(x',t)\right]^{n-1} \left[1 - \int_0^x \mathrm{d}x' \frac{f(x',t)}{S(t)}\right]^{N-n}. \qquad (2.62)$$

Then the first bracket is again expanded according to the binomial theorem, the second bracket is treated using Eq. (B.10). Using further Eq. (2.18), the main asymptotics assumes the form

$$p_{n:N}(x,t) \sim n\binom{N}{n}[S(t)]^{N-n+1}\frac{x}{2Dt}\mathrm{e}^{-(N-n+1)x^2/4Dt}, \qquad t \to \infty. \qquad (2.63)$$

If we introduce the *renormalized diffusion coefficient*,

$$D_n = \frac{D}{N-n+1}, \qquad (2.64)$$

an important conclusion emerges. On the right-hand side of Eq. (2.63), one recognizes the asymptotic single-particle PDF (2.19) conditioned on nonabsorption:

$$p_{n:N}(x,t) \sim \frac{n}{(N-n+1)} \binom{N}{n} [S(t)]^{N-n+1} f(x, D_n t \,|\, \mathbf{T} > t), \qquad t \to \infty. \qquad (2.65)$$

The only difference is that here time t is multiplied by the renormalized diffusion coefficient D_n instead of the "bare" single-particle diffusion coefficient D in Eq. (2.19). The initial order of the particle n controls in a decisive way the main asymptotics. The smaller the order n, the faster is the decay of the PDF (2.65) (for a given x). Consequently the sum in Eq. (2.41) is dominated by the PDF $p_{N:N}(x,t)$, which is just a different way how to comprehend the asymptotic relation (2.61).

Our next goal is the analysis of the mean positions of individual particles. For the rightmost particle, the calculation is based on Eq. (2.60). We obtain

$$\langle \mathbf{X}_{N:N}(t) \rangle = N \langle \mathbf{X}(t) \rangle - N(N-1) \frac{\langle \mathbf{X}(0) \rangle^2}{\sqrt{8\pi Dt}} + O\left(t^{-1}\right). \qquad (2.66)$$

The main asymptotic behavior is covered by the first term on the right hand side, that is, apart from the multiplication by N, the main asymptotics coincides with that for the single particle where we have $\langle \mathbf{X}(t) \rangle = \langle \mathbf{X}(0) \rangle$. The second term describes leading corrections.

The evaluation of asymptotic mean positions for all other particles is accomplished by integration of densities (2.65). This yields the main asymptotic behavior

$$\langle \mathbf{X}_{n:N}(t) \rangle \sim B_n \, t^{-(N-n)/2}, \quad n = 1, \ldots, N, \qquad (2.67)$$

with the prefactor

$$B_n = \frac{n}{(N-n+1)^{3/2}} \binom{N}{n} \frac{\langle \mathbf{X}(0) \rangle^{N-n+1}}{(\pi D)^{(N-n)/2}}. \qquad (2.68)$$

Thus the initial condition and the total number of particles enters the asymptotics only through the prefactor. Notice that the asymptotics for the nth particle for $n < N$, differs from that for the rightmost particle (and therefore also from that for the single particle), its mean position asymptotically approaches zero.

In a similar way, we readily obtain the second moments. The results are

$$\left\langle \mathbf{X}_{N:N}^2(t) \right\rangle \sim N \left\langle \mathbf{X}^2(t) \right\rangle - C_{N-1}, \qquad (2.69)$$

$$\left\langle \mathbf{X}_{n:N}^2(t) \right\rangle \sim C_n \, t^{-(N-n-1)/2}, \quad n = 1, \ldots, N-1, \qquad (2.70)$$

with the prefactors

$$C_n = \frac{4Dn}{(N-n+1)^2} \binom{N}{n} \left[\frac{\langle \mathbf{X}(0) \rangle}{\sqrt{\pi D}} \right]^{N-n+1}. \qquad (2.71)$$

For the rightmost particle, the main asymptotics is proportional to the second moment of the position of the noninteracting particle $\langle \mathbf{X}^2(t) \rangle$. Interestingly, for the second rightmost particle, the second moment converges to the constant C_{N-1} whereas, for $n < (N-1)$, the second moment decreases towards zero as the power law.

The first and the second moments for individual particles are illustrated in Fig. 2.4. After multiplying Eq. (2.41) by x^k and integrating, we get the relationship

$$\left\langle \mathbf{X}^k(t) \right\rangle = \frac{1}{N} \sum_{n=1}^{N} \left\langle \mathbf{X}_{n:N}^k(t) \right\rangle, \quad k = 0, 1, 2, \ldots \qquad (2.72)$$
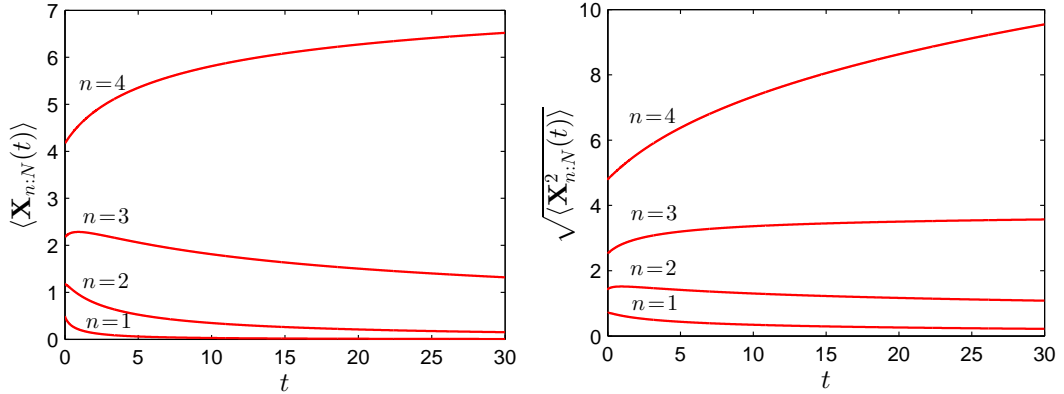
Figure 2.4: Mean positions (the left panel) and square roots of the second moments (the right panel) for individual particles in the system of $N = 4$ interacting particles. In the underlying single particle problem, we took $D = 1$ and the initial condition (2.10) with $L = 2$.

valid for any time. In the asymptotic domain, the main asymptotic of the left-hand side coincides with the $n = N$ term on the right-hand side. Differently speaking, the main asymptotics of the remaining terms in the sum is subdominant with respect to the main asymptotics of the $n = N$ term.

2.2.6   Tracer dynamics conditioned on nonabsorption

Being interested in the long-time dynamics of individual surviving particles, we introduce conditional PDFs

$$p_{n:N}(x, t \,|\, \mathbf{T}_{n:N} > t) = \frac{p_{n:N}(x, t)}{S_{n:N}(t)}. \tag{2.73}$$

In the long-time limit, the numerator is given in Eq. (2.65) and the denominator in Eq. (2.47). Thus in the long-time limit the fraction greatly simplifies. Dividing the asymptotic representation (2.65) by the leading term in Eq. (2.47) gives us the asymptotic relation

$$p_{n:N}(x, t \,|\, \mathbf{T}_{n:N} > t) \sim f(x, D_n t \,|\, \mathbf{T} > t), \qquad t \to \infty, \tag{2.74}$$

which on its right-hand side contains the Rayleigh distribution with the renormalized diffusion coefficient:

$$p_{n:N}(x, t \,|\, \mathbf{T}_{n:N} > t) \sim \frac{x}{2 D_n t}\, \mathrm{e}^{-x^2/4 D_n t}, \qquad t \to \infty. \tag{2.75}$$

This result is remarkable for its simplicity. The asymptotic conditioned dynamics of the nth tracer is the same as the dynamics of a single-diffusing particle with the diffusion coefficients $D_n = D/(N - n + 1)$. In other words, the only implication of the hard-core interaction is the renormalization of the diffusion coefficient. The left-most particle diffuses with the smallest effective diffusion coefficients $D_1 = D/N$. On the other hand the right-most particle has the same effective diffusion coefficient as a single-diffusing particle, $D_N = D$.

The above asymptotic relation means that also the moments of the conditioned dynamics are (except of the value of the diffusion coefficient) simply the moments of the single-diffusing particle. More precisely, using Eq. (2.75), we get

$$\langle \mathbf{X}_{n:N}(t) \rangle_{\mathbf{T}_{n:N} > t} \sim \sqrt{\pi D_n t}, \tag{2.76}$$

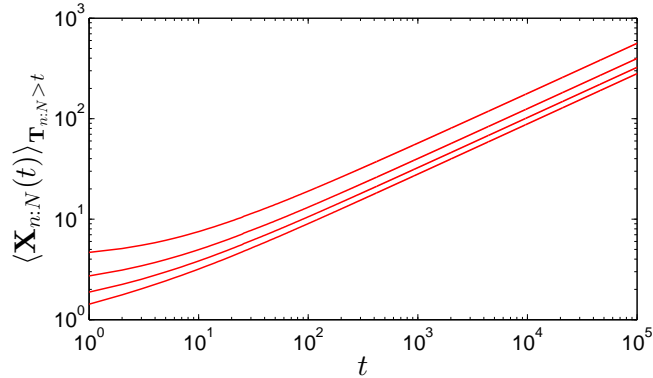$$\left\langle \mathbf{X}_{n:N}^2(t) \right\rangle_{\mathbf{T}_{n:N} > t} \sim 4 D_n t. \tag{2.77}$$

34

Figure 2.5: The double-logarithmic plot of conditioned mean positions $\langle \mathbf{X}_{n:N}(t) \rangle_{\mathbf{T}_{n:N}>t}$ of the individual particles in the system of $N=4$ interacting particles. The curves are obtained by the numerical integration using exact PDFs (2.73) with the parameters $L=2$ and $D=1$. Inequalities $\langle \mathbf{X}_{1:4}(t) \rangle_{\mathbf{T}_{1:4}>t} < ... < \langle \mathbf{X}_{4:4}(t) \rangle_{\mathbf{T}_{4:4}>t}$ hold for all $t \geq 0$, hence the curves never cross. The long-time asymptotic behavior does not depend on the initial conditions and it is given by Eq. (2.76).

Comparing the conditioned dynamics in the system with and without interaction, the interaction *does not* imply new n-dependent dynamical exponents which was the case in the unconditioned dynamics, cf. Eqs. (2.67), (2.69), and (2.70).

Finally, notice that in the present conditioned description there exists no simple relationship similar to Eq. (2.72). The N-average of conditioned kth moments is no more equal to the kth conditioned moment for the single-particle diffusion, i.e.,

$$\left\langle \mathbf{X}^k(t) \right\rangle_{\mathbf{T}>t} \neq \frac{1}{N} \sum_{n=1}^{N} \left\langle \mathbf{X}_{n:N}^k(t) \right\rangle_{\mathbf{T}_{n:N}>t}. \tag{2.78}$$

The equivalence of collective properties of the system of interacting particles and of the system of noninteracting ones no longer holds when the conditioned dynamics in both cases is assumed.

2.3   Thermodynamic limit

We now wish to focus on the dynamics of the tracer in a system of infinite number of particles. We assume that initially (for $t < 0$) the particles are distributed randomly on the half-line with a constant (mean) density ρ. At the initial instant $t = 0$ we activate the absorbing boundary at the origin. Then, for $t > 0$, the SFD system evolves in time and we are again interested in the first-passage properties and in the dynamics of the nth tagged particle.

2.3.1   Evolution of density profile

The mean density of particles $\rho(x,t)$ as the function of x and t (the density profile at t) satisfies the diffusion equation (2.5) subject to the absorbing boundary condition $\rho(0,t) = 0$, and to the initial condition: $\rho(x,0) = \rho$ for $x \geq 0$. We can derive the solution of this initial-boundary value problem by the integration of the product of the Green function (2.8) and the step initial condition over all values of y. The resulting density profile reads

$$\rho(x,t) = \rho \operatorname{erf}\left(\frac{x}{\sqrt{4Dt}}\right), \qquad x, t \geq 0. \tag{2.79}$$

Spatial derivative of $\rho(x,t)$, $D\partial\rho/\partial x$, evaluated at $x = 0$ gives us the mean particle current at $x = 0$. The integral of this current over the time interval $(0,t)$ yields the mean number of particles that have left the interval $(0,\infty)$ by time t. Explicitly, the mean number of absorbed particles is given by

$$\langle \mathbf{N}_{\mathrm{abs}}(t) \rangle = \rho \sqrt{\frac{4Dt}{\pi}}. \tag{2.80}$$

In the following analysis, the mean number of absorbed particles $\langle \mathbf{N}_{\mathrm{abs}}(t) \rangle$ and the mean number of particles located in $(0,x)$, i.e. $\int_0^x \mathrm{d}x'\rho(x',t)$, will play a similar role as probabilities $[1 - S(t)]$, $\int_0^x \mathrm{d}x' f(x',t)$ play in the finite-N case. Namely, the both quantities $\langle \mathbf{N}_{\mathrm{abs}}(t) \rangle$, $\int_0^x \mathrm{d}x'\rho(x',t)$, will be employed in order-statistics-like arguments leading to the PDF of the nth tagged particle.

2.3.2   PDF of a tagged particle

Similarly to the previous finite-N case, the analysis is based on the exact PDF for the position of the nth particle. The analytical expression which, in the present context, replaces the formula (2.39) reads

$$p_n(x,t) = \frac{\partial\mu(x,t)}{\partial x} \frac{[\mu(x,t)]^{n-1}}{(n-1)!} \, \mathrm{e}^{-\mu(x,t)}, \tag{2.81}$$

where

$$\mu(x,t) = \rho \left[\sqrt{\frac{4Dt}{\pi}} + \int_0^x \mathrm{d}y \, \mathrm{erf}\left(\frac{y}{\sqrt{4Dt}}\right) \right]. \tag{2.82}$$

Notice a straightforward probabilistic interpretation of these formulas. The first term on the right-hand side of Eq. (2.82), $\rho\sqrt{4Dt/\pi}$, is simply the mean number of absorbed particles $\langle \mathbf{N}_{\mathrm{abs}}(t) \rangle$ as given in Eq, (2.80). The second term on the right-hand side represents the mean number of particles which are, at time t, located in the space interval $(0,x)$. Hence, at time t, $\mu(x,t)$ stands for *the mean number of particles located to the left of the coordinate x, including those which were absorbed.* In Eq. (2.81) one recognizes the probability $(\partial\mu/\partial x)\,\mathrm{d}x$ of finding a noninteracting particle in the interval $(x, x + \mathrm{d}x)$ multiplied by the probability that there are $(n-1)$ particles to the left of x (including those already absorbed by the boundary).

The formal derivation of Eq. (2.81) from Eq. (2.39) proceeds as follows. At the initial time we assume that N particles are homogeneously distributed within a finite spatial interval $(0,L)$. For a large L, the probability of finding a single particle to the right of x behaves as

$$\int_x^\infty \mathrm{d}x' \int_0^L \frac{\mathrm{d}y}{L} f(x',t|y,0) \sim 1 - \frac{1}{L}\frac{\mu(x,t)}{\rho}, \quad L \to \infty, \tag{2.83}$$

where $\rho = N/L$. We insert this estimation into Eq. (2.39). The final result (2.81) follows after performing the thermodynamic limit: $L \to \infty$, $N \to \infty$, and ρ is fixed. Notably, the passage from Eq. (2.39) to Eq. (2.81) is similar in spirit to the well known passage from the binomial to the Poisson distribution (the law of rare events [164]). Actually, this analogy is more than just a formal curiosity. After the discussion of PDFs for times of absorption it will become clear that (at given t) the tracer PDF (2.81) is nothing but the PDF for the position of the nth point of the spatial inhomogeneous Poisson process with the x-dependent rate $\rho(x,t)$ and with a stochastic "initial condition" at $x = 0$.

2.3.3 First-passage properties

Survival probabilities

In the thermodynamic limit, the survival probability of the nth tagged particle is obtained by the spatial integration of the PDF (2.81). The per partes evaluation of the integral in question yields the recursion relation for the survival probability $S_n(t)$:

$$S_{n+1}(t) = S_n(t) + \mathrm{e}^{-\mu(0,t)} \frac{[\mu(0,t)]^n}{n!}, \tag{2.84}$$

with the boundary term given by $S_1(t) = \mathrm{e}^{-\mu(0,t)}$. Hence, the survival probability of the nth particle reads

$$S_n(t) = \mathrm{e}^{-\mu(0,t)} \sum_{k=0}^{n-1} \frac{[\mu(0,t)]^k}{k!}. \tag{2.85}$$

The long-time asymptotic behavior of $S_n(t)$ is controlled by the term with the highest power of $\mu(0,t)$:

$$S_n(t) \sim \frac{\left(\rho\sqrt{\frac{4Dt}{\pi}}\right)^{n-1}}{(n-1)!} \mathrm{e}^{-\rho\sqrt{4Dt/\pi}}, \qquad t \to \infty. \tag{2.86}$$

Thus, for any n, the survival probability decays with time as a stretched exponential, in contrast to its power-law decay (2.48) in the finite-N case. The particle label modifies the asymptotic behavior just through the polynomial prefactor. For $n = 1$ the stretched exponential has already been anticipated in the large-N behavior (2.54) of $S_{1:N}(t)$.

PDFs of absorption times

The stochastic process $\mathbf{N}_{\mathrm{abs}}(t)$ of absorption of noninteracting particles is the Poisson process with the mean number of points in $(0,t)$ given by Eq. (2.80). The mean number of points grows with time as $t^{1/2}$, whereas the rate of the Poisson process, i.e. the time derivative of its mean, decreases as $t^{-1/2}$. The same holds true also for interacting particles, since the overall mass transport out of the interval is not affected by the hard-core interaction. Thus the PDF for the time of absorption of the nth particle $\phi_n(t)$, $\phi_n(t) = -\mathrm{d}S_n/\mathrm{d}t$, equals the PDF for the time of occurrence of the nth Poisson point:

$$\phi_n(t) = \left[\frac{\mathrm{d}\langle \mathbf{N}_{\mathrm{abs}}(t)\rangle}{\mathrm{d}t}\right] \frac{[\langle \mathbf{N}_{\mathrm{abs}}(t)\rangle]^{n-1}}{(n-1)!} \mathrm{e}^{-\langle \mathbf{N}_{\mathrm{abs}}(t)\rangle}. \tag{2.87}$$

This fact can also be verified directly by taking the time derivative of Eq. (2.85).

In contrast to the finite-N case, now, all moments of the above distribution,

$$\left\langle \mathbf{T}_n^k \right\rangle = \int_0^\infty \mathrm{d}t\, t^k \phi_n(t), \tag{2.88}$$

are finite and can be given in a closed form. For any k, we have

$$\left\langle \mathbf{T}_n^k \right\rangle = \frac{(2k+n-1)!}{(n-1)!} \left(\frac{\pi}{4D\rho^2}\right)^k. \tag{2.89}$$

The moments decrease with increasing the initial density of particles, and, they increase with the particle order n. The mean time to absorption of the nth particle grows with n as n^2:

$$\langle \mathbf{T}_n \rangle = (n+1)n \left(\frac{\pi}{4D\rho^2}\right). \tag{2.90}$$

The variance of the time to absorption of the nth particle is proportional to n^3:

$$\left\langle [\mathbf{T}_n - \langle \mathbf{T}_n \rangle]^2 \right\rangle = 2(2n+3)(n+1)n \left(\frac{\pi}{4D\rho^2} \right)^2. \tag{2.91}$$

Hence, the relative deviation from the mean decreases as $n^{-1/2}$ for large n.

The Poisson process is omnipresent in the current semi-infinite system with the density profile $\rho(x,t)$. Let us stop the time at the instant t and let us look at the statistical properties of the *spatial* point process that describes the distribution of particles along the half-line $x \in [0, \infty)$. It is convenient to picture the absorbing boundary as the *trap* located at the point $x = 0$. The overall number of particles located inside the trap at time t, $\mathbf{N}_{\text{abs}}(t)$, is a random number drawn from the Poisson distribution described above. This number represents the *initial condition* for the spatial point process on the half-line $x \in (0, \infty)$. Conditioned on the initial state, the number of points located in $(0, x)$ is given by the Poisson distribution with mean value $\int_0^x \mathrm{d}x' \, \rho(x', t)$. Correspondingly, the tracer PDF (2.81) is nothing but the PDF for the nth point of the spatial inhomogeneous Poisson process characterized by the rate $\rho(x,t)$ and with the initial condition drawn from the Poisson distribution with the mean $\langle \mathbf{N}_{\text{abs}}(t) \rangle$. In symbols, we have

$$p_n(x,t) = \rho(x,t) \sum_{k=0}^{n-1} \frac{\left[\int_0^x \mathrm{d}x' \rho(x', t) \right]^{n-1-k}}{(n-1-k)!} \, \mathrm{e}^{-\int_0^x \mathrm{d}x' \, \rho(x',t)} \frac{\left[\langle \mathbf{N}_{\text{abs}}(t) \rangle \right]^k}{k!} \, \mathrm{e}^{-\langle \mathbf{N}_{\text{abs}}(t) \rangle}. \tag{2.92}$$

2.3.4 Tracer dynamics with absorption

We are again primarily interested in the long-time dynamics of the tracer. After employing an expansion of the integral of the error function in (2.82), the main asymptotics of the PDF (2.81) reads

$$p_n(x,t) \sim \frac{\left(\rho \sqrt{\frac{4Dt}{\pi}} \right)^{n-1}}{(n-1)!} \, \mathrm{e}^{-\rho \sqrt{4Dt/\pi}} \left[\frac{\rho \, x}{\sqrt{\pi Dt}} \, \mathrm{e}^{-\rho x^2 / \sqrt{4\pi Dt}} \right], \qquad t \to \infty. \tag{2.93}$$

The squared bracket encloses the Rayleigh distribution, and it is multiplied by the main asymptotic term of the survival probability $S_n(t)$, cf. Eq. (2.86). That is, in the long-time limit we have

$$p_n(x,t) \sim S_n(t) \left[\frac{\rho \, x}{\sqrt{\pi Dt}} \mathrm{e}^{-\rho x^2 / \sqrt{4\pi Dt}} \right], \qquad t \to \infty. \tag{2.94}$$

As for the first two moments of the tracer position we get the asymptotic formulas

$$\langle \mathbf{X}_n(t) \rangle \sim \frac{\left(\rho \sqrt{\frac{4Dt}{\pi}} \right)^{n-1}}{(n-1)!} \sqrt{\frac{\sqrt{\pi^3 Dt}}{2\rho}} \, \mathrm{e}^{-\rho \sqrt{4Dt/\pi}}, \tag{2.95}$$

$$\left\langle \mathbf{X}_n^2(t) \right\rangle \sim \frac{\left(\rho \sqrt{\frac{4Dt}{\pi}} \right)^{n-1}}{(n-1)!} \sqrt{\frac{4\pi Dt}{\rho^2}} \, \mathrm{e}^{-\rho \sqrt{4Dt/\pi}}. \tag{2.96}$$

Contrary to the finite-N case (see Eqs. (2.66), (2.67), (2.69), and (2.70)), the moments vanish for any n. The decrease is controlled by the stretched exponential which is multiplied by the n-dependent power of time.

2.3.5 Tracer dynamics conditioned on nonabsorption

Let us now focus on the dynamics of the tracer which has survived by time t. Its PDF is given by

$$p_n(x, t | \mathbf{T}_n > t) = \frac{p_n(x, t)}{S_n(t)}. \tag{2.97}$$

The long-time behavior of the above fraction follows from the asymptotic representation of the PDF $p_n(x, t)$ given in Eq. (2.94). Hence again we obtain the Rayleigh distribution:

$$p_n(x, t | \mathbf{T}_n > t) \sim \frac{x}{2D_{1/2}\sqrt{t}} \, e^{-x^2/4D_{1/2}\sqrt{t}}, \qquad t \to \infty, \tag{2.98}$$

where we have introduced the fractional-order diffusion coefficient

$$D_{1/2} = \sqrt{\frac{\pi D}{4\rho^2}}. \tag{2.99}$$

The asymptotic form (2.98) should be contrasted against the single-particle PDF (2.19), and the tracer PDF (2.74) for the finite-N case. As compared to the two scenarios, in the present thermodynamic system the conditioned dynamics of the tracer is slowed down. The first two moments of the PDF (2.98) are

$$\langle \mathbf{X}_n(t) \rangle_{\mathbf{T}_n > t} \sim \sqrt{\pi D_{1/2}\sqrt{t}}, \tag{2.100}$$

$$\left\langle \mathbf{X}_n^2(t) \right\rangle_{\mathbf{T}_n > t} \sim 4D_{1/2}\sqrt{t}. \tag{2.101}$$

Thus the average position of the tracer increases as $t^{1/4}$ in contrast to $t^{1/2}$-law as observed for a finite N (cf. Eq. (2.76)). The second moment grows as $t^{1/2}$ and hence the tracer dynamics is subdiffusive.

Interestingly enough, the diffusivity $D_{1/2}$ is different as compared to the diffusivity (1.34) obtained in a homogeneous system without the absorbing boundary. As it was pointed out in Refs. [61, 128], the diffusivity is sensitive to the way the system is prepared. In Ref. [128] it has been demonstrated that $D_{1/2}$ depends on initial conditions. In fact our result (2.99) indicates that the diffusivity also depends on boundary conditions used.

2.4 Summarizing remarks

Let us now briefly interlink different aspects of the dynamics of the nth tagged particle which were derived in the present chapter.

In the finite-N case the following overall picture emerges. Due to the hard-core repulsion, the particle which possesses a right-hand neighbor feels the (moving) reflecting barrier on the right. In the long-time limit, the barrier significantly restricts its motion, it reflects the right-moving paths and hence increases the number of left-moving paths. This left-pushing tendency is illustrated by the asymptotic formulas (2.67), (2.69), (2.70) describing the dynamics of the position and by Eq. (2.48) for the survival probability of the tagged particle. The mean position, the mean squared displacement and the survival probability of the tracer decay algebraically in time with the dynamical exponents which depend on the number of particles located to the right of it. The exponents quantify the effect of the interparticle repulsion. Of course, the rightmost particle has no right-hand neighbor and hence it behaves differently as compared to all other particles. In the transient regime, its left-hand neighbors still exist and the first particle is pushed to the right (see Fig. 2.4). In the long-time asymptotic regime,

all other particles have already disappeared and the first one simply undergoes the free diffusion. The conditioning on nonabsorption removes a part of the left-moving trajectories from the unconditioned ensemble. Hence it imposes, effectively, the right-oriented drift. Surprisingly enough, the conditioning significantly reduces the effect of the hard-core interaction. The cooperative impact of the both tendencies is articulated by asymptotic formulas (2.76), (2.77). The conditioned mean position of the tracer grows as $t^{1/2}$ regardless its order. The interparticle repulsion manifests itself only through the order-dependent tracer diffusion coefficient $D_n = D/(N - n + 1)$. Thus, loosely speaking, the closer the relative particle position to the boundary the less mobile should that particle be in order to survive for a long time.

The above reasoning holds for the system which initially contains a finite number of particles. In the thermodynamic limit, i.e., assuming initially an infinite number of particles randomly distributed along a half-line with a constant mean density ρ, the long-time dynamics of a tracer is rather different. The new features are based on a simple observation that, for any tracer, there is infinite number of particles to the right of it. This implies the n-independent *exponential* damping of the unconditioned moments (2.95), (2.96) and of the survival probability (2.86). In all asymptotic laws, the initial order of the tracer appears only in the algebraic pre-exponential factor. The conditioned dynamics of the tracer is subdiffusive and independent of n (see Eqs. (2.98), (2.100), and (2.101)). Also in the present infinite-N case, the conditioning on nonabsorption removes a part of the left-moving trajectories from the unconditioned ensemble. However, the emerging right-oriented drift scales with time as $t^{1/4}$ (cf. Eq. (2.95)) in contrast to its $t^{1/2}$ scaling for the finite-N case (see Eq. (2.76) and also Eq. (2.20) for the single-diffusing particle). Notice that the behavior of conditioned second moments in the two settings is in parallel to what has been observed in the SFD without the absorbing boundary. Namely, for a finite N, Aslangul has shown (see Sec. 1.3) that, in the long-time limit, the tracer diffusion is normal with the effective diffusion coefficient dependent both on N and on n. On the other hand, for an infinite N, one observes an anomalous diffusion and no n-dependence of the diffusivity. The present chapter detects the same features in the SFD with an absorbing boundary. However, there are important differences. First, in the present setting the renormalized diffusion coefficients are given by the simple closed expression and they decay as $1/N$ for any fixed n and N large. Second, the generalized diffusion coefficient $D_{1/2}$ derived for the semi-infinite system differs from that for the SFD on an infinite line which exemplifies the long-lasting memory effects presented in the model.

Open questions. Among many possibilities, there exists one interesting generalization of the present setting. Namely, assume that only the nth tracer is absorbed by the boundary at the origin, whereas all other particles diffuse freely on the whole real line. This problem can be readily reformulated as the order-statistics-like problem for noninteracting particles. However, despite its simple formulation, the problem *still lacks an exact solution.* It has been studied by approximative and numerical methods in Refs. [59,147]. For the finite-N case discussed in Ref. [147] the survival probability of the nth tracer decays algebraically in the long-time limit, $S_{n:N}(t) \sim t^{-\beta_{n:N}}$, the decay exponents being different from those obtained in Eq. (2.48). The infinite-N case, i.e., the system in the thermodynamic limit, has been discussed in Ref. [59] in connection to a first-passage time density of the fractional Brownian motion.

3. First-passage properties of a tracer in a finite interval
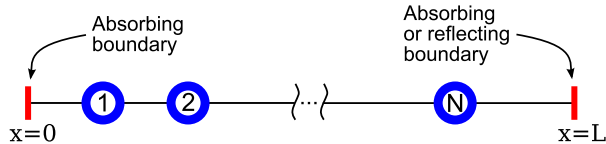
3.1 Definition of the model

Figure 3.1: Schematic illustration of the finite interval containing N particles. The left boundary is absorbing. The right boundary is either absorbing (Sec. 3.2) or reflecting (Sec. 3.3).

In the present chapter the diffusion of hard-core interacting Brownian particles in a finite one-dimensional interval will be discussed. We consider two types of boundary conditions and two types of initial conditions. The left boundary of the interval is always absorbing, the right boundary is either absorbing (Sec. 3.2) or reflecting (Sec. 3.3). The chapter is primarily based on Ref. [41].

Firstly, we assume that initially (at $t = 0$) N particles are distributed randomly in the interval $(0, L)$. During the time evolution ($t > 0$), each particle diffuses with the same diffusion constant D. The particles cannot enter the interval from the outside and they are allowed to leave it only through the absorbing boundary. Again, at initial time $t = 0$, we label the particles according to ordering of their positions from the left to the right (cf. Fig. 3.1). Hence initially we have

$$0 < \mathbf{X}_{1:N}(0) < \mathbf{X}_{2:N}(0) < \ldots < \mathbf{X}_{N:N}(0) < L, \tag{3.1}$$

The hard-core interaction guarantees that the initial ordering of particles is conserved over time. When the right boundary is reflecting then, similarly as in the semi-infinite case studied in Chap. 2, the particle No. 1 is the first one that might be absorbed. It is only after this event that the particle No. 2 can approach the origin and be absorbed. Hence when the right boundary is reflecting, the (random) times of absorption are ordered as

$$0 < \mathbf{T}_{1:N} < \mathbf{T}_{2:N} < \ldots < \mathbf{T}_{N:N} < \infty, \tag{3.2}$$

as it is the case in the semi-infinite setting, cf. Eq. (2.2). When the right boundary is *absorbing* the above ordering breaks down. In this case it is intuitively expected that an exceptionally long absorption time is exhibited by the central tracer ($n \approx N/2$), whereas the leftmost and the rightmost particles will be absorbed among the first ones.

The second initial condition discussed in the present chapter is the following. We consider the interval $(0, L)$ initially occupied by a *random* number of particles but with the constant mean density ρ. The diffusion of the tracer in the interval with such an initial condition can be modeled as follows. We imagine that for $t < 0$ the interval $(0, L)$ belongs to the whole real line on which the particles are distributed randomly with the uniform mean density ρ. Subsequently, at $t = 0$, perfectly absorbing traps are activated at $x = 0$ and $x = L$. At the instant of the activation, the interval $(0, L)$ contains N particles, N being a random number with the mean value equal to ρL. The probability that the initial number of particles equals N is given by the Poisson distribution:

$$P(N) = \frac{(\rho L)^N}{N!} \, \mathrm{e}^{-\rho L}. \tag{3.3}$$

After the activation of the traps, i.e., for $t > 0$, the particles diffuse within the finite interval $(0, L)$ which is decoupled from the line by the absorbing boundaries at $x = 0$ and $x = L$. Also in this case if a particle hits an absorbing boundary, it leaves the interval and will never return. This initial condition is physically appealing for the SFD on the interval of a random length (Sec. 3.2.3). An analogous picture emerges when the right boundary is reflecting.

The important part of Chap. 2 has been devoted to the thermodynamic limit in the semi-infinite system ($N \to \infty$, $L \to \infty$, and $\rho = N/L$ is fixed). Presently the thermodynamic limit is trivial. When the limit is performed while n is kept constant, i.e., $n \ll N$, the nth tracer looses an information about the right boundary and its dynamics becomes equivalent to that of the tracer diffusing in the semi-infinite interval with the constant initial density of particles, cf. Sec. 2.3. When the thermodynamic limit is performed e.g. for the central tracer, i.e., when $n \propto N$, the tracer looses an information about both boundaries and we recover the classical SFD on an infinite line discussed in the introductory Sec. 1.2. However, what will be studied in the present chapter is the behavior of first-passage properties for the system *approaching* the thermodynamic limit, i.e, we will find how the time of absorption of an individual tracer depends on N and L when N and L are large but still finite.

3.2 Both boundaries are absorbing

3.2.1 Single noninteracting particle

Let us now turn to the case when the both boundaries are absorbing. Now, the single-particle diffusion equation (2.5) is supplemented with absorbing boundary conditions: $f(0, t) = f(L, t) = 0$. Below we summarize essential properties of the single-particle dynamics which we will further contrast against the behavior of a tagged particle in the system with interaction. For a more thorough treatment of the single-particle problem including all derivations we refer see Refs. [151, 165].

Suppose that the particle starts its Brownian motion from the coordinate y, $y \in (0, L)$. What is the mean time before it hits any of the boundaries? This mean exit time, or mean first-passage time (MFPT) to any of the boundaries, is proportional to the product of initial distanced from the both boundaries. More precisely, it is given by

$$\langle \mathbf{T}(y) \rangle = \frac{L^2}{2D} \left(\frac{y}{L} \right) \left(1 - \frac{y}{L} \right). \tag{3.4}$$

Notice that for initial positions located in vicinity of one of the boundaries the mean exit time grows linearly with L. Whereas for initial positions located in the interior of the interval the MFPT increases as L^2. When the initial position of the particle is drawn from the homogeneous distribution, its MFPT averaged over all possible initial coordinates reads

$$\langle \mathbf{T} \rangle = \int_0^L \frac{\mathrm{d}y}{L} \langle \mathbf{T}(y) \rangle = \frac{L^2}{12D}. \tag{3.5}$$

Eq. (3.5) has a generic scaling form "(length)^2/(time) = constant" which we could anticipate from the time-dependence of the mean squared displacement of a free Brownian particle.

For absorbing boundary conditions, $f(0, t) = f(L, t) = 0$, and for the random initial condition $f(x, 0) = 1/L$, $x \in (0, L)$, the solution of the diffusion equation can be given as the eigenfunction expansion

$$f(x, t) = \frac{4}{\pi L} \sum_{k=0}^{\infty} \frac{1}{2k+1} \sin \left[\frac{\pi}{L}(2k+1)x \right] \exp \left\{ - \left[\frac{\pi}{L}(2k+1) \right]^2 Dt \right\}. \tag{3.6}$$
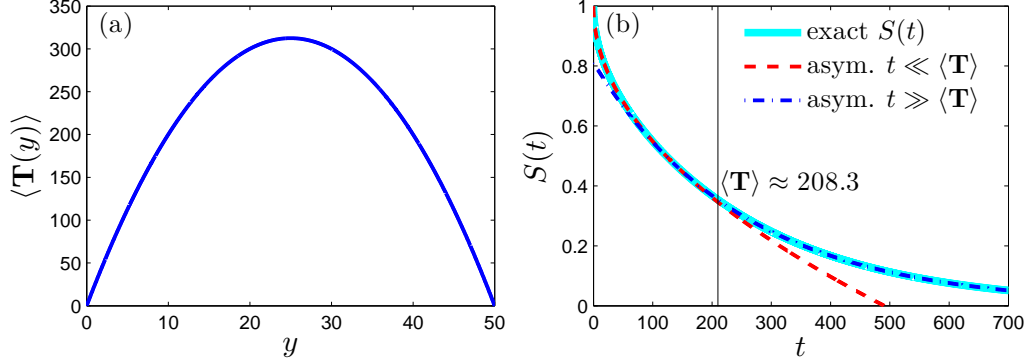
Figure 3.2: First-passage properties of a single particle for $L = 50$, $D = 1$. Panel (a) shows the MFPT (3.4) against the initial position of the particle. Panel (b) depicts the exact survival probability (3.7) (the solid line), the long-time asymptotic representation (3.9) (the dot-dashed line), and the short-time asymptotic representation (3.11) (the dashed line). Note an excellent agreement of asymptotic expressions with the exact curve even for $t \approx \langle \mathbf{T} \rangle$. The MFPT $\langle \mathbf{T} \rangle$ is given by Eq. (3.5).

The survival probability of the single noninteracting particle, $S(t)$, is given by the spatial integral of the PDF $f(x,t)$ over the whole interval (cf. Eq. (2.11)):

$$S(t) = \frac{8}{\pi^2} \sum_{k=0}^{\infty} \frac{1}{(2k+1)^2} \exp\left\{ -\left[\frac{\pi}{L}(2k+1) \right]^2 Dt \right\}. \tag{3.7}$$

The survival probability can related with the PDF for the time of absorption $\phi(t)$:

$$S(t) = 1 - \int_0^t \mathrm{d}t'\, \phi(t'), \quad \text{hence} \quad \phi(t) = -\frac{\mathrm{d}}{\mathrm{d}t} S(t). \tag{3.8}$$

For times t larger than the MFPT $\langle \mathbf{T} \rangle$ both these functions vanish exponentially fast:

$$S(t) \sim \frac{8}{\pi^2} \exp\left[-\left(\frac{\pi}{L} \right)^2 Dt \right], \qquad t \gg \langle \mathbf{T} \rangle \tag{3.9}$$

$$\phi(t) \sim \frac{8D}{L^2} \exp\left[-\left(\frac{\pi}{L} \right)^2 Dt \right], \qquad t \gg \langle \mathbf{T} \rangle. \tag{3.10}$$

The short-time asymptotic behavior can be inferred from the long-time one by the Poisson summation formula [166]. For times t shorter than MFPT we have

$$S(t) \sim 1 - \frac{4}{L}\sqrt{\frac{Dt}{\pi}}, \qquad t \ll \langle \mathbf{T} \rangle, \tag{3.11}$$

$$\phi(t) \sim \frac{2}{L}\sqrt{\frac{D}{\pi t}}, \qquad t \ll \langle \mathbf{T} \rangle. \tag{3.12}$$

The above asymptotic representations of the survival probability $S(t)$ are compared with the exact expression (3.7) in Fig. 3.2 (b).

3.2.2 Fixed initial number of interacting particles

PDF of a tagged particle

When the initial number of interacting particles equals to N, one can derive the PDF for the position of the nth particle along the same lines as in the case of one absorbing

boundary, cf. Eq. (2.39). The resulting PDF has the same form (and more importantly a similar interpretation in terms of noninteracting particles) as its counterpart (2.39). That is, also in the present case with two absorbing boundaries, we obtain

$$p_{n:N}(x,t) = \frac{N!}{(n-1)!(N-n)!} f(x,t) \left[F(x,t)\right]^{n-1} [1 - F(x,t)]^{N-n}, \tag{3.13}$$

where, now, the single-particle PDF $f(x,t)$ is given in Eq. (3.6), and also the probability $F(x,t)$ to find a noninteracting particle to the left of x, $x \in [0, L]$ is slightly modified as compared to Eq. (2.40). Now $F(x,t)$ is given by

$$F(x,t) = \frac{1}{2} \left[1 - S(t)\right] + \int_0^x \mathrm{d}x' f(x',t). \tag{3.14}$$

Eq. (3.14) formally differs from the corresponding Eq. (2.40) by the first term on the right-hand side. This term gives us the probability that a noninteracting particle is trapped by the left boundary before t. Since the initial condition $f(x,0)$ is uniform, the present case is left-right symmetric, i.e., the probability that the single noninteracting particle is trapped by the left boundary is equal to the probability that the particle is trapped by the right boundary. Both these probabilities are equal to $[1 - S(t)]/2$, where the single-particle survival probability is given in Eq. (3.7) (the generalization to the asymmetric initial condition is straightforward).

Survival probabilities

The probability that the nth particle has not touched an absorbing boundary by time t, i.e., its survival probability, is given by the spatial integral

$$S_{n:N}(t) = \int_0^L \mathrm{d}x \, p_{n:N}(x,t). \tag{3.15}$$

The integral can be expressed in terms of the probability $F(x,t)$ evaluated at boundary points of the interval. We obtain[1]

$$S_{n:N}(t) = n\binom{N}{n} \sum_{k=0}^{n-1} \frac{(-1)^k}{N-n+k+1} \binom{n-1}{k} \\ \times \left\{ [1 - F(0,t)]^{N-n+k+1} - [1 - F(L,t)]^{N-n+k+1} \right\}, \tag{3.16}$$

where the expressions in squared brackets read

$$1 - F(0,t) = \frac{1}{2} \left[1 + S(t)\right], \quad 1 - F(L,t) = \frac{1}{2} \left[1 - S(t)\right]. \tag{3.17}$$

Hence the survival probability $S_{n:N}(t)$ is again expressed solely in terms of the single-particle survival probability $S(t)$ which is given by Eq. (3.7).

In the long-time limit, the leading term of sum (3.16) reads

$$S_{n:N}(t) \sim \frac{n}{2^{N-1}} \binom{N}{n} S(t), \quad t \to \infty, \tag{3.18}$$

or, more explicitly:

$$S_{n:N}(t) \sim \frac{8}{\pi^2} \frac{n}{2^{N-1}} \binom{N}{n} \exp\left[-\left(\frac{\pi}{L}\right)^2 Dt\right], \quad t \to \infty. \tag{3.19}$$

---

[1]The derivation of Eq. (3.16) from Eq. (3.15) is analogous to the derivation of Eq. (2.43) from Eq. (2.42) with just one difference: now, the values assumed by auxiliary function $B(x,t)$, $B(x,t) = 1 - F(x,t)$, at the boundaries of the interval are given by Eqs. (3.17).

Thus the asymptotic survival probability of the nth tracer decays exponentially with time, the decay rate being independent of n. The hard-core interaction manifests itself only through the n-dependent prefactor. Moreover, the asymptotic decay rate of $S_{n:N}(t)$ is the same as that for the single noninteracting particle. This can be understood on physical grounds. Due to the mutual entropic repulsion among the particles, it is highly probable that the long-lived tagged particle eventually remains alone in the interval. Therefore, for any particle order n, the long-time dynamics of such particle should resemble that of a noninteracting particle.

The long-time decay of the survival probability is exponential for any particle. On the other hand, its short-time behavior strongly depends on the order n. The survival probability of the particle that starts its motion in a vicinity of an absorbing boundary decays to zero on time scales much shorter than the single-particle MFPT $\langle \mathbf{T} \rangle$, $\langle \mathbf{T} \rangle = L^2/12D$. Contrary to that, a particle that is initially located near the center of the interval ($n \approx N/2$) is "screened" from the both boundaries by an almost equal number of particles. Therefore, in this latter case, the survival probability is almost unity for the times comparable to (or longer than) $\langle \mathbf{T} \rangle$. This diversity in time scales is behind the fact that, for a general label n, there exists no unifying formula for the short-time behavior of $S_{n:N}(t)$. However, we may benefit from this splitting of time scales in the following discussion of large-N behavior of PDFs for exit times.

Exit time of the particle that leaves the interval as the last one

Before discussing mean exit times of individual interacting particles, let us answer the following questions. What is the longest MFPT that occurs in the problem? How does this MFPT scales with N and L? For the nth tracer, should we expect a scaling behavior different from Brownian MFPT $\propto L^2$?

Answers to all these questions would become clear after the derivation of MFPT for the particle that leaves the interval as the last one (regardless its label n). The survival probability of that particle, say $S_{\text{last}:N}(t)$, equals the probability that at a given time t there is still at least one particle diffusing in the interval. In symbols:

$$S_{\text{last}:N}(t) = 1 - [1 - S(t)]^N. \tag{3.20}$$

The mean exit time

$$\langle \mathbf{T}_{\text{last}:N} \rangle = \int_0^\infty \mathrm{d}t \, S_{\text{last}:N}(t), \tag{3.21}$$

by definition is the upper bound for any MFPT in question. The evaluation of the integral for $N \gg 1$ yields asymptotic behavior of this MFPT. It is instructive to derive the asymptotic result by two independent methods: (A) a direct method based on an approximation of $S(t)$; (B) a rigorous method that proves that $[1 - S_{\text{last}:N}(t)]$, after a proper rescaling of t, converges to the Gumbel distribution as $N \to \infty$.

(A) *The direct method.* We notice that for large N, the term $[1 - S(t)]^N$ in the integrand on the right-hand side of (3.21) contributes significantly to the value of the integral only for such t when $S(t)$ is vanishingly small. But this happens only for $t \gg \langle \mathbf{T} \rangle$. Therefore, we can safely replace $S(t)$ by its asymptotic form (3.9). After this step, we perform the substitution $u = \exp\left[-\left(\frac{\pi}{L}\right)^2 Dt\right]$ which yields

$$\langle \mathbf{T}_{\text{last}:N} \rangle \approx \frac{L^2}{\pi^2 D} \int_0^1 \mathrm{d}u \, \frac{1 - (1-u)^N}{u} = \frac{L^2}{\pi^2 D} \int_0^1 \mathrm{d}z \, \frac{1 - z^N}{1 - z} = \frac{L^2}{\pi^2 D} \sum_{k=1}^N \frac{1}{k}, \tag{3.22}$$

where another substitution, $z = 1 - u$, just adjusts the first integral to the usual integral representation of harmonic numbers H_N, $H_N = 1 + 1/2 + \ldots + 1/N$. As the last step, we

recall the asymptotic behavior of harmonic numbers: $H_N \sim [\log(N) + \gamma + 1/2N - \ldots]$ which gives us the asymptotic relation

$$\langle \mathbf{T}_{\text{last}:N} \rangle \sim \frac{L^2}{\pi^2 D} \left[\log(N) + \gamma \right], \quad N \gg 1, \tag{3.23}$$

where $\gamma \approx 0.5772156649$ is Euler's constant.

(B) *Convergence in distribution.* Alternatively to the above direct method, we can use the asymptotic theory for sample extreme (see App. A) to show that the distribution of the lifetime of the longest-living particle converges to the Gumbel distribution. This is intuitively expected since the survival probability $S(t)$ decays exponentially with time. To prove the convergence in distribution, let us choose the standardizing constants as follows:

$$a_N = \frac{L^2}{\pi^2 D}, \qquad b_N = \frac{L^2}{\pi^2 D} \log \left(\frac{8N}{\pi^2} \right). \tag{3.24}$$

Then we obtain the following large-N limit:

$$[1 - S(a_N t + b_N)]^N \sim \left(1 - \frac{\mathrm{e}^{-t}}{N} \right)^N \to \exp\left(-\mathrm{e}^{-t} \right), \quad \text{as} \quad N \to \infty. \tag{3.25}$$

In other words, we have just shown that

$$\lim_{N \to \infty} \mathrm{Prob} \left\{ \frac{\mathbf{T}_{\text{last}:N} - b_N}{a_N} < t \right\} = \exp\left(-\mathrm{e}^{-t} \right). \tag{3.26}$$

Hence, the large-N asymptotic behavior of the survival probability of the longest-living particle is given by

$$S_{\text{last}:N}(t) \sim 1 - \exp\left[-\exp\left(-\frac{\pi^2}{L^2} D t + \log \left(\frac{8N}{\pi^2} \right) \right) \right], \quad \text{as} \quad N \gg 1. \tag{3.27}$$

This result yields large-N expressions for all moments of the extreme trapping time. The first moment, given by the spatial integral (3.21), reads

$$\langle \mathbf{T}_{\text{last}:N} \rangle \sim \frac{L^2}{\pi^2 D} \left[\log(N) + \gamma - \log \left(\frac{\pi^2}{8} \right) \right], \quad N \gg 1, \tag{3.28}$$

and the variance of $\mathbf{T}_{\text{last}:N}$ asymptotically behaves as

$$\left\langle [\mathbf{T}_{\text{last}:N} - \langle \mathbf{T}_{\text{last}:N} \rangle]^2 \right\rangle \sim \frac{\pi^2}{6} \left(\frac{L^2}{\pi^2 D} \right)^2, \quad N \gg 1. \tag{3.29}$$

(C) *Comparison.* Equation (3.28) should be compared with Eq. (3.23). Notice, that the main asymptotic term for large N is identical in the both equations. In derivation of Eq. (3.23) we have replaced $S(t)$ by its long-time behavior (3.9) which is valid only for $t \gg \langle \mathbf{T} \rangle$. By this replacement, we have committed an error which is independent of N and which is of the order of L^2. The exact result (3.28) quantifies this error and shows that by the direct method we have overestimated the integral by the value $L^2 \log\left(\frac{\pi^2}{8} \right) / \pi^2 D$. The advantage of the direct method (A) resides in the fact that it provides a quick estimate for large-N asymptotics without any previous knowledge of standardizing constants (3.24). The advantage of method (B), besides the fact that it is rigorous, is that it is valid also when we perform the thermodynamic limit (and not only large-N limit with fixed L). That is, all steps of the method (B) remain unchanged if we replace L by $L = N/\rho$, where the density ρ is a fixed positive number whereas the particle number N tends to infinity.

Further we will use only the direct method. Nevertheless, in all cases, both methods can be employed when we are interested only in the main term of the large-N asymptotic behavior.

PDF of the exit time for a tagged particle

For a single *noninteracting* particle let $\phi_{\mathrm{L}}(t)$, $\phi_{\mathrm{R}}(t)$ denote the PDF of the exit time through the left, and through the right boundary, respectively. Then the integral $\int_0^t \mathrm{d}t' \, \phi_{\mathrm{L}}(t')$ equals to the probability that the single-diffusing particle has been trapped by the left boundary in $(0, t)$, and similarly $\int_0^t \mathrm{d}t' \, \phi_{\mathrm{R}}(t')$ for the right boundary. Of course, in our symmetric case we have $\phi_{\mathrm{L}}(t) = \phi_{\mathrm{R}}(t) = \phi(t)/2$ with the PDF $\phi(t)$ given in Eq. (3.10), however, it is enlightening to consider the two PDFs separately for a while.

Having prepared the two functions we are now ready to write the PDF for the time at which the nth interacting particle hits the left absorbing boundary. This PDF reads

$$\phi_{n:N}^{\mathrm{L}}(t) = \frac{N!}{(n-1)!(N-n)!} \phi_{\mathrm{L}}(t) \left[\int_0^t \mathrm{d}t' \phi_{\mathrm{L}}(t') \right]^{n-1} \left[1 - \int_0^t \mathrm{d}t' \phi_{\mathrm{L}}(t') \right]^{N-n}. \qquad (3.30)$$

That is again the hitting time of the nth interacting particle is statistically equivalent to the nth absorption event happening in the reference system of noninteracting particles. More precisely, the probability that the nth interacting particle hits the left absorbing boundary at t, $t \in (t, t + \mathrm{d}t)$, equals to the product of four terms: 1) the probability $[\phi_{\mathrm{L}}(t)\mathrm{d}t]$ that a single noninteracting particle is absorbed by the left trap in $(t, t + \mathrm{d}t)$; 2) the probability $\left[\int_0^t \mathrm{d}t' \phi_{\mathrm{L}}(t') \right]^{n-1}$ that at the time of absorption there are already $(n-1)$ particles residing in the left trap; 3) the probability $\left[1 - \int_0^t \mathrm{d}t' \phi_{\mathrm{L}}(t') \right]^{N-n}$ that the remaining $(N-n)$ particles are located anywhere except in the left trap; 4) the combinatorial prefactor which accounts for all possible labellings of the particles in the two groups from points 2) and 3). The analogous equation holds for $\phi_{n:N}^{\mathrm{R}}(t)$, i.e., for the PDF describing the time at which the nth particle is absorbed by the right boundary:

$$\phi_{n:N}^{\mathrm{R}}(t) = \frac{N!}{(n-1)!(N-n)!} \phi_{\mathrm{R}}(t) \left[\int_0^t \mathrm{d}t' \phi_{\mathrm{R}}(t') \right]^{N-n} \left[1 - \int_0^t \mathrm{d}t' \phi_{\mathrm{R}}(t') \right]^{n-1}. \qquad (3.31)$$

After summing the two equations we obtain the PDF for the time of absorption of the nth tagged particle regardless the information at which boundary the absorption takes place. Let us denote this PDF by $\phi_{n:N}(t)$, then we have

$$\phi_{n:N}(t) = \frac{N!}{(n-1)!(N-n)!} \left\{ \phi_{\mathrm{L}}(t) \left[\int_0^t \mathrm{d}t' \phi_{\mathrm{L}}(t') \right]^{n-1} \left[1 - \int_0^t \mathrm{d}t' \phi_{\mathrm{L}}(t') \right]^{N-n} \right.$$
$$\left. + \phi_{\mathrm{R}}(t) \left[\int_0^t \mathrm{d}t' \phi_{\mathrm{R}}(t') \right]^{N-n} \left[1 - \int_0^t \mathrm{d}t' \phi_{\mathrm{R}}(t') \right]^{n-1} \right\}. \qquad (3.32)$$

This equation is the generalization of Eq. (2.56) to the present case with two absorbing boundaries. Indeed, Eq. (2.56) can be obtained from Eq. (3.32) in the limit $L \to \infty$ since in this limit $\phi_{\mathrm{R}}(t)$ vanishes (the diffusing particle cannot reach an infinitely distant right boundary in a finite time) and $\phi_{\mathrm{L}}(t)$ approaches the PDF $\phi(t)$ for the time of absorption on the semi-infinite interval used in Eq. (2.56). Below we will demonstrate that Eq. (3.32) contains as a special case also the equation (2.87) for the semi-infinite system in the thermodynamic limit.

Returning to the finite-L symmetric case, we can use $\phi_{\mathrm{L}}(t) = \phi_{\mathrm{R}}(t) = \phi(t)/2$ to obtain

$$\phi_{n:N}(t) = \frac{N!}{(n-1)!(N-n)!} \frac{\phi(t)}{2^N} \left\{ [1 - S(t)]^{n-1} [1 + S(t)]^{N-n} \right.$$
$$\left. + [1 - S(t)]^{N-n} [1 + S(t)]^{n-1} \right\}. \qquad (3.33)$$

47

Alternatively, the above result can be checked by taking the time derivative of both sides of Eq. (3.16) since we have $\phi_{n:N}(t) = -\mathrm{d}S_{n:N}(t)/\mathrm{d}t$. On the other hand, Eq. (3.33) provides a straightforward probabilistic derivation of a somewhat untransparent sum occurring on the right-hand side of Eq. (3.16).

PDF (3.33) provides the complete description of the absorption time for the tagged particle for any n, N, and L. This desired information is encoded in a rather complex structure of the PDF. Consequently, the task to derive any averaged quantity form the exact result (3.33) is far from being trivial. Explicit formulas can be obtained only in a few limiting cases. The first such situation corresponds to the large-N limit of the first-passage characteristics for the central tracer. The second concerns the tracer initially located near one of the absorbing boundaries.

Exit time for the central tracer

Let us now assume that initially there are $(2N + 1)$ particles randomly distributed in the interval of the length L. The PDF for the absorption time of the central particle labeled by c, $c = N + 1$, follows form Eq. (3.33) after the substitutions $n \to (N + 1)$, $N \to (2N + 1)$. We get

$$\phi_{c:(2N+1)}(t) = \frac{(2N + 1)}{2^{2N}} \binom{2N}{N} \phi(t)[1 - S^2(t)]^N, \quad c = N + 1. \tag{3.34}$$

In order, to obtain the large-N behavior of the PDF, we choose the following standardizing constants:

$$a_N = \frac{L^2}{\pi^2 D}, \qquad b_N = \frac{L^2}{\pi^2 D} \log\left(\frac{8\sqrt{N}}{\pi^2}\right). \tag{3.35}$$

Note that the first constant, a_N, which determines the asymptotic dispersion of the absorption time is exactly the same as that for the longest-living particle, cf. Eqs. (3.24). The second constant, b_N, which determines the mean time of absorption grows slower with N as compared to that in Eq. (3.24). Mathematically this fact arises due to the second power of $S(t)$ in Eq. (3.34) (as compared to the first power of $S(t)$ in Eq. (3.20)). After the rescaling of the time variable, the following limit holds

$$\lim_{N \to \infty} \frac{L^2}{2\pi^{3/2}} \phi_{c:(2N+1)}(a_N t + b_N) = \mathrm{e}^{-t} \exp\left(-\mathrm{e}^{-2t}\right). \tag{3.36}$$

Which means that the large-N asymptotic behavior of the PDF (3.34) is given by

$$\phi_{c:(2N+1)}(t) \sim 2\pi^{3/2} \frac{D}{L^2} \mathrm{e}^{-(t-b_N)/a_N} \exp\left[-\mathrm{e}^{-2(t-b_N)/a_N}\right], \quad N \gg 1. \tag{3.37}$$

The large-N asymptotic behavior of all moments of the absorption time $\mathbf{T}_{c:(2N+1)}$ can be derived directly from the asymptotic PDF (3.37). For the mean and the variance of the absorption time we obtain

$$\left\langle \mathbf{T}_{c:(2N+1)} \right\rangle \sim \frac{L^2}{2\pi^2 D} \left[\log(N) + \gamma + 4\log\left(\frac{4}{\pi}\right)\right], \quad N \gg 1, \tag{3.38}$$

$$\left\langle \left[\mathbf{T}_{c:(2N+1)} - \left\langle \mathbf{T}_{c:(2N+1)} \right\rangle\right]^2 \right\rangle \sim \frac{1}{2}\left(\frac{L^2}{2\pi D}\right)^2, \quad N \gg 1, \tag{3.39}$$

respectively.

Thus, the mean absorption time for the central tracer exhibits a similar large-N behavior $\propto L^2 \log(N)$ as that for the longest living particle, cf. Eq. (3.28). Obviously,

the absolute value of $\left\langle \mathbf{T}_{c:(2N+1)} \right\rangle$ is smaller as compared to $\left\langle \mathbf{T}_{\mathrm{last}:(2N+1)} \right\rangle$ since the central particle can in general be absorbed earlier than the longest-living particle. The hindering introduced by surrounding particles reduces the relative fluctuations of the absorption time as N is increased. This reduction is however quite weak, the relative fluctuations decrease as $1/\log(N)$ when $N \to \infty$.

Again notice that we have just discussed the large-N limit leaving the interval length L finite. However, all conclusions holds true also for the system approaching the thermodynamic limit ($N \to \infty$, $L \to \infty$ and ρ is fixed) since the limit in Eq. (3.36) is valid also in this latter case (that is after the substitution $L = N/\rho$).

Exit time for the tracer initially located near the boundary

The second setting, when we can derive explicit results from the exact PDF (3.33) is when the tracer is initially located near the absorbing boundary, e.g. near the left one, and both N and L are large (and n is finite, $n \ll N$). In this case the exact PDF $\phi_{n:N}(t)$ converges to the PDF (2.56) for the absorption time of the nth particle in the semi-infinite system. Formally, we can write

$$\lim_{N \to \infty} \phi_{n:N}(t) = \phi_n(t), \quad N/L = \rho, \quad \rho \text{ is constant.} \tag{3.40}$$

Technically, the limit is performed after we replace the single-particle characteristics $S(t)$, $\phi(t)$ by their small-time representations (3.11), (3.12). Then the second summand on the right-hand side of Eq. (3.33), which describes the absorption at the right boundary, vanishes. The remaining term gives us exactly the right-hand side of Eq. (2.56).

3.2.3 Fixed initial density of interacting particles particles

PDF of a tagged particle

Let us now discuss the second possible initial condition. We now assume that N is the Poisson random variable distributed according to Eq. (3.3). For a given N, the PDF of the nth tagged particle diffusing in such a system is given by Eq. (3.13). The PDF of the nth tagged particle regardless the initial number of particles is obtained from the PDF (3.13) by the weighted summation over all possible initial numbers of particles:

$$p_n(x,t) = \sum_{N=n}^{\infty} p_{n:N}(x,t) P(N). \tag{3.41}$$

For a fixed n, the summation starts with $N = n$ since for $N < n$ we can formally write $p_{n:N}(x,t) = 0$: the nth particle simply does not exist in this case. The summation yields

$$p_n(x,t) = \rho L f(x,t) \frac{[\rho L F(x,t)]^{n-1}}{(n-1)!} \, \mathrm{e}^{-\rho L F(x,t)}, \tag{3.42}$$

where the probability $F(x,t)$ is defined in Eq. (3.14).

In the present fixed-ρ setting the expression $p_n(x,t)\mathrm{d}x$ has a similar meaning as its counterpart $p_{n:N}(x,t)\mathrm{d}x$ in the fixed-N case. Both quantities gives us the probability that at time t the $n$the particle is located in $(x, x+\mathrm{d}x)$. However, we should mention one important difference. Since presently N is random, it is no longer sure that the nth particle is initially located in $(0, L)$ (the interval may contain N particles with $N < n$). Therefore, at $t = 0$, the PDF $p_n(x,t)$ is not normalized to one, in contrast to the PDF $p_{n:N}(x,t)$ for the fixed-N case. Presently we have

$$\int_0^L \mathrm{d}x \, p_n(x,0) = 1 - P(N < n), \tag{3.43}$$

where $P(N < n)$ stands for the probability that the initial number of particles is less than n. For a fixed n, the latter probability vanishes exponentially with increasing interval length L:

$$P(N < n) = \mathrm{e}^{-\rho L} \sum_{k=0}^{n-1} \frac{(\rho L)^k}{k!}. \tag{3.44}$$

Notice also that the sum of individual tracer PDFs (2.41) now becomes

$$\sum_{n=1}^{\infty} p_n(x,t) = \rho L\, f(x,t), \tag{3.45}$$

where ρL, the mean number of particles initially distributed in $(0, L)$, takes over the role of the fixed number of particles N in Eq. (2.41).

Survival probabilities

The probability that, at time t, the nth tagged particle is diffusing in $(0, L)$ is defined by the integral

$$S_n(t) = \int_0^L \mathrm{d}x\, p_n(x,t). \tag{3.46}$$

If we expand the exponential in Eq. (3.42) into the power series, the required integration can be carried out and we obtain

$$S_n(t) = \frac{(\rho L)^n}{(n-1)!} \sum_{k=0}^{\infty} \frac{(-1)^k}{n+k} \frac{(\rho L)^k}{k!} \left\{ [F(L,t)]^{n+k} - [F(0,t)]^{n+k} \right\}. \tag{3.47}$$

Eq. (3.47) is valid for any t. For $t = 0$ we get

$$S_n(0) = 1 - \mathrm{e}^{-\rho L} \sum_{k=0}^{n-1} \frac{(\rho L)^k}{k!}, \tag{3.48}$$

which is nothing but Eq. (3.43). Hence apart from the normalization, the probability $S_n(t)$ possesses an analogous meaning as the survival probability $S_{n:N}(t)$ given by Eq. (3.16). Further we will refer to $S_n(t)$ as to the survival probability of the nth tracer.

The long-time analysis of $S_n(t)$ becomes more transparent when we depart from an alternative form of $S_n(t)$. Namely, the survival probability $S_n(t)$ can be obtained from $S_{n:N}(t)$ after performing the following summation

$$S_n(t) = \sum_{N=n}^{\infty} S_{n:N}(t) P(N), \tag{3.49}$$

where $P(N)$ is the Poisson distribution (3.3). In the long-time limit, *each summand in the above sum is proportional to $S(t)$*, cf. Eq. (3.18). Thus the asymptotic survival probability is given by

$$S_n(t) \sim \rho L \frac{(\rho L/2)^{n-1}}{(n-1)!} \mathrm{e}^{-\rho L/2} S(t). \tag{3.50}$$

Again, the long-time behavior of the survival probability id dictated by the single-particle exponential decay of $S(t)$. Eq. (3.50) represents the overall contribution to the long-time properties of *all possible initial particle numbers N for which $n \leq N$*.

Large-L limit

It turns out that the large-L behavior of first-passage characteristics of the nth tracer can be obtained from the large-N asymptotic behavior for the finite-N case. This intuitively plausible fact may not be obvious at a first glance, since the survival probabilities in the both cases are given by rather different formulas, cf. Eqs. (3.16), (3.47). For instance, consider the survival probability for the particle that is trapped as the last one. Presently, it reads

$$S_{\text{last}}(t) = \sum_{N=1}^{\infty} S_{\text{last}:N}(t) P(N) = 1 - \exp[-\rho L S(t)], \qquad (3.51)$$

where the single particle survival probability $S(t)$ is given by Eq. (3.7), and the corresponding survival probability for the finite-N case, $S_{\text{last}:N}(t)$, has been introduced in Eq. (3.20).

The large-L behavior of $S_{\text{last}}(t)$ is derived after choosing the standardizing constants as

$$a_L = \frac{L^2}{\pi^2 D}, \qquad b_L = \frac{L^2}{\pi^2 D} \log\left(\frac{8\rho L}{\pi^2}\right). \qquad (3.52)$$

Notice that the two constants are exactly the constants a_N, b_N, for the finite-N case as given in Eq. (3.24), after the substitution $N = L\rho$ in b_N.

After the rescaling of the time variable the following limit, which is an analogue of the limit (3.26), holds

$$\lim_{L \to \infty} \text{Prob}\left\{ \frac{\mathbf{T}_{\text{last}} - b_L}{a_L} < t \right\} = \exp\left(-\text{e}^{-t}\right). \qquad (3.53)$$

Therefore, the large-L asymptotic behavior of the survival probability

$$S_{\text{last}}(t) \sim 1 - \exp\left[-\exp\left(-\frac{\pi^2}{L^2} D t + \log\left(\frac{8\rho L}{\pi^2}\right) \right) \right], \qquad L \to \infty, \qquad (3.54)$$

is given essentially by the expression (3.26) with N replaced by ρL. All other limits, i.e., the limits which concern the central tracer and/or the tracer located near one of the boundaries, can be derived along the same lines. These results can be obtained directly from the corresponding finite-N formulas just by the substitution $N \to \rho L$.

Random interval length

The present fixed-ρ setting is a convenient starting point to study the following scenario for which the finite-N assumption would be unnatural. Let us now derive the asymptotic tagged particle survival probability in the case when L is drawn from the exponential distribution with the mean $1/\rho_{\text{tr}}$. Physically, this corresponds to the model of diffusion on the real line with randomly distributed perfectly absorbing traps. The concentration of traps is uniform and it equals ρ_{tr}. In the model we assume that the initial (i.e., for $t < 0$) density of particles ρ is also uniform. Then, at the initial time $t = 0$ the randomly distributed traps are activated. We are interested in the average survival probability of the tagged particle in such a system. Notice that for noninteracting particles, there exists a large body of literature on the subject, see, e.g., Refs. [167–174] and references therein.

The average of the survival probability $S_n(t)$ over the probability distribution of the interval lengths is given by

$$\bar{S}_n(t) = \int_0^{\infty} \text{d}L\, \rho_{\text{tr}}\, \text{e}^{-\rho_{\text{tr}} L} S_n(t). \qquad (3.55)$$

In order to investigate the long-time properties, we insert the asymptotic expression (3.50) into the above integral. After that the integral is evaluated by a saddle-point method.[2] The result is

$$\bar{S}_n(t) \sim A(Dt)^{(2n+1)/6} \exp\left\{ -\frac{3}{2} \left[2\pi^2 \left(\rho_{\mathrm{tr}} + \frac{\rho}{2} \right) Dt \right]^{1/3} \right\}, \qquad t \to \infty, \qquad (3.56)$$

where the prefactor reads

$$A = \sqrt{\frac{2\pi}{3}} \frac{16\rho_{\mathrm{tr}}}{\pi^2} \frac{(\rho/2)^n}{(n-1)!} \frac{(2\pi^2)^{(2n+1)/6}}{(\rho_{\mathrm{tr}} + \rho/2)^{(n+2)/3}}. \qquad (3.57)$$

As it is for the single noninteracting particle [167], the decay of the survival probability is slower than that when the interval length is fixed. The stretched exponential relaxation in Eq. (3.56) results from very large (and extremely rare) interval lengths which significantly enhance the asymptotic long-time survival probability [170]. A remarkable feature, which is not present in a noninteracting model, is the dependence of the factor in the exponential on ρ. That is on the initial concentration of particles and not only on the concentration of traps ρ_{tr}. This dependence is again the consequence of the entropic repulsion among the interacting particles – the higher the initial concentration the stronger the effective force that drives the tagged particle into the trap.

3.3 The left boundary is absorbing, the right boundary is reflecting

Let us now discuss the first-passage properties of the tagged particle in a finite interval where the right boundary is reflecting and the left boundary is absorbing. The setting shares many common features with both the semi-infinite system of Chap. 2 and the finite system with two absorbing boundaries discussed in the present chapter. Therefore, instead of a full thorough derivation of all the, we restrict ourselves to a brief exposition of the main similarities and differences of the present scenario as compared to the two aforementioned cases.

3.3.1 Single noninteracting particle

Now, the PDF of the single noninteracting particle, $f(x,t)$, satisfies the diffusion equation (2.5) subject to the absorbing boundary condition at the origin, $f(0,t) = 0$, to the reflecting boundary condition at the right end of the interval, $\partial f/\partial x|_{x=L} = 0$, and to the homogeneous initial condition $f(x,0) = 1/L$, $x \in (0, L)$. The solution of this

---

[2]The integral in Eq. (3.55) has the form

$$I(t;n) = \int_0^\infty \mathrm{d}L \ L^n \exp\left[-\alpha L - \frac{\beta t}{L^2} \right], \quad \alpha, \beta > 0.$$

The substitution $L = t^{1/3}x$ brings us to the expression

$$I(t;n) = t^{(n+1)/3} \int_0^\infty \mathrm{d}x \ x^n \exp\left[-t^{1/3} \left(\alpha x + \frac{\beta}{x^2} \right) \right].$$

In the long-time limit, the above integral is approximated by the Laplace's method [175, 176]:

$$I(t;n) \sim C_n \, t^{(2n+1)/6} \exp\left[-\frac{3}{2} \left(2\beta\alpha^2 t \right)^{1/3} \right], \qquad C_n = \sqrt{\frac{2\pi}{3}} \frac{(2\beta)^{(2n+1)/6}}{\alpha^{(n+2)/3}}.$$

initial-boundary value problem can be expressed as the eigenfunction expansion:

$$f(x,t) = \frac{4}{\pi L} \sum_{k=0}^{\infty} \frac{(-1)^k}{2k+1} \cos\left[\frac{\pi}{2L}(2k+1)(L-x)\right] \exp\left\{-\left[\frac{\pi}{2L}(2k+1)\right]^2 Dt\right\}. \quad (3.58)$$

Again, as it is the case for two absorbing boundaries (cf. Eq. (3.6)), each term of the above series decays exponentially in time with the decay rate being higher for higher values of k.

The survival probability of the single noninteracting particle,

$$S(t) = \int_0^L dx\, f(x,t), \quad (3.59)$$

is given by the sum

$$S(t) = \frac{8}{\pi^2} \sum_{k=0}^{\infty} \frac{1}{(2k+1)^2} \exp\left\{-\left[\frac{\pi}{2L}(2k+1)\right]^2 Dt\right\}, \quad (3.60)$$

which in the long-time limit is dominated by the first term

$$S(t) \sim \frac{8}{\pi^2} \exp\left[-\left(\frac{\pi}{2L}\right)^2 Dt\right], \qquad t \to \infty. \quad (3.61)$$

The survival probability (3.60) should be compared with the survival probability (3.7) for the finite interval with two absorbing boundaries. The two survival probabilities coincide except for the fact that the damping factors in exponentials in Eq. (3.60) depend on $2L$ whereas their counterparts in Eq. (3.7) depend on L. This fact follows from the reflection principle. Any trajectory that hits the reflecting boundary at $x = L$ and then is absorbed at $x = 0$ possesses an image which passes freely through the point $x = L$ and is absorbed at $x = 2L$. Thus, as for the first-passage properties, the diffusion of a single particle in the finite interval with the reflecting boundary at $x = L$ is equivalent to the diffusion of the particle in the twice as large interval with two absorbing boundaries.[3]

3.3.2 Fixed initial number of particles

The very basic fact that presently we have only one absorbing boundary implies that we can adopt all general formulas from Chap. 2 with just minor changes. Namely, the PDF of the position of the nth tracer possesses exactly the same structure (and interpretation) as that occurring in Eq. (2.39). Now the probability $F(x,t)$ is given by

$$F(x,t) = [1 - S(t)] + \int_0^x dx'\, f(x',t), \quad (3.62)$$

which is formally equivalent to Eq. (2.40). However, presently, the single-particle quantities $f(x,t)$, $S(t)$, used in Eq. (3.62) are defined in Eqs. (3.58), (3.60), respectively.

The second quantity which we can adopt formally without changes is the survival probability for the tagged particle (2.43) which reads

$$S_{n:N}(t) = n\binom{N}{n} \sum_{k=0}^{n-1} \frac{(-1)^k}{N-n+k+1} \binom{n-1}{k} [S(t)]^{N-n+k+1}. \quad (3.63)$$

---

[3]The equivalence holds for the first-passage properties only. The dynamics of the particle, e.g., the time-evolution of its mean position, is rather different in the two systems. Indeed, in the present setting the particle is pushed out of the interval by an entropic repulsion emerging from the collisions with the reflecting boundary, whereas in the setting with two absorbing boundaries there is no boundary-induced entropic repulsion at all.

Notice that each summand of the above sum decays exponentially with time, cf. Eq. (3.61). Hence the main asymptotic term in the long-time regime is that with $k = 0$. It reads

$$S_{n:N}(t) \sim \frac{n}{N - n + 1} \binom{N}{n} [S(t)]^{N-n+1}, \qquad t \to \infty. \tag{3.64}$$

After inserting the asymptotic representation (3.61) into the above result we obtain the explicit form of the tagged particle asymptotic survival probability:

$$S_{n:N}(t) \sim C_{n:N} \exp\left[-(N - n + 1)\left(\frac{\pi}{2L}\right)^2 Dt\right], \qquad t \to \infty, \tag{3.65}$$

where the prefactor is given by

$$C_{n:N} = \frac{n}{N - n + 1} \binom{N}{n} \left(\frac{8}{\pi^2}\right)^{N-n+1}. \tag{3.66}$$

Thus the asymptotic survival probability of the nth tagged particle decays exponentially with time. The decay rate increases with the number of particles located between the tagged particle and the reflecting wall at $x = L$, i.e., with $(N - n)$. In particular, the survival probability of the rightmost particle ($n = N$) decays exactly with the same rate as that of the single-diffusing particle. In this respect the result (3.65) is similar to the one obtained in Chap. 2 for a semi-infinite interval with the absorbing boundary at the origin (where the single-particle survival probability decays as the power law $t^{-1/2}$, cf. Eq. (2.48)). On the other hand, the asymptotic behavior (3.65) is rather different from that in the system with two absorbing boundaries, where the decay rate of the asymptotic tagged particle survival probability is independent of both n, and N, cf. Eq. (3.19).

We can proceed further and adopt the PDF for the exit time of the nth particle (2.56) and/or investigate the large-N behavior of the first-passage characteristics. For instance, it turns out that the large-N asymptotic behavior of $S_{N:N}$ is given by Eq. (3.27) with L being replaced by $2L$. This is intuitively plausible since now the rightmost particle is the particle that is certainly absorbed as the last one. Further, the large-N limit of $\phi_{1:N}(t)$ is exactly the same as in the case with two absorbing boundaries, cf. Eq. (3.40).

3.3.3 Fixed initial density of particles

For a given N, Eqs. (3.64), (3.65) clearly demonstrate the consequences of the entropic repulsion among the particles: the more particles are located between the tagged particle and the reflecting boundary the higher the decay rate of the tagged particle survival probability. Hence, in the case when ρ is given (i.e., N is drawn from the Poisson distribution (3.3)), one could expect that the decay rate of the tagged particle survival probability is controlled by an average number of particles located between the tagged particle and the reflecting boundary. However, this is not the case.

The survival probability of the nth tracer averaged over the initial number of particles is obtained by the summation

$$S_n(t) = \sum_{N=n}^{\infty} S_{n:N}(t) P(N), \tag{3.67}$$

where $S_{n:N}(t)$ comes from Eq. (3.63), and $P(N)$ is the Poisson distribution (3.3). In the long-time limit, *only the first term* contributes significantly to the sum (3.67), since all

other terms decay much faster with time, cf. Eqs. (3.64), (3.65). Thus the asymptotic survival probability reads

$$S_n(t) \sim \rho L \frac{(\rho L)^{n-1}}{(n-1)!} \, \mathrm{e}^{-\rho L} S(t). \tag{3.68}$$

The above result is formally similar with Eq. (3.50). However, the physical backgrounds of both asymptotic representations are rather different. In the present case described by Eq. (3.68), the long-time behavior of the survival probability $S_n(t)$ is dominated by those events when the tagged particle is initially the right-most one ($n = N$). On the other hand, Eq. (3.50) represents the overall contribution of all possible initial conditions for which $n \leq N$.

3.4 Summarizing remarks

In the present chapter we have studied first-passage properties of the nth tagged particle diffusing in a finite interval with two types of boundary conditions: 1) the both boundaries are absorbing; 2) the left boundary is absorbing and the right boundary is reflecting. Let us now summarize the main physical consequences of the hard-core interaction.

When the right boundary is reflecting, the particles located between the reflecting boundary and the nth tagged particle create an effective (entropic) repulsive force which shortens the time spent by the nth tagged particle in the interval. This is behind the dependence of the decay rate of the asymptotic survival probability (3.65) on $(N - n)$. This behavior is parallel of what has been observed in the semi-infinite system of Chap. 2, where, however, the asymptotic survival probability (2.48) has decayed as the power law. When, instead of the precise initial number of particles, the initial mean density is given then Eq. (3.68) yields the asymptotic survival probability averaged over all possible initial particle numbers. In fact, Eq. (3.68) represents only the first term of the sum (3.67). Thus, in the fixed-ρ case, the long-time properties are controlled solely by the initial configuration in which the nth particle is the right-most one.

The situation is rather different when both boundaries are absorbing. For a given N, the long-time regime is governed by the scenario when the tagged particle remains alone in the interval, cf. Eq. (3.19). Then the long-time dynamics of the tracer resembles that of the single noninteracting particle. The only trace of the hard-core interaction is contained in the pre-exponential factor of the asymptotic survival probability (3.19). For a given ρ, all terms of the sum (3.49) are asymptotically proportional to the survival probability of the single noninteracting particle. Hence all initial conditions with all possible initial particle numbers contribute to the asymptotics (3.49).

The exact PDF for the exit time of the nth tagged particle, cf. Eq. (3.32), allows us to study the large-N (and/or large-L) behavior of the time spent by the particle in the interval before it is absorbed. For the single noninteracting particle, the Brownian scaling holds, i.e., the mean time of absorption is proportional to L^2. The hard-core interaction changes this scaling law by introducing a (marginal) logarithmic dependence on N. More precisely, the mean time to absorption of the central tracer grows with N as $L^2 \log(N)$, and its relative fluctuations decrease as $1/\log(N)$, cf. Eqs. (3.38), (3.39). The same holds true for the particle which leaves the interval as the last one (for both types of boundary conditions), cf. Eqs. (3.28), (3.29). The large-N behavior of the tracer initially located in the vicinity of the absorbing boundary approaches that of the tracer diffusing in the semi-infinite system in the thermodynamic limit discussed in Chap. 2, Sec. 2.3.3.

Finally, when L is random (and ρ is given), the tagged-particle asymptotic survival probability (3.56) exhibits a stretched-exponential decay. This behavior is observed also in the case without the hard-core interaction. A remarkable consequence of the hard-core interaction is the dependence of the asymptotic survival probability (3.56) on the combination $(\rho_{\mathrm{tr}} + \rho/2)$. That is, the lifetime of the tagged particle is reduced not only by increasing the concentration of the traps ρ_{tr} (as it is the case for noninteracting particles) but it is also the *initial* density ρ of the interacting particles which controls the time-asymptotic decay rate of the survival probability.

4. Basics of stochastic thermodynamics

Stochastic thermodynamics is a discipline exhibiting a rapid development over the past two decades. The progress is driven by many applications to small (nano-sized) systems of current interest (such as individual Brownian particles, biomolecules, quantum dots) and, from the theoretical point of view, by recent discoveries of rather general relations called fluctuation theorems. The adjective "stochastic" in the name of the field means that the dynamics of the system under consideration is governed by stochastic evolution equations, which in our case is the Langevin equation. The key quantities of the classical thermodynamics such as heat, work and entropy are (within the framework of the stochastic thermodynamics) defined along individual trajectories of the system. Thus defined quantities are valid for *finite*, and even small systems which are driven *arbitrarily far from equilibrium*, in contrast to their classical counterparts which are used for *macroscopic* systems *in equilibrium* (or in a linear-response regime).

The main aim of the present chapter is to introduce basic concepts and relations which are necessary for the study presented in Chap. 5. First, we identify the work and the heat for the system whose dynamics obeys the Langevin equation (Sec. 4.1), second we introduce two fluctuation theorems which proved to be useful in experiments (Sec. 4.2), and third, we provide references to several reviews and to just a few selected original works in the field (Sec. 4.3).

4.1 Definition of stochastic work and heat

Nonequilibrium processes in biology and nanosystems are generally strongly affected by thermal fluctuations. A paradigmatic model for gaining a better understanding of nonequilibrium processes in such systems is a colloidal particle diffusing in water and driven by an externally controlled potential. In the overdamped regime (characterized by low Reynolds numbers) the position of the particle evolves according to the Langevin equation

$$d\mathbf{X}(t) = \mathcal{F}(\mathbf{X}(t), t)dt + \sqrt{2D}\,d\mathbf{B}(t), \qquad (4.1)$$

where D controls the strength of the thermal noise and $\mathbf{B}(t)$ is the standard Wiener process. Specifically, in the present case of a thermal environment, the noise strength is proportional to the heat-bath temperature, $D = k_{\mathrm{B}}T$ (the particle mobility is set to one). The external force, $\mathcal{F}(x,t)$, is derived from the potential $U(x,t)$, $\mathcal{F}(x,t) = -\partial U/\partial x$, which represents, e.g., the confinement imposed by an optical trap.

If the potential is modulated in time following a given externally imposed protocol, the position of the particle evolves along a stochastic trajectory. Any single trajectory of the particle in the time interval $[0, t]$ yields a single value of the work $\mathbf{W}(t)$ done on the particle by an external filed. The work $\mathbf{W}(t)$ is a *functional* of the position process $\mathbf{X}(t')$, $0 \le t' \le t$, and it is distributed with a probability density function $p(w, t)$. The probability $p(w, t)dw$ that the work $\mathbf{W}(t)$ falls into an infinitesimal interval $(w, w + dw)$ equals the probabilistic weight of all trajectories giving work values in that interval. Analogical reasoning holds true for the heat exchanged with the heat reservoir, $\mathbf{Q}(t)$.

The stochastic heat and work are identified with the aid of the first law of thermodynamics. In the overdamped regime which we consider here, the "internal energy" of the particle is given by its mean potential energy $\langle U(\mathbf{X}(t), t)\rangle$. The total differential of

the potential energy

$$dU = \left(\frac{\partial U}{\partial x}\right)_t dx + \left(\frac{\partial U}{\partial t}\right)_x dt \tag{4.2}$$

is decomposed into two parts. If we substitute into the above expression the (random) position of the particle at time t, $x \to \mathbf{X}(t)$, the following interpretation emerges [36, 37]. The first term on the right-hand side describes the infinitesimal increment of the potential energy due to the particle relaxation in the *time-independent* potential. We identify this term with the heat accepted by the system from heat bath:

$$\delta\mathbf{Q}(t) = -\mathcal{F}(\mathbf{X}(t), t)d\mathbf{X}(t). \tag{4.3}$$

This relation is physically plausible since in the overdamped regime the total mechanical force times the displacement corresponds to dissipated energy. The minus sign corresponds to the convention that the heat transferred into the system is positive.

The second term on the right-hand side of Eq. (4.2) describes the increment of the potential energy due to the time-variation of the potential while the particle position is held constant. In this case, the potential energy of the particle is either raised or lowered purely due to the externally controlled modulation of potential U. Correspondingly, this term describes as the work performed on the particle:

$$\delta\mathbf{W}(t) = \left(\frac{\partial U}{\partial t}\right)_{\mathbf{X}(t)} dt, \tag{4.4}$$

and hence altogether we have

$$dU(\mathbf{X}(t), t) = \delta\mathbf{Q}(t) + \delta\mathbf{W}(t). \tag{4.5}$$

The above definition of the stochastic work is in agreement with the definition of "thermodynamic work" used in equilibrium theory [177]. However, the definition is not identical to that used in introductory courses of classical mechanics, where to "work = force times displacement".[1] For the discussion of (un)ambiguity of the definition used see Refs. [178–181] and references therein. See also Refs. [182, 183] for implications of different work definitions in context of fluctuation relations.

4.2   Crooks fluctuation theorem and Jarzynski equality

Many important processes in biophysics take place in the liquid environment which is maintained at a constant temperature. In classical thermodynamics, work w required to transfer the system from the specified initial equilibrium state i to the specified final equilibrium state f by the means of an *isothermal* process is equal to the increase of the system's free energy ΔF, $\Delta F = F_f - F_i$, only if the process is carried out *quasistatically.* That is the variation of the external parameters must be so slow that the system is at any instant in the state of thermodynamic equilibrium with the heat bath (the environment). Theoretically such a process would take an infinite time. Contrary to this, any finite-time process is accompanied by the dissipation and the required work fulfills $w \geq \Delta F$. The extra amount of work performed on the system during the nonequilibrium process as compared to the equilibrium one is dissipated as heat which is accepted by the heat bath. The Crooks fluctuation theorem [184, 185] states something remarkable. Consider the process $i \to f$, carried out at *an arbitrary*

---

[1]The mechanical definition of work is used whenever it is meaningful to split the total potential energy U into two contributions: $U = U_0(x) + U_{ext}(x, t)$, the first being an intrinsic time-independent potential and the second describes the external driving. Then the "mechanical work", $\delta W_{mech} = -(\partial U_{ext}/\partial x)dx$, satisfies the integrated first law of the form $\Delta U_0 = Q(t) + W_{mech}(t)$.

rate. At the initial state i the system resides in a thermal equilibrium and the external potential is equal to $U(x, 0)$. Afterwards, in a finite time interval $[0, t]$, the potential is varied according to a given (forward) protocol $U(x, \tau)$, $\tau \in [0, t]$. Then the PDF of the work performed on the particle during the described nonequilibrium process fulfills

$$\frac{p(w, t)}{p_{\mathrm{R}}(-w, t)} = \exp[\beta(w - \Delta F)], \tag{4.6}$$

where $1/\beta = k_{\mathrm{B}}T$ is the thermal energy, and $p_{\mathrm{R}}(w, t)$ stands for the PDF of the work performed on the particle during the *reversed process*: the process that departs from the equilibrium state f (in this state the potential is equal to $U(x, t)$) and, during the process, the potential is varied according to the time-reversed protocol $U(x, t - \tau)$, $\tau \in [0, t]$.

If we multiply the both sides of the Crooks theorem by $p_{\mathrm{R}}(-w, t)\mathrm{e}^{-\beta w}$ and then integrate over all possible values of w we obtain perhaps the most widely known fluctuation theorem, the Jarzynski equality [186]

$$\int_{-\infty}^{+\infty} \mathrm{d}w\, \mathrm{e}^{-\beta w} p(w, t) = \left\langle \mathrm{e}^{-\beta \mathbf{W}(t)} \right\rangle = \mathrm{e}^{-\beta \Delta F}. \tag{4.7}$$

The equality relates the free energy difference between two equilibrium configurations of the system to the exponential average of the work done during a finite-time far-from-equilibrium (forward) process.

Notice that the both above relations are perfectly consistent with the classical thermodynamics. If the process $i \to f$ is reversible, then the work done during the reversed process has exactly the same distribution as that in the forward one and the Crooks relation implies that $w = \Delta F$. This should be understood in the sense that the work loses its stochastic nature and it simply becomes a number. On the other hand, for an arbitrary process the Jensen relation $\langle \mathrm{e}^x \rangle \geq \mathrm{e}^{\langle x \rangle}$ applied on the Jarzynski equality gives us $\langle \mathbf{W}(t) \rangle \geq \Delta F$.

The both fluctuation theorems provide us a completely new possibility how to measure equilibrium thermodynamic properties of small systems. Instead of trying to perform an equilibrium manipulation e.g. with the single RNA macromolecule, one can carry out a far-from-equilibrium experiment and use one of the fluctuation theorems to recover the free energy differences. The latter procedure is favorable in systems with complex free-energy landscapes where the condition of equilibrium manipulation cannot be achieved in a reasonable time. Indeed, the Crooks fluctuation theorem has been experimentally used e.g. in RNA pulling experiments with optical tweezers [187] proving to be a reliable tool for extracting the free energy differences. In the (bidirectional) experiment the both distributions $p(w, t)$ and $p_{\mathrm{R}}(-w, t)$ are measured, then, according to Eq. (4.6), ΔF equals to value of w at which the two histograms $p(w, t)$, $p_{\mathrm{R}}(-w, t)$ intersect when plotted against the common w axis.

In situations when the forward and reverse work distributions are separated by a large gap on the w axis the above bidirectional method is biased by a rather large error [188]. In these cases, the Jarzynski equality, or its modification due to Hummer and Szabo [189] can be used to extract ΔF from a unidirectional experiment only [190–196]. In general, however, the application of Eq. (4.7) can be difficult, because the exponential average $\langle \exp[-\beta \mathbf{W}(t)] \rangle$ is dominated by rare trajectories with exceptionally low work values $w \ll \Delta F$. In experiments these rare trajectories are almost never observed and even in computer simulations it is difficult to generate them with a sufficient statistical weight. A possible solution is to extend measured histograms to the tail regime $w \ll \Delta F$ by fitting to theoretical predictions. To this end, some generic behavior in the tail regime needs to be assumed and attempts have been made recently in this

direction [197–199]. For example, in the case of DNA/RNA unfolding, Palassini and Ritort [197] suggested that the lower tail of the work distribution is unbounded and decays as

$$p(w,t) \sim \frac{q}{\Omega} \left(\frac{|w - w_c|}{\Omega} \right)^{\nu} e^{-\left(\frac{|w-w_c|}{\Omega} \right)^{\delta}}, \qquad w \to -\infty, \tag{4.8}$$

with $q > 0$ and $\Omega > 0$, w_c is a characteristic work value. For the Jarzynski equality (4.7) to hold, it needs to be either $\delta > 1$, or $\Omega < 1$ and $\delta = 1$. Interestingly, the asymptotic behavior of the work distribution for a driven Brownian particle in a harmonic potential was found to satisfy Eq. (4.8) with $\delta = 1$ and $\nu = -1/2$ [199,200]. One of the important results of the analysis presented in the next chapter is that Eq. (4.8) holds with $\delta = 1$ also for an asymmetric and anharmonic potential, the exponent ν in this case quantifies a degree of anharmonicity.

A further information on experiments with single biomolecules (mechanical manipulation of biomolecules by optical tweezers, or an atomic force microscope) can be found e.g. Refs. [201–207]. Recent progress in fluctuation theorems and free energy recovery is reviewed in Ref. [188].

The above discussion may evoke an impression that the work fluctuations are observable in small systems only. Notice, however, that both the Jarzynski equality and the Crooks theorem does not refer explicitly to the system size. As a matter of fact, the two fluctuation theorems have been confirmed in an experiment involving a macroscopic torsional pendulum [208,209]. See also Ref. [210] for an experiment with a granular gas.

4.3 Further reading

The stochastic thermodynamics, despite its long history [211], experiences a rather rapid development in recent years. The growing interest in the field is certainly stimulated by discoveries of fluctuation theorems (FTs). Two prominent examples of FTs, the Crooks theorem and the Jarzynski equality, have been discussed in Sec. 4.2. The theorems are remarkable for their generality and they extend our understanding of thermodynamics far beyond its original area of validity (i.e., to small systems driven arbitrarily far from the thermal equilibrium). Besides new relationships for free-energy differences, the theorems resulted in a long-awaited breakthrough in our understanding of how macroscopic irreversibility (dictated by the second law) emerges from a time-reversal symmetric microscopic dynamics [212].

Probably the first appearance of fluctuation relations in the literature can be found in papers by Bochkov and Kuzovlev [213,214]. The two works, however, have remained unnoticed until recently, see Refs. [182,183,215] for detailed discussion. A fluctuation theorem for entropy production was first observed in simulations of sheared fluids by Evans et al. [216,217]. Shortly after that a related FT for the deterministic dynamics has been proven by Gallavotti and Cohen [218], for the Langevin dynamics by Kurchan [219], and for fairly general Markov processes by Lebowitz and Spohn [220] and Maes [221]. The (experimental) usefulness of fluctuation relations has been recognized after Jarzynski [186,222] and Crooks [184,185] demonstrated how to relate equilibrium quantities to non-equilibrium work measurements. A fluctuation theorem (analogous to Jarzynski equality) that applies to transitions between two different non-equilibrium steady states has been derived by Hatano and Sasa [223].

Since 2000 a number of significant contributions to stochastic thermodynamics and to fluctuation theorems have been published (see e.g. Refs. [224–235] to name just a few). Fortunately, the rapidly growing amount of literature has became a subject

of numerous reviews, lecture notes and introductory texts [35, 212, 236–250]. In particular, for a pedagogical introduction to fluctuation relations and related topics we recommend recent book [249]. For a comprehensive overview of the stochastic thermodynamics including the fluctuation relations, their classification and interrelations see the review by Seifert [35], which is possibly the most complete survey in the field. Further, nonequilibrium work relations for Langevin dynamics are summarized by Kurchan [242]. Fluctuation theorems for the systems governed by the Master equation are reviewed by Harris and Schütz [243]. For other reviews focusing on different aspects related to fluctuation relations we refer to Van den Broeck [247] (performance of Brownian machines), Sevick et al. [212] (irreversibility of macroscopic dynamics), Maes [237, 238] (entropy in out-of-equilibrium systems), Ritort [204, 239] and Bustamante et al. [240] (FTs from experimental perspective), and Gaspard [241] (statistical mechanics based on Hamiltonian dynamics).

Finally, it should be noted that also quantum versions of FTs are nowadays subject to an active (mainly theoretical) development. For the reviews we refer to Refs. [251, 252].

5. Work distribution in logarithmic-harmonic potential

5.1 Definition of the model

Consider an overdamped motion of a Brownian particle in the logarithmic-harmonic potential

$$U(x,t) = -g\log(x) + \frac{1}{2}k(t)x^2, \quad g > 0, \quad x > 0, \tag{5.1}$$

where the parameter g specifies the strength of the logarithmic part and $k(t)$ is a time-dependent force constant. The potential is illustrated in Fig. 5.1 for two values of g. For $g < 0$, the potential tends to minus infinity as coordinate x approaches the origin from the right. For $g > 0$ the logarithmic part grows to positive infinity as $x \to 0^+$ and the whole potential forms an asymmetric and anharmonic potential well, cf. Fig. 5.1 b). We always assume the latter setting.

In the deterministic limit, i.e., in absence of thermal noise, the particle moves along the positive x-axis as driven by the time-dependent force $\mathcal{F}(x,t) = -\partial U/\partial x$ (without inertia). Taking into account the thermal noise, the combined process $\{\mathbf{X}(t), \mathbf{W}(t)\}$ is described by the system of Langevin equations

$$d\mathbf{X}(t) = \left[\frac{g}{\mathbf{X}(t)} - k(t)\mathbf{X}(t)\right]dt + \sqrt{2D}\,d\mathbf{B}(t), \tag{5.2}$$

$$d\mathbf{W}(t) = \frac{1}{2}\dot{k}(t)\mathbf{X}^2(t)\,dt, \tag{5.3}$$

where D quantifies the strength of the noise, $\mathbf{B}(t)$ is the standard Wiener process and $\dot{k}(t)$ stands for the time derivative of force constant $k(t)$. Specifically, the noise strength is proportional to the heat-bath temperature, $D = k_{\mathrm{B}}T$ (the particle mobility is set to one). The first equation is nothing but the Langevin equation (4.1), the second equation follows from the definition (4.4) where we have replaced the symbol "δ", which emphasized that the work is not a state function, by the differential symbol "d" which is more common for Langevin equations.

Primarily we are interested in the distribution of work performed on the particle when the potential $U(x,t)$ changes in time according to the prescribed protocol $k(t')$, $t' \in [0,t]$. Because the work is a functional of the whole stochastic trajectory, e.g. in the present case we have

$$\mathbf{W}(t) = \frac{1}{2}\int_0^t dt'\, \dot{k}(t')\mathbf{X}^2(t'), \tag{5.4}$$

it is not easy to gain an explicit insight into behavior of work distributions in far-from-equilibrium processes. Hence in general exact analytical results can be obtained only in a few exceptional cases. An analytical progress is possible for Markovian two level systems driven by a time-dependent external field [205,206,253–257] and for continuous diffusive systems driven by simple (harmonic as a general rule) external potentials [198–200, 258–277]. The present work broadens the second group adding there exact results for the anharmonic and asymmetric potential. In particular, setting $g = 0$, our model reduces to the so called "breathing parabola" model. The work PDF for the breathing parabola model has been studied analytically in Refs. [198], [199], [274], [275], [276] and [277]. In Refs. [198], [199], the authors considered an expansion around a single trajectory attributed to a prescribed rare value of the work and derived asymptotic
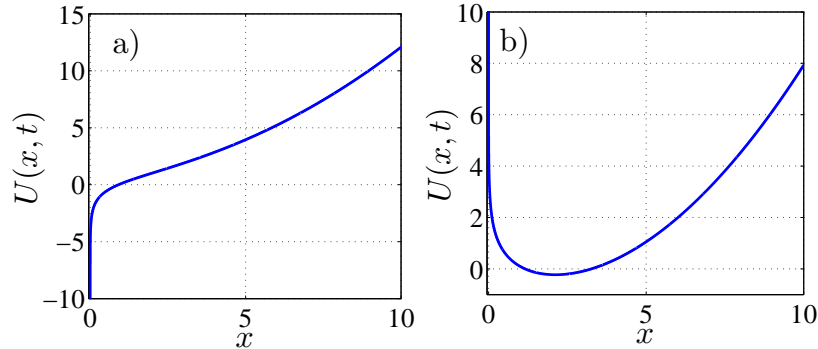
Figure 5.1: Sketch of the potential in Eq. (5.1) for $k(t) = 0.2$ and a) negative $g = -0.9$ and b) positive $g = 0.9$. The analysis in the main text corresponds to the case b) $g \geq 0$. Decreasing the force constant $k(t)$, the well broadens and its minimum shifts further from the origin.

results for the tails of the work PDF in the small the small limit of vanishing noise. The solution reported in [274] is formally exact for arbitrary protocol $k(t)$, explicit results are given in the limit of slow driving, when the process is close to a quasi-static equilibrium and the work PDF can be approximated by a Gaussian. In Ref. [275] the work-weighted propagator was derived by the path integral method. In Ref. [276] the Onsager-Machlup's formalism is discussed. Ref. [277] extends the analysis beyond an overdamped limit. Another closely related setting, where the work PDF can be calculated analytically, is for a parabolic potential with a time-dependent position of the minimum ("sliding parabola"). See Refs. [258–273] for a further discussion of different analytical approaches which yield distributions of work, heat, and power in the latter model.

Finally it should be noted that the exact PDF of the particle position for the logarithmic-harmonic potential was obtained in Refs. [278, 279]. In the following, we recover this result as a byproduct of the Lie algebraic approach to the solution of the Fokker-Planck equation for the combined process $\{\mathbf{X}(t), \mathbf{W}(t)\}$. The solvability of this problem stems from the fact that the operators entering the Fokker-Planck equation form a Lie algebra [280–282]. More precisely, if one considers the Fokker-Planck equation for the joint PDF of position and work (cf. Eq. (5.13)), the corresponding differential operators no *do not* generate a Lie algebra. However, if one starts with the Fokker-Planck equation for the joint PDF and performs a Laplace transformation with respect to the work variable w, a Lie algebraic structure is recovered. Solution of the Fokker-Planck equation then provides the characteristic function for the work process. Then the moments of the work distribution may be obtained by taking an appropriate derivative of the characteristic function. The tails of the work PDF can be extracted using asymptotic analysis of Laplace transforms. The present chapter is based on Ref. [200].

5.2 Solution of the Fokker-Planck equation for arbitrary protocol

5.2.1 Green function for logarithmic potential

An important auxiliary quantity in deriving all subsequent results is the Green function

$$q(x,t|x_0) = \exp\left[t\left(\frac{\partial^2}{\partial x^2} - \frac{g}{D}\frac{\partial}{\partial x}\frac{1}{x}\right)\right]\delta(x-x_0), \quad x_0 > 0, \tag{5.5}$$

which represents the solution of the Fokker-Planck equation

$$\frac{\partial}{\partial t}q(x,t|x_0) = \left(\frac{\partial^2}{\partial x^2} - \frac{g}{D}\frac{\partial}{\partial x}\frac{1}{x}\right)q(x,t|x_0), \qquad q(x,0|x_0) = \delta(x-x_0), \tag{5.6}$$

for the diffusion in the time-independent logarithmic potential. In the mathematical literature the diffusion process described by the Fokker-Planck equation (5.6) is known as the *Bessel process* [283, 284]. It represents e.g. the diffusion of the radial coordinate of a Brownian particle in d-dimensional space ($g \propto (d-1)$). Notably, the diffusion in the logarithmic potential has recently regained a considerable attention of the physical community due to its frequent occurrence in real situations [285], rich first-passage proprties [286] and intriguing relaxation behavior [287–292].

Let us now present the explicit form of the Green function. Notice that for a further convenience the above equation is written in the rescaled time variable, $tD \to t$, and hence the diffusion constant appears in the combination with parameter g of the logarithmic potential. The fraction (g/D) determines the relative strength of the logarithmic potential as compared to the strength of thermal fluctuations. One of the peculiarities of the diffusion in the logarithmic potential is the following (see e.g. Ref. [284]). When the potential "is weak" as compared to the strength of thermal fluctuations, the particle may reach the origin despite the fact that the potential diverges at $x = 0$ (cf. Fig. 5.1, panel b)). This may happen when

$$g/D < 1. \tag{5.7}$$

In this case, we assume that there is a *reflecting boundary* placed at $x = 0$ (since we do not want to let the diffusing particle to escape from the log-harmonic well). On the other hand, when the logarithmic potential "is sufficiently strong", the probability that the particle will ever hit the origin equals to zero. This holds true when

$$g/D \geq 1. \tag{5.8}$$

In the latter case we do not need to prescribe a boundary condition at the origin.

The explicit form of the Green function that satisfies the above boundary conditions is given by

$$q(x,t|x_0) = \frac{x_0}{2t}\left(\frac{x}{x_0}\right)^{\nu+1}\exp\left(-\frac{x^2+x_0^2}{4t}\right)\mathrm{I}_\nu\left(\frac{xx_0}{2t}\right), \tag{5.9}$$

where $\mathrm{I}_\nu(.)$ is the modified Bessel function of order ν,

$$\nu = \frac{1}{2}\left(\frac{g}{D}-1\right), \qquad \nu \geq -\frac{1}{2}. \tag{5.10}$$

In all subsequent results the parameter g enters solely through combination ν defined in Eq. (5.10). In particular, the combination ν will determine the exponent of the pre-exponential factor of the asymptotic behavior of the work PDF for $|w| \to \infty$. We will

demonstrate that the resulting asymptotic formula is precisely of the form of Eq. (4.8) (cf. Eq. (5.50)), where the symbol ν in (4.8) agrees with its present meaning (5.10).

Equation (5.9) is the unique norm-preserving solution of the diffusion problem in the domain $x \geq 0$, i.e., the probability current at $x = 0$ vanishes. Therefore, performing the limit $g \to 0$ and using $I_{-1/2}(z) = \sqrt{2/\pi} \cosh(z)/\sqrt{z}$, we obtain the standard solution for free diffusion with a reflecting boundary at $x = 0$:

$$\lim_{g \to 0} q(x, t|x_0) = \frac{1}{\sqrt{4\pi t}} \left[e^{-(x-x_0)^2/4t} + e^{-(x+x_0)^2/4t} \right]. \tag{5.11}$$

5.2.2 Joint Green function for work and position

Let us denote by $p(x, w, t|x_0, 0)$ the joint PDF for the process $\{\mathbf{X}(t), \mathbf{W}(t)\}$ given that at time $t = 0$ the particle is at position x_0, $x_0 > 0$, and no work has been done on it yet,

$$p(x, w, 0|x_0, 0) = \delta(x - x_0)\delta(w), \qquad x_0 > 0. \tag{5.12}$$

The time evolution of the joint PDF is given by the Fokker-Planck equation

$$\frac{\partial}{\partial t} p(x, w, t|x_0, 0) = \left[D \frac{\partial^2}{\partial x^2} - \frac{\partial}{\partial x} \left(\frac{g}{x} - k(t)x \right) - \frac{1}{2}\dot{k}(t)x^2 \frac{\partial}{\partial w} \right] p(x, w, t|x_0, 0). \tag{5.13}$$

The differential operators on the right-hand side *do not* possess closed commutation relations. However, after performing the two-sided Laplace transformation [293]

$$\widetilde{p}(x, \xi, t|x_0) = \int_{-\infty}^{+\infty} dw\, e^{-\xi w} p(x, w, t|x_0, 0), \tag{5.14}$$

the Fokker-Planck equation (5.13) assumes the form

$$\frac{\partial}{\partial t}\widetilde{p}(x, \xi, t|x_0) = \left[D\widehat{J}_0 + 2k(t)\widehat{J}_1 - 4\xi\dot{k}(t)\widehat{J}_2 + (\nu + 1)k(t) \right] \widetilde{p}(x, \xi, t|x_0), \tag{5.15}$$

where the differential operators

$$\widehat{J}_0 = \frac{\partial^2}{\partial x^2} - \frac{g}{D}\frac{\partial}{\partial x}\frac{1}{x}, \qquad \widehat{J}_1 = \frac{1}{2}\left(x\frac{\partial}{\partial x} - \nu \right), \qquad \widehat{J}_2 = \frac{1}{8}x^2, \tag{5.16}$$

satisfy the *closed* commutation relations

$$[\widehat{J}_0, \widehat{J}_1] = \widehat{J}_0, \qquad [\widehat{J}_0, \widehat{J}_2] = \widehat{J}_1, \qquad [\widehat{J}_1, \widehat{J}_2] = \widehat{J}_2. \tag{5.17}$$

This allows us to derive the exact solution of Eq. (5.15) by the Lie algebraic method, as discussed, e.g., in Refs. [280–282]. First, we write the solution of Eq. (5.15) in the factorized form

$$\widetilde{p}(x, \xi, t|x_0) = \exp\left[(\nu+1)\int_0^t dt'k(t') \right] \exp\left[b_2(t)\widehat{J}_2 \right] \exp\left[b_1(t)\widehat{J}_1 \right] \exp\left[b_0(t)\widehat{J}_0 \right] \delta(x - x_0), \tag{5.18}$$

then we use commutation relations (5.17) to derive the ordinary differential equations for time-dependent coefficients $b_0(t)$, $b_1(t)$, $b_2(t)$. After some algebra, it turns out that the coefficient $b_2(t)$ satisfies the Riccati differential equation

$$\dot{b}_2(t) = \frac{D}{2}b_2^2(t) + 2k(t)b_2(t) - 4\xi\dot{k}(t), \qquad b_2(0) = 0. \tag{5.19}$$

Assume we are able to solve this equation. Then the other coefficients are given by

$$b_1(t) = 2\int_0^t dt'k(t') + D\int_0^t dt'b_2(t'), \quad b_0(t) = D\int_0^t dt'e^{b_1(t')}. \tag{5.20}$$

65

In the last step, we act, using Eqs. (5.5) and (5.9), with the operator $\exp\left[b_0(t)\widehat{J}_0\right]$ on the delta function in Eq. (5.18), and subsequently we apply to the emerging result the two remaining exponential operators in Eq. (5.18). This yields

$$\widetilde{p}(x,\xi,t|x_0) = \exp\left[\int_0^t \mathrm{d}t'k(t') - \frac{1}{2}\nu D\int_0^t \mathrm{d}t'b_2(t') + \frac{1}{8}b_2(t)x^2\right]q(xe^{\frac{1}{2}b_1(t)}, b_0(t)|x_0). \quad (5.21)$$

In the derivation we have utilized the operator identity

$$\exp\left(\eta x\frac{\partial}{\partial x}\right)f(x) = f\left(xe^\eta\right). \quad (5.22)$$

The exact solution (5.21) is the central result of the present section and it constitutes the starting point of all subsequent analyses.

It should be noted that the Laplace-transformed Fokker-Planck operator in Eq. (5.15) is a linear combination of generators of the Lie algebra of $SU(1,1)$ group. However, instead of standard generators [294], we prefer to use the operators (5.16). The advantage of the present approach is that it treats the boundary conditions in a very natural and straightforward way. Indeed, the exact solution (5.21) is built on the basis of Green function $q(x,t|x_0)$ which ensures that also for the dynamics described by the transformed Green function (5.21) the probability current through the origin $x = 0$ vanishes (see Sec. 5.2.1 for a discussion of boundary conditions).

5.3 PDF of particle position and its long-time asymptotics

After integrating the joint PDF $p(x,w,t|x_0,0)$ over the work variable, the transition PDF $p(x,t|x_0)$ for the particle coordinate alone is obtained. Equivalently, the w-integration is accomplished by evaluating the result (5.21) at $\xi = 0$. Notice that the variable ξ enters the solution (5.21) only through the Riccati equation (5.19). When taking $\xi = 0$, this equation reduces to the Bernoulli differential equation, where the unique solution satisfying $b_2(0) = 0$ is the trivial one, $b_2(t) = 0$. The remaining coefficients in Eq. (5.21) are then given by

$$b_1(t) = 2\int_0^t \mathrm{d}t'k(t'), \qquad b_0(t) = D\int_0^t \mathrm{d}t'\exp\left[2\int_0^{t'}\mathrm{d}t''k(t'')\right]. \quad (5.23)$$

Hence the PDF for the particle position reads[1]

$$p(x,t|x_0) = \frac{x_0\,e^{\frac{\nu+2}{2}b_1(t)}}{2b_0(t)}\left(\frac{x}{x_0}\right)^{\nu+1}\exp\left(-\frac{x^2e^{b_1(t)}+x_0^2}{4b_0(t)}\right)\mathrm{I}_\nu\left(\frac{xx_0\,e^{\frac{1}{2}b_1(t)}}{2b_0(t)}\right). \quad (5.24)$$

This result is valid for an arbitrary driving protocol $k(t)$. If $k(t)$ is a positive constant, say $k(t) = k_0$, and $k_0 > 0$, then the system approaches the Gibbs canonical equilibrium at long times. If the constant force is superimposed with a periodically oscillating component, a gradual constitution of a nontrivial steady state occurs. In this steady state, the PDF does not depend on the initial condition x_0 and, for any given $x > 0$, it is a periodic function of time with the fundamental period given by that of $k(t)$.

To exemplify the PDF in the steady state, let us take

$$k(t) = k_0 + k_1\sin(\omega t), \qquad k_0 > 0. \quad (5.25)$$

---

[1]This result agrees with Eq. (19) in Ref. [278], where it has been derived in connection with a diffusion problem with logarithmic factors in drift and diffusion coefficients. See also Refs. [279, 295].

The asymptotic analysis of Eq. (5.24) for long times requires the evaluation of the limit

$$\lim_{t \to \infty} \frac{e^{\alpha\, b_1(t)}}{b_0(t)}, \quad \alpha \leq 1 \ . \tag{5.26}$$

If $\alpha < 1$, the limit exists and, using L'Hôpital's rule, it equals zero. Hence for any finite x and x_0, the argument $z = xx_0 e^{b_1(t)/2}/[2b_0(t)]$ in the Bessel function appearing in Eq. (5.24) becomes small for large t and we can write $I_\nu(z) \sim (\frac{1}{2}z)^\nu/\Gamma(\nu+1)$. If $\alpha = 1$, the limit does not exist and $e^{b_1(t)}/b_0(t) \sim 1/f(t)$ for $t \to \infty$, where

$$f(t) = D \exp\left[\frac{2k_1}{\omega}\cos(\omega t)\right] \sum_{n=-\infty}^{+\infty} I_n\left(-\frac{2k_1}{\omega}\right) \frac{e^{in\omega t}}{2k_0 + in\omega}, \quad k_0 > 0. \tag{5.27}$$

Accordingly, for $t \to \infty$ we have

$$p(x,t|x_0) \sim p_{\text{as}}(x,t) = \frac{1}{\Gamma(\nu+1)}\left(\frac{1}{f(t)}\right)^{\nu+1}\left(\frac{x}{2}\right)^{2\nu+1}\exp\left[-\left(\frac{x}{2}\right)^2\frac{1}{f(t)}\right] \ . \tag{5.28}$$

In the limit $k_1 \to 0$ or $\omega \to 0$, $f(t) \to D/(2k_0)$, and $p(x,t|x_0)$ approaches the Gibbs equilibrium distribution.

Finally, the limit $g \to 0$ in Eq. (5.24) yields the exact transition PDF for the breathing parabola model with reflecting boundary at the origin. Correspondingly, Eq. (5.28) yields exact time-asymptotic PDF in the same model. Since the parameter g enters only via ν defined in Eq. (5.10), $g \to 0$ limit corresponds to $\nu \to -1/2$ in Eqs. (5.24), (5.28).

5.4 Work fluctuations

5.4.1 Characteristic functions

By integration of the joint PDF in Eq. (5.21) over the spatial variable x, we obtain the characteristic function for the work done on the particle during the time interval $[0,t]$.

Let us first consider the particle dynamics conditioned on the initial position x_0. In this case the characteristic function for the work reads

$$\Phi(\xi,t|x_0) = \int_0^{+\infty} dx\, \widetilde{p}(x,\xi,t|x_0) \ . \tag{5.29}$$

At the same time the, this function is the two-sided Laplace transformation of the work PDF conditioned on x_0 (cf. Eq. (5.14)). Carrying out the spatial integration of the formula (5.21), we find

$$\Phi(\xi,t|x_0) = \left(\frac{2e^{b_1(t)-\frac{1}{2}D\int_0^t dt' b_2(t')}}{2e^{b_1(t)} - b_0(t)b_2(t)}\right)^{\nu+1}\exp\left[\frac{b_2(t)}{2e^{b_1(t)} - b_0(t)b_2(t)}\left(\frac{x_0}{2}\right)^2\right] \ . \tag{5.30}$$

A physically more important situation is when the particle coordinate is initially equilibrated with respect to the initial value $k(0) = k_0$, $k_0 > 0$, of the force constant. In order to obtain the characteristic function for this situation we have to integrate over x_0 the product of the conditioned characteristic function $\Phi(\xi,t|x_0)$ and the equilibrium PDF p_{eq} which is given by the right-hand side of Eq. (5.28) with $f(t) = D/(2k_0)$. The result of this integration is

$$\Phi(\xi,t) = \left\langle e^{-\xi \mathbf{W}(t)}\right\rangle = \left(\frac{4k_0 e^{b_1(t)-\frac{1}{2}D\int_0^t dt' b_2(t')}}{4k_0 e^{b_1(t)} - [D + 2k_0 b_0(t)]\, b_2(t)}\right)^{\nu+1} \ . \tag{5.31}$$

Notice that equation (5.31) is valid for an arbitrary driving protocol $k(t)$. The Laplace variable ξ enters $\Phi(\xi, t)$ through coefficients $b_i(t)$, $i = 0, 1, 2$ (cf. the Riccati equation (5.19) and Eqs. (5.20)). In particular, for $\xi = \beta$, $\Phi(\beta, t)$ is nothing but the exponential average that appears in the Jarzynski equality (4.7) (notice that in the present setting we have $\beta = 1/D$ since the particle mobility is set to one).

In the limit $g \to 0$ ($\nu \to -1/2$), Eqs. (5.30), (5.31) give the corresponding characteristic functions for the breathing parabola model *with reflecting boundary at $x = 0$*. These characteristic functions are also valid for the breathing parabola model *without reflecting boundary*, if rather obvious changes are made of the meaning of the initial coordinate x_0 in Eq. (5.30), and of the initial Gibbs equilibrium state underlying Eq. (5.31). In the breathing parabola model without reflecting boundary, Eq. (5.30) is valid for $x_0 \in (-\infty, +\infty)$ and Eq. (5.31) corresponds to the initial Gibbs equilibrium in the parabolic potential $U(x_0) = k_0 x_0^2/2$. The equivalence of the characteristic functions for the problems with and without reflecting boundary is due to the symmetry of the parabolic potential, which implies that *the work done on the particle that crosses the origin is the same as the work done on the particle reflected at the origin.* This reasoning (which is a kind of the reflection principle for the work variable) can be supported by an independent calculation if one notices that both models, the present model with the logarithmic-harmonic potential and the breathing parabola one, possess the same operator algebra.

5.4.2 Simple example

A reasonable example of a driving protocol which allows for an explicit solution of the Riccati equation (5.19) in terms of elementary functions can be given, is

$$k(t) = \frac{k_0}{1 + \gamma t}, \quad k_0 > 0, \quad \gamma > 0. \tag{5.32}$$

Notice that the same protocol was considered in Refs. [198, 199].

Solution of the Riccati equation

In order to study work fluctuations for the protocol (5.32) the Riccati equation (5.19) needs to be solved. This nonlinear differential equation is equivalent to the linear second-order differential equation with variable coefficients [296]

$$\ddot{y}(t) - 2k(t)\dot{y}(t) - 2D\xi \dot{k}(t)y(t) = 0, \qquad \dot{y}(0) = 0. \tag{5.33}$$

Specifically, if $y(t)$ solves Eq. (5.33), then the logarithmic derivative

$$b_2(t) = -\frac{2}{D} \frac{\dot{y}(t)}{y(t)} \tag{5.34}$$

is the solution of Eq. (5.19).

For the sake of transparency, let us take $k_0 = 1$, $\gamma = 1$. Then the second order equation (5.33) with the protocol (5.32) can be written as

$$\frac{d}{dt} \left[(1 + t)^2 \dot{y}(t) \right] = 2D\xi \, y(t). \tag{5.35}$$

The above equation suggests that we may look for the solution of the form

$$y(t) = (1 + t)^\lambda, \tag{5.36}$$

where λ is an unknown constant to be determined. After introducing the ansatz (5.36) into Eq. (5.35) the quadratic equation for λ is obtained:

$$\lambda(\lambda + 1) = 2D\xi. \tag{5.37}$$

Hence the general solution of Eq. (5.35) is given by

$$y(t) = C_1(1 + t)^{\lambda_1} + C_2(1 + t)^{\lambda_2} \tag{5.38}$$

where $\lambda_{1,2}$ are the two solutions of the quadratic equation (5.37). The general solution (5.38) contains two undetermined constants C_1, C_2. One of the constants is ruled out by the initial condition $\dot{y}(0) = 0$:

$$C_1\lambda_1 + C_2\lambda_2 = 0. \tag{5.39}$$

Having eliminated one of the two constants, the solution (5.38) will be proportional to the remaining one. The actual value of the remaining (nonzero) constant is irrelevant since the sought-after function $b_2(t)$ is proportional to the logarithmic derivative of $y(t)$, cf. Eq. (5.34).

The solution of the Riccati equation for general values of k_0, γ can be derived along the similar lines. After some algebra we get

$$b_2(t) = -\frac{2}{D}\frac{d}{dt}\log\left\{(1 + \gamma t)^{\frac{1}{2\gamma}[(2k_0+\gamma)-A(\xi)]}\left[(1 + \gamma t)^{A(\xi)} - \frac{(2k_0 + \gamma) + A(\xi)}{(2k_0 + \gamma) - A(\xi)}\right]\right\}, \tag{5.40}$$

where

$$A(\xi) = \sqrt{(2k_0 + \gamma)^2 - 8k_0\gamma D\xi}. \tag{5.41}$$

Work distribution

For the sake of transparency, we take $\gamma = 1$ and $k_0 = 1$ in the following. The exact expression for $b_2(t)$ can be integrated as required in Eqs. (5.20). This somewhat lengthy but straightforward calculation gives us functions $b_0(t)$ and $b_1(t)$, and eventually, the exact expression for the characteristic function (5.31) is obtained:

$$\Phi(\xi, t) = \left(\frac{2A(\xi)(1 + t)^{\frac{1}{2}[3+A(\xi)]}}{A(\xi)\left[(1 + t)^{A(\xi)} + 1\right] + (3 - 2D\xi)\left[(1 + t)^{A(\xi)} - 1\right]}\right)^{\nu+1}. \tag{5.42}$$

According to Eq. (5.32), the time derivative $\dot{k}(t)$ is negative, the potential well widens with time and hence Eq. (5.4) implies that the work done on the particle *is negative* for any $t > 0$ and for any trajectory. Therefore the domain of analyticity of $\Phi(\xi, t)$ is the complex half-plane $\text{Re}[\xi] < a$, where a, $a \in \mathbb{R}$, is the abscissa of convergence. The Jarzynski equality guarantees that the Laplace transform $\Phi(\xi, t)$ is well defined for $\xi = 1/D$. As a matter of fact, from Eq. (5.42), we have $\Phi(1/D, t) = \exp\left[(\nu + 1)\log(1 + t)\right]$. Hence even without any examination of formula (5.42) we know (on physical grounds) that it is certainly analytic when $\text{Re}[\xi] \leq 1/D$.

Successive derivatives of the characteristic function with respect to ξ evaluated at $\xi = 0$ yield the moments of the work distribution. The mean work done on the particle during the time interval $[0, t]$ is given by

$$\langle \mathbf{W}(t) \rangle = -(\nu + 1)\frac{D}{9}\left[6\log(1 + t) + \frac{t^3 + 3t^2 + 3t}{(1 + t)^3}\right]. \tag{5.43}$$

It is a monotonically decreasing function of t, where for small times, the decrease is linear, while in the long-time limit, it is logarithmic. For the variance we find

$$\left\langle [\mathbf{W}(t) - \langle \mathbf{W}(t) \rangle]^2 \right\rangle = (\nu + 1) \left(\frac{D}{9} \right)^2 \frac{t^3 + 3t^2 + 3t}{(1+t)^6}$$
$$\times \left[t^3 + 3t^2 + 3t + 24(1+t)^3 \log(1+t) \right]. \tag{5.44}$$

This increases monotonically, where the increase is quadratic for small times and logarithmic for long times. The strength g of the logarithmic potential barrier enters the above formulas only through the multiplicative prefactor $(\nu + 1)$. This holds true for all cumulants of the work. For stronger repulsion, the particle predominantly diffuses in a region further away from the origin. The decrease of its typical potential energy results in a larger absolute value of the mean work. At the same time, the width of the work PDF increases, since the initial particle position is sampled from a broader Gibbs distribution.

The characteristic function (5.42) entails the complete information about the work distribution $p(w,t)$. In particular it allows one to derive the tails of the work PDF for both $w \to 0^-$ and $w \to -\infty$ without carrying out the inverse Laplace transformation of the complete exact expression for $\Phi(\xi, t)$ [293].

The asymptotics of $p(w,t)$ for $w \to 0^-$ (at fixed t) is related to the asymptotics of $\Phi(\xi, t)$ for $\xi \to -\infty$, which follows from (5.42),

$$\Phi(\xi, t) \sim \left(\sqrt{8} \, (1+t)^{\frac{3}{2}} \frac{\exp\left[-\sqrt{2} \log(1+t) \sqrt{-D\xi} \right]}{\sqrt{-D\xi}} \right)^{\nu+1}, \quad \xi \to -\infty. \tag{5.45}$$

By taking the inverse Laplace transform of this asymptotic form (cf. Ref. [297]), we obtain a parabolic cylinder function (cf. Ref. [298]) with argument proportional to $\sqrt{D/|w|}$. Considering the limit of large arguments of this function [298], we find

$$p(w,t) \sim c_1(t) \left(\frac{|w|}{D} \right)^{\nu - \frac{1}{2}} e^{-c_2(t) \frac{D}{|w|}}, \quad w \to 0^-, \tag{5.46}$$

where

$$c_2(t) = \left[\frac{\nu+1}{\sqrt{2}} \log(1+t) \right]^2, \quad c_1(t) = \frac{1}{D} \sqrt{\frac{8}{\pi}} (1+t)^{\frac{3}{2}} \left[\frac{2(1+t)^{\frac{3}{2}}}{(\nu+1)\log(1+t)} \right]^{\nu}. \tag{5.47}$$

For any g and any t, the PDF almost vanishes in an interval $(w_c(t), 0)$, where its width $|w_c(t)|$ is controlled by the "damping constant" $c_2(t)$. The width increases both with time and the strength of the logarithmic potential. This can be understood from the fact that any trajectory yielding a small (absolute) value of the work, must necessarily depart from a position close to the origin and remain in its vicinity during the whole time interval $[0,t]$. The probabilistic weight of such trajectories decreases with both t and g.

The asymptotics of the work PDF $p(w,t)$ for $w \to -\infty$ (at fixed t) is determined by the expansion of the characteristic function $\Phi(\xi, t)$ at such $\xi_0(t)$, which represents the singularity of $\Phi(\xi, t)$ lying closest to its abscissa of convergence [293]. To find $\xi_0(t)$, we numerically solved the transcendental equation $1/\Phi(\xi_0(t), t) = 0$. In the vicinity of the singularity,

$$\Phi(\xi, t) \sim r(t) \left(-\frac{1}{D[\xi - \xi_0(t)]} \right)^{\nu+1}, \quad \xi \to \xi_0(t), \tag{5.48}$$
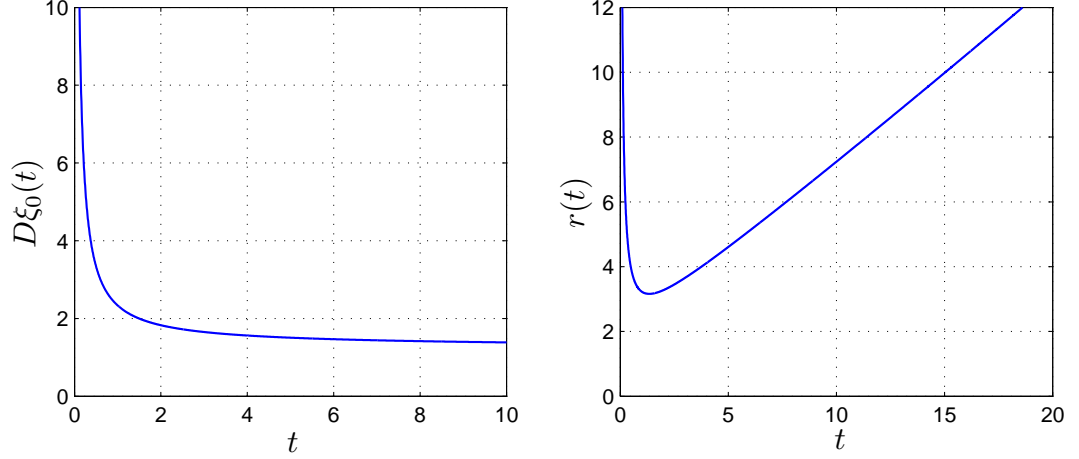
70

Figure 5.2: Positions of the singularity in the expression (5.48) (left panel), and the prefactor (5.49) (right panel) as functions of time. These functions control, through Eq. (5.50), the large $|w|$ asymptotics of the work PDF. In the right panel we have taken $D = 1$ and $g = 1$.
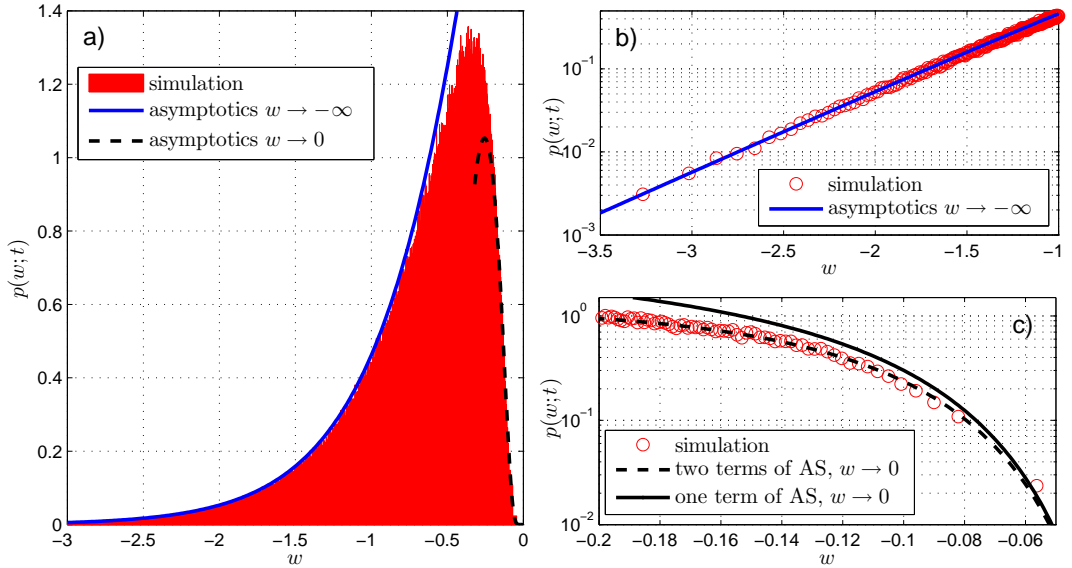

Figure 5.3: a) Simulated work PDF in comparison with the asymptotic behavior predicted by Eq. (5.50) ($|w|$ large, solid line) and Eq. (5.51) ($|w|$ small, dashed line) for parameters $g = 1.5$, $D = 1$ and $t = 1$. In the simulations 10^6 trajectories were generated with the time step $\Delta t = 0.001$ (adapted when the particle is near the origin, see text). b) Semi-logarithmic plot of simulated $p(w, t)$ vs. w (circles), demonstrating the agreement with Eq. (5.50) (solid line) for large $|w|$. c) Semi-logarithmic plot of simulated $p(w; t)$ vs. w (circles) in comparison with the first leading term of the asymptotic expansion for small $|w|$ (Eq. (5.46), solid line), and when including the second leading term according to Eq. (5.51) (dashed line).

with

$$r(t) = (-D)^{\nu+1} \lim_{\xi \to \xi_0(t)} [\xi - \xi_0(t)]^{\nu+1} \Phi(\xi, t). \tag{5.49}$$

From this result we obtain the required tail of the work PDF:

$$p(w, t) \sim \frac{1}{D} \frac{r(t)}{\Gamma(\nu+1)} \left(\frac{|w|}{D} \right)^{\nu} e^{-D\xi_0(t)\frac{|w|}{D}}, \qquad w \to -\infty, \tag{5.50}$$

where $D\xi_0(t)$ is a real, positive, decreasing function of t, it is plotted in Fig. 5.2 (the left panel). For small t, the work PDF is very narrow ($D\xi_0(t)$ large). With increasing t, the weight of the trajectories yielding large (absolute) values of the work increases. This is reflected by the decrease of $D\xi_0(t)$.[2] Contrary to the function $c_2(t)$ in (5.46), the present "damping constant" $D\xi_0(t)$ does not depend on the strength of the logarithmic potential. The parameter g enters only the pre-exponential factor in Eq. (5.50).

In order to verify the exact asymptotic expansions of the work PDF, we have performed extensive Langevin dynamics simulations using the Heun algorithm [299] for several sets of parameters and different time intervals. A typical PDF together with the predictions for its asymptotic behavior according to Eqs. (5.46) and (5.50) is shown in Fig. 5.3. In order to avoid nonphysical negative values of the particle position in the numerics, which can originate from a fixed time discretization, we have implemented a time-adapted Heun scheme. If a negative (attempted) coordinate along a trajectory is generated, the time step Δt is reduced until the attempted particle position is positive. In order to achieve a better agreement of the analytical asymptotic representation and the simulated data for small $|w|$ (cf. Fig. 5.3), we have derived also the second leading term in the asymptotic expansion for $|w| \to 0$. After somewhat lengthy but straightforward calculation, we obtain

$$p(w, t) \sim c_1(t) \left[\left(\frac{|w|}{D} \right)^{\nu-\frac{1}{2}} - \sqrt{\frac{4}{(\nu+1)\log(1+t)}} \left(\frac{|w|}{D} \right)^{\nu+\frac{1}{2}} \right] e^{-c_2(t)\frac{D}{|w|}}, \quad w \to 0^-, \tag{5.51}$$

where $c_1(t)$ and $c_2(t)$ are given in Eq. (5.47).

5.5   Summarizing remarks

In the present chapter, we have calculated the characteristic function for the work in a simple setting which, however, may be realized in experiments [300, 301]. Based on a Lie algebraic approach we have succeeded to derive the closed expression (5.21) for the joint PDF of work and position for a Brownian particle in a time-dependent anharmonic potential. In order to deduce further explicit results from Eq. (5.21) for a given driving protocol, the Riccati equation (5.19) needs to be solved. We have focused on the protocol (5.32) for which both the solution of the Riccati equation and the work characteristic function can be expressed in terms of elementary functions. The protocol should exemplify typical asymptotic features of the work PDF for *monotonic* external drivings. It has been shown that the tail of work PDF for large negative work values, cf. Eq. (5.50), is in agreement with the formula proposed by Palassini and Ritort, cf. Eq. (4.8), with $\delta = 1$ and ν being dependent on the strength of the logarithmic potential. The latter exponent, given by Eq. (5.10) in our model, can be interpreted as follows. Notice that ν is composed of two parts: $\nu = -1/2 + g/(2D)$. The first part is independent of the strength of the logarithmic potential ($\nu = -1/2$

---

[2]For $t = 2$ and $g = 0$ we obtain $D\xi_0(2) \dot{=} 1.827$, $r(2)/\Gamma(1/2) \dot{=} 1.021$, which is in perfect agreement with Eq. (5.30) in [199].
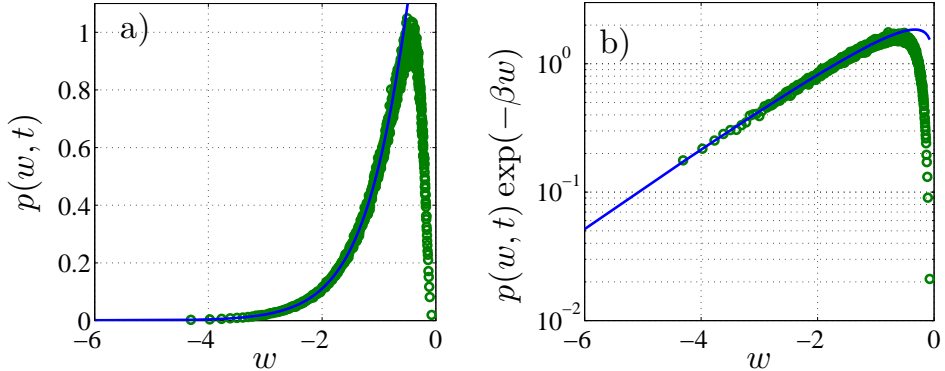
Figure 5.4: a) Simulated work distribution $p(w,t)$ (symbols) at time $t = 1$ for the protocol $k(t) = k_0 \exp(-\gamma t)$ with $k_0 = 1$, $\gamma = 1$, and parameters $g = 1.5$ and $D = 1$; in b) the associated Jarzynski integrand $p(w,t)\exp(-\beta w)$ is displayed in a semi-logarithmic representation. The solid blue line is a fit of Eq. (5.50) to the left tail. The best parameters are $r(1) \approx 2.833$, $D\xi_0(1) \approx 1.757$. In the simulations 10^6 trajectories were generated with time step $\Delta t = 10^{-3}$.

for the purely harmonic potential), and the second one quantifies the deviation of the external potential from the parabolic one. Thus the pre-exponential factor in the tail formula for the work PDF reflects the anharmonicity of the external potential.

The solution of the Riccati equation for several reasonable driving protocols, e.g., for the exponential protocol

$$k(t) = k_0 \exp(-\gamma t), \tag{5.52}$$

or for $k(t) = k_0 + k_1 t$, $k(t) = k_1 t^n$, can be written in terms of higher transcendental functions. Corresponding results are rather involved and are briefly discussed in App. C. In these cases, the complexity of the solution makes the analytical progress impossible. However, the sequence of steps used in the derivation of formula (5.50) suggests that the asymptotic form (5.50) should be applicable for any monotonous driving with nonuniversal (protocol-dependent) parameters $r(t)$, $D\xi_0(t)$. To test this hypothesis, the numerical analysis of the work PDF has been performed for the above mentioned protocols showing an excellent agreement with the formula (5.50). The outcome of the simulation for the exponential protocol is fitted by the formula (5.50) in Figs. 5.4, 5.5.

For *nonmonotonous* driving protocols the work can assume any real value. Then the work PDF has the support $(-\infty, +\infty)$ and its two-sided Laplace transform will be analytic within a stripe parallel to the imaginary axis. In this case, the $w \to +\infty$ tail of the work PDF is determined by the singularity, which is closest to the stripe on its left side, and $w \to -\infty$ tail is controlled by the closest singularity on the right side. We hence expect an asymptotics

$$p(w,t) \sim \frac{1}{D} \frac{r_\pm(t)}{\Gamma(\nu+1)} \left(\frac{|w|}{D}\right)^\nu e^{-D\xi_\pm(t)\frac{|w|}{D}} \quad , \quad w \to \pm\infty \; , \tag{5.53}$$

where the coefficients $\xi_\pm(t)$, $r_\pm(t)$, depend on the driving protocol $k(t)$. Periodic driving protocols play an important role in the analysis of Brownian motors. A deeper analysis of the work PDF for this class of protocols seems to be worthy of further study.

Interestingly enough, the validity of the derived results can be extended beyond the diffusion in the anharmonic potential with a *single* minimum. Namely, the reflection principle for the work variable presented in the last paragraph of Sec. 5.4.1 allows us to consider an anharmonic *bistable* potential. Indeed, for $g = 0$, the reflection principle
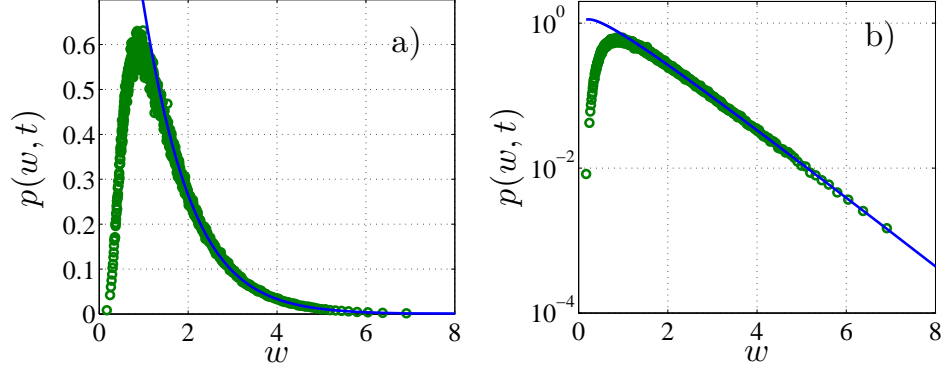
73

Figure 5.5: Simulated work distribution (symbols) at time $t = 1$ for a protocol $k(t) = k_0 \exp(-\gamma t)$ with $\gamma = -1$, and otherwise the same parameters as in Fig. 5.4. In a) $p(w,t)$ is plotted in a linear representation and in b) in a semi-logarithmic one. The solid blue line is a fit of Eq. (5.50) to the right tail with the best parameters are $r(1) \approx 1.916$, $D\xi_0(1) \approx 1.124$. In the simulations 10^6 trajectories were generated with time step $\Delta t = 10^{-3}$.

guarantees the equivalence of the work distributions in the present model (with the reflecting boundary at the origin) and in the parabolic one defined on the whole real line. Considering $g > 0$, the application of the reflection principle makes sense only if there exist trajectories which can reach the origin (where they are reflected). As we know, such trajectories indeed exist if $g/D < 1$, cf. Eq. (5.7). Assuming this condition, imagine that instead of the reflection at $x = 0$, the particle passes through the origin into the second log-harmonic well located on the negative half-line $x < 0$. More precisely, the reflection principle yields the equivalence of the work distributions in the present semi-infinite system described by the potential $U(x,t) = -g\log(x) + k(t)x^2/2$, $x > 0$, and in that described by the double-well potential $\widetilde{U}(x,t) = -g\log(|x|) + k(t)x^2/2$ defined for $x \in (-\infty, +\infty)$. Thus all conclusions concerning the work PDF in the present setting holds true also for the extended symmetric bistable model. (For the previous study of the work distribution in a bistable potential see Ref. [302].)

Conclusions and outlook

In the thesis we have concentrated on two topics. First, in Chaps. 1, 2 and 3 we have discussed the single-file diffusion. Second, in Chaps. 4, and 5 we have addressed stochastic thermodynamics and in particular the work distribution for the Brownian particle diffusing in the time-dependent anharmonic potential. We would like to emphasize that detailed concluding sections discussing main physical features of individual models are presented at the ends of Chaps. 2, 3, and 5, see Secs. 2.4, 3.4, and 5.5, respectively. Therefore, let us now mention some rather general aspects and outlook for the future.

As for the single-file diffusion, after the review of known results (Chap. 1), we have focused on the dynamics and first-passage properties of a tagged-particle in open single-file systems (Chaps. 2 and 3). The model is exactly solvable. This is guaranteed by the statistical equivalence of trajectories of interacting particles and the trajectories of noninteracting ones. In the thesis we have developed the mapping between two sets of trajectories for SFD in the presence of absorbing boundaries. The mapping has turned out to be particularly useful for derivation of exact one-time characteristics like PDF for position of a given tagged particle. Starting from this PDF, the effects induced by the presence of boundaries and by interparticle interactions were described in detail for various initial and boundary conditions (cf. Chaps. 2 and 3).

There are many directions in which the present analysis could be generalized. For instance, a challenging problem is to develop the probabilistic reasoning for the single-file system coupled to a reservoir of particles. Another still unsolved task is the exact description of a first-passage time for the setting, when only the tracer interacts with the absorbing boundary, whereas all other particles diffuse freely on an unbounded real line. A rather hard and important problem is SFD under the action of external forces. This setting opens the possibility to address, besides the dynamics itself, also the stochastic energetics of a tagged particle. Since the dynamics of a tagged particle becomes subdiffusive one expects anomalous fluctuation theorems to hold.

Notice that SFD model provides us an "exactly solvable playground" for our understanding of subdiffusion. Gaining an intuition with this particular model could significantly contribute to development of a theory for general anomalous dynamics.

As for the stochastic thermodynamics, in Chap. 4, after a brief review of basic notions (definitions of stochastic work and heat), we have discussed the two most widely known fluctuation theorems (the Crooks theorem and the Jarzynski equality) and their roles in free-energy measurements. Then, in Chap. 5, we have introduced and solved the model for the Brownian motion in the time-dependent anharmonic potential. For the model the exact form of the work characteristic function has been obtained. This success is based on the fact that (after the Laplace transform in work variable) the differential operators entering the Fokker-Planck equation possess closed commutation relations. This allowed us to reduce the Fokker-Planck equation for the joint PDF of work and position (using the Lie-algebraic method) to the Riccati equation and some quadratures. For the model, the PDF of the particle position can be derived in a closed form for any external driving. But it is just for a few specific driving protocols that characteristic function for work can be obtained in a closed form, yielding the desired information about the work PDF including all moments and the both tails.

The model clearly illustrates a disparity in our understanding of properties of the PDF for the particle position on one hand and of those of PDFs for energetic characteristics like work on the other. While the behavior of the PDF for the position is well understood for a wide range of external potentials, the opposite holds true for the corresponding work PDFs. To this end, the only general (well known) result is that near

equilibrium (slow driving) and in the vicinity of its maximum the work PDF could be approximated by a Gaussian function. Certainly this state is very unsatisfactory and we hope that study of exactly solvable models could shed some light on the qualitative features of the work PDF.

Our findings concerning the work PDF (together with previous studies cited in Chaps. 4, 5) indicate the following universality. It seems that the exponential tail with polynomial prefactor as given by Eq. (5.50) is a rather universal feature of the Langevin dynamics starting from the equilibrium initial condition. The parameters of the external driving affect merely the "damping constant" of the asymptotic exponential decay, and the exponent of the algebraic pre-exponential factor. Actually, in the present setting, this exponent quantifies the anharmonicity of the external potential. These findings could improve the fitting of the histogram of experimentally measured work values. In addition, from the comparison against numerical results it follows that the range of validity of the scaling form (5.50) includes also a region of typical (i.e., not too rare) values of work, cf. Figs. 5.3, 5.4 and 5.5. Hence the fitting parameters could be obtained with a sufficient precision. In a further research it would be very interesting to classify the conditions for which the asymptotics of the work PDF could be different from that described by Eq. (5.50). To this end, it is necessary to understand how (i) a shape of the external potential, (ii) a time-dependence of external driving (slow, fast, monotonous, oscillating), and also (iii) initial conditions control the overall features of the work PDF.

Appendices

A. Limit distribution of the extreme

Let $\mathbf{X}_1, \mathbf{X}_2, \ldots, \mathbf{X}_n$ be independent and identically distributed random variables, each with the cumulative distribution function $F(x)$. The asymptotic theory of the sample extreme $\mathbf{X}_{n:n} = \max\{\mathbf{X}_1, \mathbf{X}_2, \ldots, \mathbf{X}_n\}$, is concerned with the limit behavior of the maximum $\mathbf{X}_{n:n}$ as $n \to \infty$. The theory, in a certain sense, resembles the central limit theory for partial sums of random variables. In the present Appendix we just list possible asymptotic distributions of $\mathbf{X}_{n:n}$. For a readable introduction to asymptotic theory we refer the reader to Chapter 10 of Ref. [53]. The book [53] contains about 1500 references, including numerous applications of order statistics. A more advanced discussion of limit distributions can be found in Ref. [303].

For an arbitrary distribution $F(x)$, the maximum $\mathbf{X}_{n:n}$ will in general not possess a limiting distribution. However, if there exist standardizing constants $a_n > 0$ and b_n and the distribution $G(x)$ such that

$$F_{n:n}(a_n x + b_n) = [F(a_n x + b_n)]^n \to G(x) \quad \text{at all continuity points of } G, \qquad \text{(A.1)}$$

i.e., if the distribution of the maximum $F_{n:n}(x)$ converges to the limit distribution $G(x)$, then the limit distribution $G(x)$ *must be one of just three types*. The three types are: (A) a Fréchet distribution when $f(x)$, $f(x) = \mathrm{d}F/\mathrm{d}x$, decays as a power law $x^{-\alpha-1}$, $\alpha > 0$, as $x \to \infty$; (B) a Weibull distribution when the support of $f(x)$ is bounded; (C) a Gumbel distribution when $f(x)$ decays faster than a power law as $x \to \infty$. The three distributions read

$$\text{(Fréchet)} \qquad G_1(x; \alpha) = \begin{cases} 0 & x \le 0, \alpha > 0 \\ \exp(-x^{-\alpha}) & x > 0; \end{cases} \qquad \text{(A.2)}$$

$$\text{(Weibull)} \qquad G_2(x; \alpha) = \begin{cases} \exp\left[-(-x)^{-\alpha}\right] & x \le 0, \alpha > 0 \\ 1 & x > 0; \end{cases} \qquad \text{(A.3)}$$

$$\text{(Gumbel)} \qquad G_3(x; \alpha) = \exp(-\mathrm{e}^{-x}) \qquad -\infty < x < +\infty. \qquad \text{(A.4)}$$

Throughout the thesis the Gumbel distribution appears in Eq. (1.47) as the distribution for the position of the (single-file) diffusion front and in Eqs. (3.26), (3.53) as the distribution for the absorption time of the longest-living particle in a finite interval. The Fréchet distribution can be found in Eq. (2.50), it gives the asymptotic distribution for the time of absorption of the longest-living particle in the semi-infinite system. Notice that the limit PDF for the central tracer in a finite system, Eq. (3.37), after an appropriate normalization becomes proportional to $\mathrm{e}^{-x}\exp(-\mathrm{e}^{-2x})$, which resembles the PDF of the Gumbel distribution $g_3(x; \alpha) = \mathrm{e}^{-x}\exp(-\mathrm{e}^{-x})$.

B. Asymptotic expansion of conditioned PDF

The main aim of this Appendix is to justify relations (2.18) and (2.22). To this end, we treat separately the numerator and the denominator in Eq. (2.17).

As for the numerator, we insert the explicit expression (2.8) into the mean value in Eq. (2.9). This yields

$$f(x,t) = \frac{2\,e^{-x^2/4Dt}}{\sqrt{4\pi Dt}} \left\langle \sinh\left(\frac{x\mathbf{X}(0)}{2Dt}\right) e^{-\mathbf{X}^2(0)/4Dt} \right\rangle. \tag{B.1}$$

Using the power series representation for the functions inside the averaging brackets, we obtain

$$\left\langle \sinh\left(\frac{x\mathbf{X}(0)}{2Dt}\right) e^{-\mathbf{X}^2(0)/4Dt} \right\rangle = \frac{x}{2Dt} \sum_{k,l=0}^{\infty} \frac{(-1)^l 2^{-2l}}{l!\,(2k+1)!} \left(\frac{1}{Dt}\right)^{k+l} \left(\frac{x^2}{4Dt}\right)^k \left\langle \mathbf{X}^{2(k+l)+1}(0) \right\rangle. \tag{B.2}$$

The above double sum is treated by the index substitution $p = k + l$:

$$f(x,t) = \frac{x\,e^{-x^2/4Dt}}{2Dt} \frac{\langle \mathbf{X}(0) \rangle}{\sqrt{\pi Dt}} \sum_{p=0}^{\infty} \sum_{k=0}^{p} c(k,p) \left(\frac{x^2}{4Dt}\right)^k \left(\frac{1}{Dt}\right)^p, \tag{B.3}$$

where the time-independent coefficients $c(k,p)$ carry the information concerning the initial condition. Explicitly, they read

$$c(k,p) = \frac{(-1)^{p-k}\,2^{2k-2p}}{(p-k)!\,(2k+1)!} \frac{\langle \mathbf{X}^{2p+1}(0) \rangle}{\langle \mathbf{X}(0) \rangle}. \tag{B.4}$$

We now prepare similar expansion for the survival probability $S(t)$ as defined in Eq. (2.11). Inserting the power series [304]

$$\mathrm{erf}(z) = \frac{2}{\sqrt{\pi}} \sum_{k=0}^{\infty} \frac{(-1)^k z^{2k+1}}{k!\,(2k+1)} \tag{B.5}$$

into the averaging in (2.11), we immediately obtain

$$S(t) = \frac{\langle \mathbf{X}(0) \rangle}{\sqrt{\pi Dt}} \sum_{p=0}^{\infty} \frac{(-1)^p}{2^{2p}p!(2p+1)} \frac{\langle \mathbf{X}^{2p+1}(0) \rangle}{\langle \mathbf{X}(0) \rangle} \left(\frac{1}{Dt}\right)^p. \tag{B.6}$$

Interestingly, the numerical factors $2^{2p}p!(2p+1)$ in the denominators of individual terms of (B.6) form a sequence $1, 12, 160, 2688, 55296, \ldots$ (for $p = 0, 1, 2, 3, 4, \ldots$), which is A167558 sequence in Sloane's On-Line Encyclopedia of Integer Sequences [305]. This sequence originally emerged in a completely different situation without any obvious connection to the expansion of the error function (see also A167546).

One can arrive at an alternative equivalent expansion of the function $S(t)$ by staring with the first equality in Eq. (2.11) from the main text. The series (B.3) is integrated term by term and it assumes the form

$$S(t) = \frac{\langle \mathbf{X}(0) \rangle}{\sqrt{\pi Dt}} \sum_{p=0}^{\infty} \sum_{k=0}^{p} k!\,c(k,p) \left(\frac{1}{Dt}\right)^p. \tag{B.7}$$

By term by term comparison of the series (B.6) and (B.7) one obtains a non-trivial identity

$$\sum_{k=0}^{p} \frac{(-1)^k \, 2^{2k} k\,!}{(p-k)!\,(2k+1)!} = \frac{1}{p\,!(2p+1)}.\tag{B.8}$$

Returning to the main goal of the Appendix, we divide the series (B.3) by (B.6). Notice that the prefactor $\langle \mathbf{X}(0)\rangle/\sqrt{\pi Dt}$ appears in both (B.3) and (B.6), therefore it cancels. Representing the fraction $1/S(t)$ by a geometric series, we finally obtain the sought-after asymptotic expansion

$$
\begin{aligned}
f(x, Dt \mid \mathbf{T} > t) = {}& \frac{x}{2Dt}\, \mathrm{e}^{-x^2/4Dt} \left[1 + \sum_{k=0}^{1} c(k,1) \left(\frac{x^2}{4Dt} \right)^k \frac{1}{Dt} + O\!\left(t^{-2} \right) \right] \\
& \times \left[1 + \frac{1}{12} \frac{\langle \mathbf{X}^3(0)\rangle}{\langle \mathbf{X}(0)\rangle} \frac{1}{Dt} + O\!\left(t^{-2} \right) \right].
\end{aligned}\tag{B.9}
$$

The asymptotic expansion of the corresponding distribution function, i.e.,

$$\int_0^x \mathrm{d}x'\, \frac{f(x',t)}{S(t)} = 1 - \mathrm{e}^{-x^2/4Dt} \left[1 + O\!\left(t^{-1} \right) \right],\tag{B.10}$$

has been employed in steps leading from Eq. (2.59) to Eq. (2.60), and from Eq. (2.62) to Eq. (2.63).

C. Different driving protocols

In order to derive explicit results from Eq. (5.21) for a given protocol, the Riccati equation (5.19) needs to be solved. This nonlinear differential equation is equivalent to the linear second-order differential equation (5.33). Specifically, if $y(t)$ solves (5.33), then the logarithmic derivative (5.34) is the solution of Eq. (5.19). Hence the characteristic function (5.31) can be expressed in terms of the function $y(t)$. The solution of (5.33) for several reasonable driving protocols can be expressed in terms of higher transcendental functions.

Firstly let us consider the exponential protocol

$$k(t) = k_0 e^{-\gamma t}. \tag{C.1}$$

For the sake of simplicity we assume that $k_0 = 1$, and $\gamma = 1$. Then the substitution $\tau = 2e^{-t}$ transforms the second-order equation (5.33) into the form

$$\frac{d^2 y}{d\tau^2} + \left(1 + \frac{1}{\tau}\right)\frac{dy}{d\tau} + \frac{D\xi}{\tau} y = 0, \tag{C.2}$$

which after another substitution, $y(\tau) = e^{-\tau} w(\tau)$, reduces to Kummer's differential equation

$$\tau \frac{d^2 w}{d\tau^2} + (1 - \tau)\frac{dw}{d\tau} - (1 - D\xi) w = 0. \tag{C.3}$$

Thus the general solution of the original problem (5.33) for the exponential driving is given by the linear combination

$$y(\tau) = C_1 e^{-\tau} {}_1F_1(1 - D\xi, 1; \tau) + C_2 e^{-\tau} U(1 - D\xi, 1; \tau), \qquad \tau = 2e^{-t}, \tag{C.4}$$

of confluent hypergeometric functions of the first and of the second kind [304]. An alternative form of the solution can be derived by the Laplace transform method of Ref. [255]. Having obtained the exact expression for $y(t)$, one can try to derive the characteristic function for the work as given by Eq. (5.31). To this end, one of the constants C_1, C_2 is ruled out by the initial condition $\dot{y}(0) = 0$. The remaining constant cancels after forming the logarithmic derivative $\dot{y}(t)/y(t)$ which is proportional to the solution $b_2(t)$ of the Riccati equation, cf. Eq. (5.34). Differently speaking, we are free to supplement Eq. (5.31) with the initial condition prescribing $y(0)$, e.g. $y(0) = 1$. However, and this is the main obstacle on our way to the exact characteristic function, the function $b_2(t)$ still must be integrated according to Eqs. (5.20). Unfortunately the integration cannot be accomplished analytically.

Intuitively one may guess that the most simple results should be obtained for the linear protocol

$$k(t) = k_0 + k_1 t. \tag{C.5}$$

However, this is not the case. The transformation of the time variable $k_1\tau = (k_0 + k_1 t)^2$ reduces the second-order differential equation (5.33) again to Kummer's equation. Presently we have

$$\tau \frac{d^2 y}{d\tau^2} + \left(\frac{k_0}{2} - \tau\right)\frac{dy}{d\tau} + \frac{D\xi}{2} y = 0, \qquad \tau = \frac{1}{k_1}(k_0 + k_1 t)^2. \tag{C.6}$$

And again, there seems to be no reasonable way how to get a closed formula for the characteristic function (5.31) starting from the exact formula for $y(t)$.

Bibliography

[1] CHOWDHURY, D., SANTEN, L., AND SCHADSCHNEIDER, A. Statistical physics of vehicular traffc and some related systems. *Phys. Rep. 329* (2000), 199. DOI: 10.1016/S0370-1573(99)00117-9.

[2] BOUCHERIE, R. J., AND VAN DIJK, N. M., Eds. *Queueing Networks.* Springer, New York, 2011. ISBN 978-1-4419-6471-7, DOI: 10.1007/978-1-4419-6472-4.

[3] HELBING, D., MOLNÁR, P., FARKAS, I. J., AND BOLAY, K. Self-organizing pedestrian movement. *Env. Plan. B 28* (2001), 361. DOI: 10.1068/b2697.

[4] JOHN, A., SCHADSCHNEIDER, A., CHOWDHURY, D., AND NISHINARI, K. Trafficlike collective movement of ants on trails: absence of a jammed phase. *Phys. Rev. Lett. 102* (2009), 108001. DOI: 10.1103/PhysRevLett.102.108001.

[5] MÄNNIK, J., DRIESSEN, R., GALAJDA, P., KEYMER, J. E., AND DEKKER, C. Bacterial growth and motility in sub-micron constrictions. *PNAS 106* (2009), 14861. DOI: 10.1073/pnas.0907542106.

[6] BRESSLOFF, P. C., AND NEWBY, J. M. Stochastic models of intracellular transport. *Rev. Mod. Phys. 85* (2013), 135. DOI: 10.1103/RevModPhys.85.135.

[7] ALBERTS, B., BRAY, D., HOPKIN, K., JOHNSON, A., LEWIS, J., RAFF, M., ROBERTS, K., AND WALTER, P. *Essential Cell Biology*, 3 ed. Garland Science, Taylor & Francis Group, New York, 2010. ISBN 978-0-8153-4129-1.

[8] HODGKIN, A. L., AND KEYNES, R. D. The potassium permeability of a giant nerve fibre. *The Journal of Physiology (London) 128* (1955), 61. Online at http://jp.physoc.org/content/128/1/61.

[9] GRANÉLI, A., YEYKAL, C. C., ROBERTSON, R. B., AND GREENE, E. C. Long-distance lateral diffusion of human Rad51 on double-stranded DNA. *PNAS 103* (2006), 1221. DOI: 10.1073/pnas.0508366103.

[10] LI, G.-W., BERG, O. G., AND ELF, J. Effects of macromolecular crowding and DNA looping on gene regulation kinetics. *Nat. Phys. 5* (2009), 294. DOI: 10.1038/nphys1222.

[11] RICHARDS, P. M. Theory of one-dimensional hopping conductivity and diffusion. *Phys. Rev. B 16* (1977), 1393. DOI: 10.1103/PhysRevB.16.1393.

[12] FEDDERS, P. A. Two-point correlation functions for a distinguishable particle hopping on a uniform one-dimensional chain. *Phys. Rev. B 17* (1978), 40. DOI: 10.1103/PhysRevB.17.40 .

[13] PERKINS, T. T., SMITH, D. E., AND CHU, S. Direct observation of tube-like motion of a single polymer chain. *Science 264* (1994), 819. DOI: 10.1126/science.8171335.

[14] HAHN, K., KÄRGER, J., AND KUKLA, V. Single-file diffusion observation. *Phys. Rev. Lett. 76* (1995), 2762. DOI: 10.1103/PhysRevLett.76.2762.

[15] GUPTA, V., NIVARTHI, S. S., MCCORMICK, A. V., AND DAVIS, H. T. Evidence for single file diffusion of ethane in the molecular sieve $AlPO_4$-5. *Chem. Phys. Lett. 247* (1995), 596. DOI: 10.1016/S0009-2614(95)01246-X.

[16] KUKLA, V., KORNATOWSKI, J., DEMUTH, D., GIRNUS, I., PFEIFER, H., REES, L. V. C., SCHUNK, S., UNGER, K. K., AND KÄRGER, J. NMR studies of single-file diffusion in unidimensional channel zeolites. *Science 272* (1996), 702. DOI: 10.1126/science.272.5262.702.

[17] KEFFER, D. The temperature dependence of single-file separation mechanisms in one-dimensional nanoporous materials. *Chem. Eng. J. 74* (1999), 33. DOI: 10.1016/S1385-8947(99)00061-3.

[18] KÄRGER, J., RUTHVEN, D. M., AND THEODOROU, D. N. *Diffusion in Nanoporous Materials*, vol. 1. Wiley-VCH Verlag & Co. KGaA, Weinheim, 2012. ISBN 978-3-527-31024-1.

[19] CHENG, C.-Y., AND BOWERS, C. R. Observation of Single-File diffusion in dipeptide nanotubes by continuous-flow hyperpolarized Xenon-129 NMR spectroscopy. *ChemPhysChem 8* (2007), 2077. DOI: 10.1002/cphc.200700336.

[20] WEI, Q.-H., BECHINGER, C., AND LEIDERER, P. Single-file diffusion of colloids in one-dimensional channels. *Science 287* (2000), 625. DOI: 10.1126/science.287.5453.625.

[21] LUTZ, C., KOLLMANN, M., LEIDERER, P., AND BECHINGER, C. Diffusion of colloids in one-dimensional light channels. *J. Phys.: Condens. Matter 16* (2004), S4075. DOI: 10.1088/0953-8984/16/38/022.

[22] LUTZ, C., KOLLMANN, M., AND BECHINGER, C. Single-file diffusion of colloids in one-dimensional channels. *Phys. Rev. Lett. 93* (2004), 026001. DOI: 10.1103/PhysRevLett.93.026001.

[23] CUI, B., DIAMANT, H., AND LIN, B. Screened hydrodynamic interaction in a narrow channel. *Phys. Rev. Lett. 89* (2002), 188302. DOI: 10.1103/PhysRevLett.89.188302.

[24] LIN, B., MERON, M., CUI, B., RICE, S. A., AND DIAMANT, H. From random walk to single-file diffusion. *Phys. Rev. Lett. 94* (2005), 216001. DOI: 10.1103/PhysRevLett.94.216001.

[25] TIERNO, P., SAGUÉS, F., JOHANSEN, T. H., AND SOKOLOV, I. M. Evidence of Rouse-like dynamics in magnetically ratchetting colloidal chains. *Soft Matter 7* (2011), 7944. DOI: 10.1039/c1sm05601h.

[26] SIEMS, U., KREUTER, C., ERBE, A., SCHWIERZ, N., SENGUPTA, S., LEIDERER, P., AND NIELABA, P. Non-monotonic crossover from single-file to regular diffusion in micro-channels. *Sci. Rep. 2* (2012), 1015. DOI: 10.1038/srep01015.

[27] HARRIS, T. E. Diffusion with "collisions" between particles. *J. Appl. Probab. 2* (1965), 323. DOI: 10.2307/3212197.

[28] CHOU, T., MALLICK, K., AND ZIA, R. K. P. Non-equilibrium statistical mechanics: from a paradigmatic model to biological transport. *Rep. Prog. Phys. 74* (2011), 116601. DOI: 10.1088/0034-4885/74/11/116601.

[29] BLYTHE, R. A., AND EVANS, M. R. Nonequilibrium steady states of matrix-product form: a solver's guide. *J. Phys. A: Math. Theor. 40* (2007), R333. DOI: 10.1088/1751-8113/40/46/R01.

[30] EVANS, M. R., AND HANNEY, T. Nonequilibrium statistical mechanics of the zero-range process and related models. *J. Phys. A: Math. Gen. 38* (2005), R195. DOI: 10.1088/0305-4470/38/19/R01.

[31] SCHÜTZ, G. M. Critical phenomena and universal dynamics in one-dimensional driven diffusive systems with two species of particles. *J. Phys. A: Math. Gen. 36* (2003), R339. DOI: 10.1088/0305-4470/36/36/201.

[32] KRAPIVSKY, P. L., REDNER, S., AND BEN-NAIM, E. *A Kinetic View of Statistical Physics.* Cambridge University Press, Cambridge, 2010. ISBN-13 978-0-521-85103-9.

[33] RISKEN, H. *The Fokker-Planck Equation: Methods of Solutions and Applications*, 2 ed. Springer-Verlag, Berlin, 1989. ISBN 0-387-50498-2.

[34] SEKIMOTO, K. *Stochastic Energetics.* Lecture notes in physics 799. Springer, Berlin, 2010. ISBN 978-3-642-05410-5, DOI: 10.1007/978-3-642-05411-2.

[35] SEIFERT, U. Stochastic thermodynamics, fluctuation theorems and molecular machines. *Rep. Prog. Phys. 75* (2012), 126001. DOI: 10.1088/0034-4885/75/12/126001.

[36] SEKIMOTO, K. Kinetic characterization of heat bath and the energetics of thermal ratchet models. *J. Phys. Soc. Jpn. 66* (1997), 1234. DOI: 10.1143/JPSJ.66.1234.

[37] SEKIMOTO, K. Langevin equation and thermodynamics. *Prog. Theor. Phys. Suppl. 130* (1998), 17. DOI: 10.1143/PTPS.130.17.

[38] PERCUS, J. K. On tagged particle dynamics in highly confined fluids. *J. Stat. Phys. 138* (2010), 40. DOI: 10.1007/s10955-009-9917-8.

[39] RYABOV, A., AND CHVOSTA, P. Single-file diffusion of externally driven particles. *Phys. Rev. E 83* (2011), 020106. DOI: 10.1103/PhysRevE.83.020106.

[40] RYABOV, A., AND CHVOSTA, P. Survival of interacting Brownian particles in crowded one-dimensional environment. *J. Chem. Phys. 136* (2012), 064114. DOI: 10.1063/1.3684954.

[41] RYABOV, A. Single-file diffusion in an interval: first passage properties. *J. Chem. Phys. 138* (2013), 154104. DOI: 10.1063/1.4801326.

[42] RYABOV, A., AND CHVOSTA, P. Tracer dynamics in semi-infinite system with absorbing boundary. *Phys. Rev. E 89* (2014), 022132. DOI: 10.1103/PhysRevE.89.022132.

[43] ASLANGUL, C. Diffusion of two repulsive particles in a one-dimensional lattice. *J. Phys. A: Math. Gen. 32* (1999), 3993. DOI: 10.1088/0305-4470/32/22/301.

[44] AMBJÖRNSSON, T., AND SILBEY, R. Diffusion of two particles with a finite interaction potential in one dimension. *J. Chem. Phys. 129* (2008), 165103. DOI: 10.1063/1.2999602.

[45] AMBJÖRNSSON, T., LIZANA, L., LOMHOLT, M. A., AND SILBEY, R. J. Single-file dynamics with different diffusion constants. *J. Chem. Phys. 129* (2008), 185106. DOI: 10.1063/1.3009853.

[46] POTTS, J. R., HARRIS, S., AND GIUGGIOLI, L. An anti-symmetric exclusion process for two particles on an infinite 1D lattice. *J. Phys. A: Math. Theor. 44* (2009), 485003. DOI: 10.1088/1751-8113/44/48/485003.

[47] MINC, H. *Permanents.* Encyclopedia of mathematics and its applications. Addison-Wesley Publishing Company, London, 1978. ISBN 0-201-13505-1.

[48] GESSEL, I. M., AND ZEILBERGER, D. Random walk in a Weyl chamber. *Proc. Amer. Math. Soc. 115* (1992), 27. DOI: 10.2307/2159560.

[49] GRABINER, D. J. Brownian motion in a Weyl chamber, non-colliding particles, and random matrices. *Annales de l'Institut Henri Poincare (B) Probability and Statistics 35* (1999), 177. DOI: 10.1016/S0246-0203(99)80010-7.

[50] RÖDENBECK, C., KÄRGER, J., AND HAHN, K. Calculating exact propagators in single-file systems via the reflection principle. *Phys. Rev. E 57* (1998), 4382. DOI: 10.1103/PhysRevE.57.4382.

[51] LIZANA, L., AND AMBJÖRNSSON, T. Single-file diffusion in a box. *Phys. Rev. Lett. 100* (2008), 200601. DOI: 10.1103/PhysRevLett.100.200601.

[52] LIZANA, L., AND AMBJÖRNSSON, T. Diffusion of finite-sized hard-core interacting particles in a one-dimensional box: Tagged particle dynamics. *Phys. Rev. E 80* (2009), 051103. DOI: 10.1103/PhysRevE.80.051103.

[53] DAVID, H. A., AND NAGARAJA, H. N. *Order Statistics*, 3 ed. John Wiley & Sons, Inc., New Jersey, 2003. ISBN 978-0-471-38926-2.

[54] BURLATSKII, S. F., AND OSHANIN, G. S. Probability distribution for trajectories of a polymer chain segment. *Theor. and Math. Phys. 75* (1988), 659. DOI: 10.1007/BF01036268.

[55] GROSBERG, A. Y., AND KHOKHLOV, A. R. *Statistical Physics of Macromolecules.* AIP Press, New York, 1994. Chap. 6. ISBN-13 978-1563960710.

[56] TOROCZKAI, Z., AND WILLIAMS, E. D. Nanoscale fluctuations at solid surfaces. *Phys. Tod. 52* (1999), 24. DOI: 10.1063/1.882897.

[57] MANDELBROT, B. B., AND VAN NESS, J. W. Fractional Brownian motions, fractional noises and applications. *SIAM reviews 10* (1968), 422. DOI: 10.1137/1010093.

[58] TALONI, A., CHECHKIN, A., AND KLAFTER, J. Generalized elastic model yields a fractional Langevin equation description. *Phys. Rev. Lett. 104* (2010), 160602. DOI: 10.1103/PhysRevLett.104.160602.

[59] SANDERS, L. P., AND AMBJÖRNSSON, T. First passage times for a tracer particle in single file diffusion and fractional Brownian motion. *J. Chem. Phys. 136* (2012), 175103. DOI: 10.1063/1.4707349.

[60] MARCHESONI, F., AND TALONI, A. Subdiffusion and long-time anticorrelations in a stochastic single file. *Phys. Rev. Lett. 97* (2006), 106101. DOI: 10.1103/PhysRevLett.97.106101.

[61] LIZANA, L., AMBJÖRNSSON, T., TALONI, A., BARKAI, E., AND LOMHOLT, M. A. Foundation of fractional Langevin equation: Harmonization of a many-body problem. *Phys. Rev. E 81* (2010), 051118. DOI: 10.1103/PhysRevE.81.051118.

[62] LOMHOLT, M. A., LIZANA, L., AND AMBJÖRNSSON, T. Dissimilar bouncy walkers. *J. Chem. Phys. 134* (2011), 045101. DOI: 10.1063/1.3526941.

[63] LOMHOLT, M. A., AND AMBJÖRNSSON, T. Universality and non-universality of mobility in heterogeneous single-file systems and Rouse chains. *Phys. Rev. E 89* (2014), 032101. DOI: 10.1103/PhysRevE.89.032101.

[64] KÄRGER, J. Straightforward derivation of the long-time limit of the mean-square displacement in one-dimensional diffusion. *Phys. Rev. A 45* (1992), 4173. DOI: 10.1103/PhysRevA.45.4173.

[65] LEVITT, D. G. Dynamics of a single-file pore: Non-Fickian behavior. *Phys. Rev. A 8* (1973), 3050. DOI: 10.1103/PhysRevA.8.3050.

[66] LEVITT, D. G. One-dimensional time-dependent distributions. *J. Stat. Phys. 7* (1973), 329. DOI: 10.1007/BF01014908.

[67] LEBOWITZ, J. L., AND PERCUS, J. K. Kinetic equations and density expansions: Exactly solvable one-dimensional system. *Phys. Rev. 155* (1967), 122. DOI: 10.1103/PhysRev.155.122.

[68] JEPSEN, D. W. Dynamics of a simple many-body system of hard rods. *J. Math. Phys. 6* (1965), 405. DOI: 10.1063/1.1704288.

[69] HAHN, K., AND KÄRGER, J. Propagator and mean-square displacement in single-file systems. *J. Phys. A: Math. Gen. 28* (1995), 3061. DOI: 10.1088/0305-4470/28/11/010.

[70] ASLANGUL, C. Classical diffusion of N interacting particles in one dimension: General results and asymptotic laws. *Europhys. Lett. 44* (1998), 284. DOI: 10.1209/epl/i1998-00471-9.

[71] LIZANA, L., LOMHOLT, M. A., AND AMBJÖRNSSON, T. Single-file diffusion with non-thermal initial conditions. *Physica A 395* (2014), 148. DOI: 10.1016/j.physa.2013.10.025.

[72] ALEXANDER, S., AND PINCUS, P. Diffusion of labeled particles on one-dimensional chains. *Phys. Rev. B 18* (1978), 2011. DOI: 10.1103/PhysRevB.18.2011.

[73] VAN BEIJEREN, H., KEHR, K. W., AND KUTNER, R. Diffusion in concentrated lattice gases. III. Tracer diffusion on a one-dimensional lattice. *Phys. Rev. B 28* (1983), 5711. DOI: 10.1103/PhysRevB.28.5711.

[74] DELFAU, J.-B., COSTE, C., AND JEAN, M. S. Single-file diffusion of particles with long-range interactions: Damping and finite-size effects. *Phys. Rev. E 84* (2011), 011101. DOI: 10.1103/PhysRevE.84.011101.

[75] MANZI, S. J., HERRERA, J. J. T., AND PEREYRA, V. D. Single-file diffusion in a box: Effect of the initial configuration. *Phys. Rev. E 86* (2012), 021129. DOI: 10.1103/PhysRevE.86.021129.

[76] ARRATIA, R. The motion of a tagged particle in the simple symmetric exclusion system on Z. *Ann. Probab. 11* (1983), 227. DOI: 10.1214/aop/1176993602.

[77] SABHAPANDIT, S. Statistical properties of a single-file diffusion front. *J. Stat. Mech.* (2007), L05002. DOI: 10.1088/1742-5468/2007/05/L05002.

[78] DERRIDA, B., AND GERSCHENFELD, A. Current fluctuations of the one dimensional symmetric simple exclusion process with step initial condition. *J. Stat. Phys. 136* (2009), 1. DOI: 10.1007/s10955-009-9772-7.

[79] DERRIDA, B., AND GERSCHENFELD, A. Current fluctuations in one dimensional diffusive systems with a step initial density profile. *J. Stat. Phys. 137* (2009), 978. DOI: 10.1007/s10955-009-9830-1.

[80] PRÄHOFER, M., AND SPOHN, H. Current fluctuations for the totally asymmetric simple exclusion process. *In and Out of Equilibrium. Progress in Probability 51* (2002), 185. DOI: 10.1007/978-1-4612-0063-5_7.

[81] SASAMOTO, T. Fluctuations of the one-dimensional asymmetric exclusion process using random matrix techniques. *J. Stat. Mech.* (2007), P07007. DOI: 10.1088/1742-5468/2007/07/P07007.

[82] IMAMURA, T., AND SASAMOTO, T. Dynamics of a tagged particle in the asymmetric exclusion process with the step initial condition. *J. Stat. Phys. 128* (2007), 799. DOI: 10.1007/s10955-007-9326-9.

[83] ANTAL, T., KRAPIVSKY, P. L., AND RÁKOS, A. Logarithmic current fluctuations in nonequilibrium quantum spin chains. *Phys. Rev. E 78* (2008), 061115. DOI: 10.1103/PhysRevE.78.061115.

[84] TRACY, C. A., AND WIDOM, H. A Fredholm determinant representation in ASEP. *J. Stat. Phys. 132* (2008), 291. DOI: 10.1007/s10955-008-9562-7.

[85] TRACY, C. A., AND WIDOM, H. Asymptotics in ASEP with step initial condition. *Commun. Math. Phys. 290* (2009), 129. DOI: 10.1007/s00220-009-0761-0.

[86] TRACY, C. A., AND WIDOM, H. On ASEP with step Bernoulli initial condition. *J. Stat. Phys. 137* (2009), 825. DOI: 10.1007/s10955-009-9867-1.

[87] SASAMOTO, T., AND SPOHN, H. The crossover regime for the weakly asymmetric simple exclusion process. *J. Stat. Phys. 140* (2010), 209. DOI: 10.1007/s10955-010-9990-z.

[88] FERRARI, P. L., AND FRINGS, R. On the partial connection between random matrices and interacting particle systems. *J. Stat. Phys. 141* (2010), 613. DOI: 10.1007/s10955-010-0070-1.

[89] ASLANGUL, C. Single-file diffusion with random diffusion constants . *J. Phys. A: Math. Gen. 33* (2000), 851. DOI: 10.1088/0305-4470/33/5/303.

[90] FLOMENBOM, O. Dynamics of heterogeneous hard spheres in a file. *Phys. Rev. E 82* (2010), 031126. DOI: 10.1103/PhysRevE.82.031126.

[91] GONÇALVES, P., AND JARA, M. Scaling limits of a tagged particle in the exclusion process with variable diffusion coefficient. *J. Stat. Phys. 132* (2008), 1135. DOI: 10.1007/s10955-008-9595-y.

[92] KOLLMANN, M. Single-file diffusion of atomic and colloidal systems: Asymptotic laws. *Phys. Rev. Lett. 90* (2003), 180602. DOI: 10.1103/PhysRevLett.90.180602.

[93] NELISSEN, K., MISKO, V. R., AND PEETERS, F. M. Single-file diffusion of interacting particles in a one-dimensional channel. *Europhys. Lett. 80* (2007), 56004. DOI: 10.1209/0295-5075/80/56004.

[94] FELDERHOF, B. U. Fluctuation theory of single-file diffusion. *J. Chem. Phys. 131* (2009), 064504. DOI: 10.1063/1.3204469.

[95] COSTE, C., DELFAU, J.-B., EVEN, C., AND JEAN, M. S. Single-file diffusion of macroscopic charged particles. *Phys. Rev. E 81* (2010), 051201. DOI: 10.1103/PhysRevE.81.051201.

[96] DELFAU, J.-B., COSTE, C., EVEN, C., AND JEAN, M. S. Single-file diffusion of interacting particles in a finite-sized channel. *Phys. Rev. E 82* (2010), 031201. DOI: 10.1103/PhysRevE.82.031201.

[97] OOSHIDA, T., GOTO, S., MATSUMOTO, T., NAKAHARA, A., AND OTSUKI, M. Continuum theory of single-file diffusion in terms of label variable. *J. Phys. Soc. Jpn. 80* (2011), 074007. DOI: 10.1143/JPSJ.80.074007.

[98] EUÁN-DÍAZ, E. C., MISKO, V. R., PEETERS, F. M., HERRERA-VELARDE, S., AND CASTAÑEDA-PRIEGO, R. Single-file diffusion in periodic energy landscapes: The role of hydrodynamic interactions. *Phys. Rev. E 86* (2014), 031123. DOI: 10.1103/PhysRevE.86.031123.

[99] CECCONI, F., DIOTALLEVI, F., MARCONI, U. M. B., AND PUGLISI, A. Fluid-like behavior of a one-dimensional granular gas. *J. Chem. Phys. 120* (2004), 35. DOI: 10.1063/1.1630957.

[100] VILLAMAINA, D., PUGLISI, A., AND VULPIANI, A. The fluctuation-dissipation relation in sub-diffusive systems: the case of granular single-file diffusion. *J. Stat. Mech.* (2008), L10001. DOI: 10.1088/1742-5468/2008/10/L10001.

[101] SPOHN, H. Tracer dynamics in Dyson's model of interacting Brownian particles. *J. Stat. Phys. 47* (1987), 669. DOI: 10.1007/BF01206151.

[102] KALINAY, P., AND PERCUS, J. K. Projection of two-dimensional diffusion in a narrow channel onto the longitudinal dimension. *J. Chem. Phys. 122* (2005), 204701. DOI: 10.1063/1.1899150.

[103] KALINAY, P., AND PERCUS, J. K. Exact dimensional reduction of linear dynamics: application to confined diffusion. *J. Stat. Phys. 123* (2006), 1059. DOI: 10.1007/s10955-006-9081-3.

[104] KALINAY, P., AND PERCUS, J. K. Stretched Markov nature of single-file self-dynamics. *Phys. Rev. E 76* (2007), 041111. DOI: 10.1103/PhysRevE.76.041111.

[105] KALINAY, P., AND PERCUS, J. K. Two definitions of the hopping time in a confined fluid of finite particles. *J. Chem. Phys. 129* (2008), 154117. DOI: 10.1063/1.2996363.

[106] MON, K. K., AND PERCUS, J. K. Self-diffusion of fluids in narrow cylindrical pores. *J. Chem. Phys. 117* (2002), 2289. DOI: 10.1063/1.1490337.

[107] KALINAY, P. Calculation of the mean first passage time tested on simple two-dimensional models. *J. Chem. Phys. 126* (2007), 194708. DOI: 10.1063/1.2734148.

[108] MON, K. K. Brownian dynamics mean first passage time of two hard disks diffusing in a channel. *J. Chem. Phys. 130* (2009), 184701. DOI: 10.1063/1.3127764.

[109] LUCENA, D., TKACHENKO, D. V., NELISSEN, K., MISKO, V. R., FERREIRA, W. P., FARIAS, G. A., AND PEETERS, F. M. Transition from single-file to two-dimensional diffusion of interacting particles in a quasi-one-dimensional channel. *Phys. Rev. E 85* (2012), 031147. DOI: 10.1103/PhysRevE.85.031147.

[110] DELFAU, J.-B., COSTE, C., AND JEAN, M. S. Enhanced fluctuations of interacting particles confined in a box. *Phys. Rev. E 85* (2012), 041137. DOI: 10.1103/PhysRevE.85.041137.

[111] DELFAU, J.-B., COSTE, C., AND JEAN, M. S. Single-file diffusion of particles in a box: Transient behaviors. *Phys. Rev. E 85* (2012), 061111. DOI: 10.1103/PhysRevE.85.061111.

[112] DELFAU, J.-B., COSTE, C., AND JEAN, M. S. Transverse single-file diffusion near the zigzag transition. *Phys. Rev. E 87* (2013), 032163. DOI: 10.1103/PhysRevE.87.032163.

[113] LUCENA, D., FERREIRA, W. P., MUNARIN, F. F., FARIAS, G. A., AND PEETERS, F. M. Tunable diffusion of magnetic particles in a quasi-one-dimensional channel. *Phys. Rev. E 87* (2013), 012307. DOI: 10.1103/PhysRevE.87.012307.

[114] LUCENA, D., GALVÁN-MOYA, J. E., FERREIRA, W. P., AND PEETERS, F. M. Single-file and normal diffusion of magnetic colloids in modulated channels. *Phys. Rev. E 89* (2014), 032306. DOI: 10.1103/PhysRevE.89.032306.

[115] GALVÁN-MOYA, J. E., LUCENA, D., FERREIRA, W. P., AND PEETERS, F. M. Magnetic particles confined in a modulated channel: Structural transitions tunable by tilting a magnetic field. *Phys. Rev. E 89* (2014), 032309. DOI: 10.1103/PhysRevE.89.032309.

[116] BARKAI, E., AND SILBEY, R. Theory of single file diffusion in a force field. *Phys. Rev. Lett. 102* (2009), 050602. DOI: 10.1103/PhysRevLett.102.050602.

[117] BARKAI, E., AND SILBEY, R. Diffusion of tagged particle in an exclusion process. *Phys. Rev. E 81* (2010), 041129. DOI: 10.1103/PhysRevE.81.041129.

[118] TALONI, A., AND MARCHESONI, F. Single-file diffusion on a periodic substrate. *Phys. Rev. Lett. 96* (2006), 020601. DOI: 10.1103/PhysRevLett.96.020601.

[119] BURLATSKY, S. F., OSHANIN, G., MOGUTOV, A. V., AND MOREAU, M. Directed walk in a one-dimensional lattice gas. *Phys. Lett. A 166* (1992), 230. DOI: 10.1016/0375-9601(92)90368-V.

[120] BURLATSKY, S. F., OSHANIN, G., MOREAU, M., AND REINHARDT, W. P. Motion of a driven tracer particle in a one-dimensional symmetric lattice gas. *Phys. Rev. E 54* (1996), 3165. DOI: 10.1103/PhysRevE.54.3165.

[121] ILLIEN, P., BÉNICHOU, O., MEJÍA-MONASTERIO, C., OSHANIN, G., AND VOITURIEZ, R. Active transport in dense diffusive single-file systems. *Phys. Rev. Lett. 111* (2013), 038102. DOI: 10.1103/PhysRevLett.111.038102.

[122] HANES, R. D. L., SCHMIEDEBERG, M., AND EGELHAAF, S. U. Brownian particles on rough substrates: Relation between intermediate subdiffusion and asymptotic long-time diffusion. *Phys. Rev. E 88* (2013), 062133. DOI: 10.1103/PhysRevE.88.062133.

[123] EVERS, F., HANES, R. D. L., ZUNKE, C., CAPELLMANN, R. F., BE-
WERUNGE, J., DALLE-FERRIER, C., JENKINS, M. C., LADADWA, I., HEUER,
A., CASTAÑEDA-PRIEGO, R., AND EGELHAAF, S. U. Colloids in light fields:
Particle dynamics in random and periodic energy landscapes. *Eur. Phys. J. Spe-
cial Topics 222* (2013), 2995. DOI: 10.1140/epjst/e2013-02071-2.

[124] BURADA, P. S., HÄNGGI, P., MARCHESONI, F., SCHMID, G., AND TALKN-
ER, P. Diffusion in confined geometries. *ChemPhysChem 10* (2009), 45. DOI:
10.1002/cphc.200800526.

[125] BEN-NAIM, E., AND KRAPIVSKY, P. L. Strong mobility in weakly disor-
dered systems. *Phys. Rev. Lett. 102* (2009), 190602. DOI: 10.1103/Phys-
RevLett.102.190602.

[126] BAUER, M., GODEC, A., AND METZLER, R. Diffusion of finite-size particles in
two-dimensional channels with random wall configurations. *Phys. Chem. Chem.
Phys. 16* (2014), 6118. DOI: 10.1039/C3CP55160A.

[127] FLOMENBOM, O., AND TALONI, A. On single-file and less dense processes.
Europhys. Lett. 83 (2008), 20004. DOI: 10.1209/0295-5075/83/20004.

[128] LEIBOVICH, N., AND BARKAI, E. Everlasting effect of initial conditions on
single-file diffusion. *Phys. Rev. E 88* (2013), 032107. DOI: 10.1103/Phys-
RevE.88.032107.

[129] PERCUS, J. K. Anomalous self-diffusion for one-dimensional hard cores. *Phys.
Rev. A 9* (1974), 557. DOI: 10.1103/PhysRevA.9.557.

[130] BENA, I., AND MAJUMDAR, S. N. Universal extremal statistics in a freely
expanding Jepsen gas. *Phys. Rev. E 75* (2007), 051103. DOI: 10.1103/Phys-
RevE.75.051103.

[131] SABHAPANDIT, S., BENA, I., AND MAJUMDAR, S. N. Statistics of the total
number of collisions and the ordering time in a freely expanding hard-point gas.
J. Stat. Mech. (2008), P05012. DOI: 10.1088/1742-5468/2008/05/P05012.

[132] ROY, A., NARAYAN, O., DHAR, A., AND SABHAPANDIT, S. Tagged particle
diffusion in one-dimensional gas with Hamiltonian dynamics. *J. Stat. Phys. 150*
(2013), 851. DOI: 10.1007/s10955-012-0673-9.

[133] FLOMENBOM, O. Clustering in anomalous files of independent particles. *Euro-
phys. Lett. 94* (2011), 58001. DOI: 10.1209/0295-5075/94/58001.

[134] FLOMENBOM, O. Renewal–anomalous–heterogeneous files. *Phys. Lett. A 374*
(2010), 4331. DOI: 10.1016/j.physleta.2010.08.029.

[135] BANDYOPADHYAY, T. Single-file diffusion of subdiffusive particles. *Europhys.
Lett. 81* (2008), 16003. DOI: 10.1209/0295-5075/81/16003.

[136] BARMA, M., AND RAMASWAMY, R. Escape times in interacting biased random
walks. *J. Stat. Phys. 43* (1986), 561. DOI: 10.1007/BF01020653.

[137] WEISS, G. H., SHULER, K. E., AND LINDENBERG, K. Order statistics for
first passage times in diffusion processes. *J. Stat. Phys. 31* (1983), 255. DOI:
10.1007/BF01011582.

[138] YUSTE, S. B., AND LINDENBERG, K. Order statistics for first passage times in one-dimensional diffusion processes. *J. Stat. Phys. 85* (1996), 501. DOI: 10.1007/BF02174217.

[139] LINDENBERG, K., SESHADRI, V., SHULER, K. E., AND WEISS, G. H. Lattice random walks for sets of random walkers. First passage times. *J. Stat. Phys. 23* (1980), 11. DOI: 10.1007/BF01014427.

[140] YUSTE, S. B., ACEDO, L., AND LINDENBERG, K. Order statistics for d-dimensional diffusion processes. *Phys. Rev. E 64* (2001), 052102. DOI: 10.1103/PhysRevE.64.052102.

[141] ACEDO, L., AND YUSTE, S. B. Survival probability and order statistics of diffusion on disordered media. *Phys. Rev. E 66* (2002), 011110. DOI: 10.1103/PhysRevE.66.011110.

[142] YUSTE, S. B., AND ACEDO, L. Order statistics of the trapping problem. *Phys. Rev. E 64* (2001), 061107. DOI: 10.1103/PhysRevE.64.061107.

[143] YUSTE, S. B. Escape times of j random walkers from a fractal labyrinth. *Phys. Rev. Lett. 79* (1997), 3565. DOI: 10.1103/PhysRevLett.79.3565.

[144] YUSTE, S. B. Order statistics of diffusion on fractals. *Phys. Rev. E 57* (1998), 6327. DOI: 10.1103/PhysRevE.57.6327.

[145] YUSTE, S. B., AND ACEDO, L. Multiparticle trapping problem in the half-line. *Physica A 297* (2001), 321. DOI: 10.1016/S0378-4371(01)00244-8.

[146] BEN-NAIM, E. Mixing of diffusing particles. *Phys. Rev. E 82* (2010), 061103. DOI: 10.1103/PhysRevE.82.061103.

[147] BEN-NAIM, E., AND KRAPIVSKY, P. L. First-passage exponents of multiple random walks. *J. Phys. A: Math. Theor. 43* (2010), 495008. DOI: 10.1088/1751-8113/43/49/495008.

[148] SPITZER, F. Interaction of Markov processes. *Adv. Math. 5* (1970), 246. DOI: 10.1016/0001-8708(70)90034-4.

[149] MASI, A. D., AND FERRARI, P. A. Flux fluctuations in the one dimensional nearest neighbors symmetric simple exclusion process. *J. Stat. Phys. 107* (2002), 677. DOI: 10.1023/A:1014577928229.

[150] FERRARI, P. A. Limit theorems for tagged particles. *Markov Processes Relat. Fields 2* (1996), 17. Online at http://www.ime.usp.br/ pablo/papers/reprints-old/50.pdf.

[151] REDNER, S. *A Guide to First-Passage Processes*. Cambridge University Press, Cambridge, 2001. ISBN 0 521 65248 0.

[152] POLLETT, P. Quasi-stationary distributions: a bibliography. Online at http://www.maths.uq.edu.au/∼pkp/papers/qsds/qsds.pdf (2012).

[153] STEINSALTZ, D., AND EVANS, S. N. Markov mortality models: implications of quasistationarity and varying initial distributions. *Theor. Popul. Biol. 65* (2004), 319. DOI: 10.1016/j.tpb.2003.10.007.

[154] YAGLOM, A. M. Certain limit theorems of the theory of branching random processes. *Dokl. Akad. Nauk SSSR 56* (1947), 795. MR0022045 (in Russian).

[155] NÅSELL, I. The quasi-stationary distribution of the closed endemic SIS model. *Adv. Appl. Probab. 28* (1996), 895. DOI: 10.2307/1428186.

[156] FERRARI, P. A., MARTÍNEZ, S., AND MARTÍN, J. S. Phase transition for absorbed Brownian motion with drift. *J. Stat. Phys. 86* (1997), 213. DOI: 10.1007/BF02180205.

[157] CATTIAUX, P., COLLET, P., LAMBERT, A., MARTÍNEZ, S., MÉLÉARD, S., AND MARTÍN, J. S. Quasi-stationary distributions and diffusion models in population dynamics. *Ann. Probab. 37* (2009), 1647. DOI: 10.1214/09-AOP451.

[158] MÉLÉARD, S., AND VILLEMONAIS, D. Quasi-stationary distributions and population processes. *Probability Surveys 9* (2012), 340. DOI: 10.1214/11-PS191.

[159] DIMARZIO, E. A. Proper accounting of conformations of a polymer near a surface. *J. Chem. Phys. 42* (1965), 2101. DOI: 10.1063/1.1696251.

[160] ROE, R.-J. Conformation of an isolated polymer molecule at an interface. II. Dependence on molecular weight. *J. Chem. Phys. 43* (1965), 1591. DOI: 10.1063/1.1696976.

[161] SILBERBERG, A. Adsorption of flexible macromolecules. III. Generalized treatment of the isolated macromolecule; the effect of selfexclusion. *J. Chem. Phys. 46* (1967), 1105. DOI: 10.1063/1.1840775.

[162] DIMARZIO, E. A., AND RUBIN, R. J. Adsorption of a chain polymer between two plates. *J. Chem. Phys. 55* (1971), 4318. DOI: 10.1063/1.1676755.

[163] TAITELBAUM, H., HAVLIN, S., AND WEISS, G. H. Effects of hard-core interaction on nearest-neighbor distances at a single trap for random walks and for diffusion processes. *Chemical Physics 146* (1990), 351. DOI: 10.1016/0301-0104(90)80055-3.

[164] FELLER, W. *An Introduction to Probability Theory and Its Applications*, 3 ed., vol. 1. John Wiley & Sons, Inc., New York, 1968. ISBN-13 978-0471257080.

[165] WEISS, G. H. *Aspects and Applications of the Random Walk*. North-Holland, Amsterdam, 1994. ISBN 0 444 81606 2.

[166] FELLER, W. *An Introduction to Probability Theory and Its Applications*, 3 ed., vol. 2. John Wiley & Sons, Inc., New York, 1971. ISBN-13 978-0471257097.

[167] BEN-AVRAHAM, D., AND HAVLIN, S. *Diffusion and Reactions in Fractals and Disordered Systems.* Cambridge University Press, Cambridge, 2000. ISBN 0 521 62278 6.

[168] HAVLIN, S., AND BEN-AVRAHAM, D. Diffusion in disordered media. *Advances in Physics 51* (2002), 187. DOI: 10.1080/00018730110116353.

[169] ANLAUF, J. K. Asymptotically exact solution of the one-dimensional trapping problem. *Phys. Rev. Lett. 52* (1984), 1845. DOI: 10.1103/PhysRevLett.52.1845.

[170] GRASSBERGER, P., AND PROCACCIA, I. The long time properties of diffusion in a medium with static traps. *J. Chem. Phys. 77* (1982), 6281. DOI: 10.1063/1.443832.

[171] WEISS, G. H., AND HAVLIN, S. Trapping of random walks on the line. *J. Stat. Phys. 37* (1984), 17. DOI: 10.1007/BF01012902.

[172] YUSTE, S. B., AND ACEDO, L. Order statistics of Rosenstock's trapping problem in disordered media. *Phys. Rev. E 68* (2003), 036134. DOI: 10.1103/PhysRevE.68.036134.

[173] YUSTE, S. B., AND ACEDO, L. Some exact results for the trapping of subdiffusive particles in one dimension. *Physica A 336* (2004), 334. DOI: 10.1016/j.physa.2003.12.048.

[174] REDNER, S., AND KANG, K. Asymptotic solution of interacting walks in one dimension. *Phys. Rev. Lett. 51* (1983), 1729. DOI: 10.1103/PhysRevLett.51.1729.

[175] AGMON, N., AND GLASSER, M. L. Complete asymptotic expansion for integrals arising from one-dimensional diffusion with random traps. *Phys. Rev. A 34* (1986), 656. DOI: 10.1103/PhysRevA.34.656.

[176] HENRICI, P. *Applied And Computational Complex Analysis*, vol. 2. John Wiley & Sons, Inc., New York. ISBN 0 471 01525 3 (v.2).

[177] REIF, F. *Fundamentals of Statistical and Thermal Physics*. McGrow-Hill Inc., New York, 1965. Section 6.6. ISBN 07-051800-9.

[178] VILAR, J. M. G., AND RUBI, J. M. Failure of the work-Hamiltonian connection for free-energy calculations. *Phys. Rev. Lett. 100* (2008), 020601. DOI: 10.1103/PhysRevLett.100.020601.

[179] PELITI, L. On the work–Hamiltonian connection in manipulated systems. *J. Stat. Mech.* (2008), P05002. DOI: 10.1088/1742-5468/2008/05/P05002.

[180] HOROWITZ, J., AND JARZYNSKI, C. Comment on "Failure of the work-Hamiltonian connection for free-energy calculations". *Phys. Rev. Lett. 101* (2008), 098901. DOI: 10.1103/PhysRevLett.101.098901.

[181] ZIMANYI, E. N., AND SILBEY, R. J. The work-Hamiltonian connection and the usefulness of the Jarzynski equality for free energy calculations. *J. Chem. Phys. 130* (2009), 171102. DOI: 10.1063/1.3132747.

[182] HOROWITZ, J., AND JARZYNSKI, C. Comparison of work fluctuation relations. *J. Stat. Mech.* (2007), P11002. DOI: 10.1088/1742-5468/2007/11/P11002.

[183] JARZYNSKI, C. Comparison of far-from-equilibrium work relations. *C. R. Physique 8* (2007), 495. DOI: 10.1016/j.crhy.2007.04.010.

[184] CROOKS, G. E. Nonequilibrium measurements of free energy differences for microscopically reversible Markovian systems. *J. Stat. Phys. 90* (1998), 1481. DOI: 10.1023/A:1023208217925.

[185] CROOKS, G. E. Entropy production fluctuation theorem and the nonequilibrium work relation for free energy differences. *Phys. Rev. E 60* (1999), 2721. DOI: 10.1103/PhysRevE.60.2721.

[186] JARZYNSKI, C. Nonequilibrium equality for free energy differences. *Phys. Rev. Lett. 78* (1997), 2690. DOI: 10.1103/PhysRevLett.78.2690.

[187] COLLIN, D., RITORT, F., JARZYNSKI, C., SMITH, S. B., TINOCO, I., AND BUSTAMANTE, C. Verification of the Crooks fluctuation theorem and recovery of RNA folding free energies. *Nature 437* (2005), 321. DOI: 10.1038/nature04061.

[188] ALEMANY, A., RIBEZZI-CRIVELLARI, M., AND RITORT, F. Recent progress in fluctuation theorems and free energy recovery. In *Nonequilibrium Statistical Physics of Small Systems*, R. Klages, W. Just, and C. Jarzynski, Eds., Reviews of Nonlinear Dynamics and Complexity. Wiley-VCH, Weinheim, Germany, 2013, ch. 5, pp. 155–180. ISBN: 978-3-527-41094-1.

[189] HUMMER, G., AND SZABO, A. Free energy reconstruction from nonequilibrium single-molecule pulling experiments. *PNAS 98* (2001), 3658. DOI: 10.1073/pnas.071034098.

[190] LIPHARDT, J., DUMONT, S., SMITH, S. B., TINOCO, I., AND BUSTAMANTE, C. Equilibrium information from nonequilibrium measurements in an experimental test of Jarzynski's equality. *Science 296* (2002), 1832. DOI: 10.1126/science.1071152.

[191] RITORT, F., BUSTAMANTE, C., AND TINOCO, I. A two-state kinetic model for the unfolding of single molecules by mechanical force. *PNAS 99* (2002), 13544. DOI: /10.1073/pnas.172525099.

[192] DANILOWICZ, C., COLJEE, V. W., BOUZIGUES, C., LUBENSKY, D. K., NELSON, D. R., AND PRENTISS, M. DNA unzipped under a constant force exhibits multiple metastable intermediates. *PNAS 100* (2003), 1694. DOI: 10.1073/pnas.262789199.

[193] ZUCKERMAN, D. M., AND WOOLF, T. B. Theory of a systematic computational error in free energy differences. *Phys. Rev. Lett. 89* (2002), 180602. DOI: 10.1103/PhysRevLett.89.180602.

[194] GORE, J., RITORT, F., AND BUSTAMANTE, C. Bias and error in estimates of equilibrium free-energy differences from nonequilibrium measurements. *PNAS 100* (2003), 12564. DOI: 10.1073/pnas.1635159100.

[195] HARRIS, N. C., SONG, Y., AND KIANG, C.-H. Experimental free energy surface reconstruction from single-molecule force spectroscopy using Jarzynski's equality. *Phys. Rev. Lett. 99* (2007), 068101. DOI: 10.1103/PhysRevLett.99.068101.

[196] ENGEL, S., ALEMANY, A., FORNS, N., MAASS, P., AND RITORT, F. Folding and unfolding of a triple-branch DNA molecule with four conformational states. *Philos. Mag. 91* (2011), 2049. DOI: 10.1080/14786435.2011.557671.

[197] PALASSINI, M., AND RITORT, F. Improving free-energy estimates from unidirectional work measurements: theory and experiment. *Phys. Rev. Lett. 107* (2011), 060601. DOI: 10.1103/PhysRevLett.107.060601.

[198] ENGEL, A. Asymptotics of work distributions in nonequilibrium systems. *Phys. Rev. E 80* (2009), 021120. DOI: 10.1103/PhysRevE.80.021120.

[199] NICKELSEN, D., AND ENGEL, A. Asymptotics of work distributions: the pre-exponential factor. *Eur. Phys. J. B 82* (2011), 207. DOI: 10.1140/epjb/e2011-20133-y.

[200] RYABOV, A., DIERL, M., CHVOSTA, P., EINAX, M., AND MAASS, P. Work distribution in a time-dependent logarithmic–harmonic potential: exact results and asymptotic analysis. *J. Phys. A: Math. Theor. 46* (2013), 075002. DOI: 10.1088/1751-8113/46/7/075002.

[201] Janshoff, A., Neitzert, M., Oberdörfer, Y., and Fuchs, H. Force spectroscopy of molecular systems – single molecule spectroscopy of polymers and biomolecules. *Angew. Chem. Int. Ed. 39* (2000), 3212. DOI: 10.1002/1521-3773(20000915)39:18<3212::AID-ANIE3212>3.0.CO;2-X.

[202] Liphardt, J., Onoa, B., Smith, S. B., Tinoco, I., and Bustamante, C. Reversible unfolding of single RNA molecules by mechanical force. *Science 292* (2001), 733. DOI: 10.1126/science.1058498.

[203] Zhuang, X., and Rief, M. Single-molecule folding. *Curr. Opin. Struct. Biol. 13* (2003), 88. DOI: 10.1016/S0959-440X(03)00011-3.

[204] Ritort, F. Single-molecule experiments in biological physics: methods and applications. *J. Phys.: Condens. Matter 18* (2006), R531. DOI: 10.1088/0953-8984/18/32/R01.

[205] Mossa, A., Manosas, M., Forns, N., Huguet, J. M., and Ritort, F. Dynamic force spectroscopy of DNA hairpins: I. Force kinetics and free energy landscapes. *J. Stat. Mech.* (2009), P02060. DOI: 10.1088/1742-5468/2009/02/P02060.

[206] Manosas, M., Mossa, A., Forns, N., Huguet, J. M., and Ritort, F. Dynamic force spectroscopy of DNA hairpins: II. Irreversibility and dissipation. *J. Stat. Mech.* (2009), P02061. DOI: 10.1088/1742-5468/2009/02/P02061.

[207] Huguet, J. M., Bizarro, C. V., Forns, N., Smith, S. B., Bustamante, C., and Ritort, F. Single-molecule derivation of salt dependent base-pair free energies in DNA. *PNAS 107* (2010), 15431. DOI: 10.1073/pnas.1001454107.

[208] Douarche, F., Ciliberto, S., Petrosyan, A., and Rabbiosi, I. An experimental test of the Jarzynski equality in a mechanical experiment. *Europhys. Lett. 70* (2005), 593. DOI: 10.1209/epl/i2005-10024-4.

[209] Ciliberto, S., Joubaud, S., and Petrosyan, A. Fluctuations in out-of-equilibrium systems: from theory to experiment. *J. Stat. Mech.* (2010), P12003. DOI: 10.1088/1742-5468/2010/12/P12003.

[210] Naert, A. Experimental study of work exchange with a granular gas: the viewpoint of the fluctuation theorem. *Europhys. Lett. 97* (2012), 20010. DOI: 10.1209/0295-5075/97/20010.

[211] Van den Broeck, C. Stochastic thermodynamics. In *Selforganization by nonlinear irreversible processes*, W. Ebeling and H. Ulbricht, Eds., Springer series in synergetics. Springer, Berlin, 1986, pp. 57–61. ISBN-13: 978-3-642-71006-3, DOI: 10.1007/978-3-642-71004-9.

[212] Sevick, E. M., Prabhakar, R., Williams, S. R., and Searles, D. J. Fluctuation theorems. *Annu. Rev. Phys. Chem. 59* (2008), 603. DOI: 10.1146/annurev.physchem.58.032806.104555.

[213] Bochkov, G. N., and Kuzovlev, Y. E. General theory of thermal fluctuations in nonlinear systems. *Sov. Phys. JETP 45* (1977), 125. Online at http://www.jetp.ac.ru/cgi-bin/e/index/e/45/1/p125?a=list.

[214] Bochkov, G. N., and Kuzovlev, Y. E. Fluctuation-dissipation relations for nonequilibrium processes in open systems. *Sov. Phys. JETP 49* (1979), 543. Online at http://www.jetp.ac.ru/cgi-bin/e/index/e/49/3/p543?a=list.

[215] BOCHKOV, G. N., AND KUZOVLEV, Y. E. Fluctuation-dissipation relations. Achievements and misunderstandings. *Physics-Uspekhi 56* (2013), 590. DOI: 10.3367/UFNe.0183.201306d.0617.

[216] EVANS, D. J., COHEN, E. G. D., AND MORRISS, G. P. Probability of second law violations in shearing steady states. *Phys. Rev. Lett. 71* (1993), 2401. DOI: 10.1103/PhysRevLett.71.2401.

[217] EVANS, D. J., AND SEARLES, D. J. Equilibrium microstates which generate second law violating steady states. *Phys. Rev. E 50* (1994), 1645. DOI: 10.1103/PhysRevE.50.1645.

[218] GALLAVOTTI, G., AND COHEN, E. G. D. Dynamical ensembles in nonequilibrium statistical mechanics. *Phys. Rev. Lett. 74* (1995), 2694. DOI: 10.1103/PhysRevLett.74.2694.

[219] KURCHAN, J. Fluctuation theorem for stochastic dynamics. *J. Phys. A: Math. Gen. 31* (1998), 3719. DOI: 10.1088/0305-4470/31/16/003.

[220] LEBOWITZ, J. L., AND SPOHN, H. A Gallavotti–Cohen-type symmetry in the large deviation functional for stochastic dynamics. *J. Stat. Phys. 95* (1999), 333. DOI: 10.1023/A:1004589714161.

[221] MAES, C. The fluctuation theorem as a Gibbs property. *J. Stat. Phys. 95* (1999), 367. DOI: 10.1023/A:1004541830999.

[222] JARZYNSKI, C. Equilibrium free-energy differences from nonequilibrium measurements: A master-equation approach. *Phys. Rev. E 56* (1997), 5018. DOI: 10.1103/PhysRevE.56.5018.

[223] HATANO, T., AND SASA, S. Steady-state thermodynamics of Langevin systems. *Phys. Rev. Lett. 86* (2001), 3463. DOI: 10.1103/PhysRevLett.86.3463.

[224] CROOKS, G. E. Path-ensemble averages in systems driven far from equilibrium. *Phys. Rev. E 61* (2000), 2361. DOI: 10.1103/PhysRevE.61.2361.

[225] MAES, C., AND NETOČNÝ, K. Time-reversal and entropy. *J. Stat. Phys. 110* (2003), 269. DOI: 10.1023/A:1021026930129.

[226] SEIFERT, U. Entropy production along a stochastic trajectory and an integral fluctuation theorem. *Phys. Rev. Lett. 95* (2005), 040602. DOI: 10.1103/PhysRevLett.95.040602.

[227] IMPARATO, A., AND PELITI, L. Fluctuation relations for a driven Brownian particle. *Phys. Rev. E 74* (2006), 026106. DOI: 10.1103/PhysRevE.74.026106.

[228] CLEUREN, B., VAN DEN BROECK, C., AND KAWAI, R. Fluctuation and dissipation of work in a Joule experiment. *Phys. Rev. Lett. 96* (2006), 050601. DOI: 10.1103/PhysRevLett.96.050601.

[229] MAES, C., AND NETOČNÝ, K. Minimum entropy production principle from a dynamical fluctuation law. *J. Math. Phys. 48* (2007), 053306. DOI: 10.1063/1.2738753.

[230] ESPOSITO, M., AND LINDENBERG, K. Continuous-time random walk for open systems: fluctuation theorems and counting statistics. *Phys. Rev. E 77* (2008), 051119. DOI: 10.1103/PhysRevE.77.051119.

[231] ESPOSITO, M., AND VAN DEN BROECK, C. Three faces of the second law. I. Master equation formulation. *Phys. Rev. E 82* (2010), 011143. DOI: 10.1103/PhysRevE.82.011143.

[232] ESPOSITO, M., AND VAN DEN BROECK, C. Three faces of the second law. II. Fokker-Planck formulation. *Phys. Rev. E 82* (2010), 011144. DOI: 10.1103/PhysRevE.82.011144.

[233] SEIFERT, U., AND SPECK, T. Fluctuation-dissipation theorem in nonequilibrium steady states. *Europhys. Lett. 89* (2012), 10007. DOI: 10.1209/0295-5075/89/10007.

[234] RAHAV, S., AND JARZYNSKI, C. Nonequilibrium fluctuation theorems from equilibrium fluctuations. *New J. Phys. 15* (2013), 125029. DOI: 10.1088/1367-2630/15/12/125029.

[235] MAES, C., AND NETOČNÝ, K. A nonequilibrium extension of the Clausius heat theorem. *J. Stat. Phys. 154* (2014), 188. DOI: 10.1007/s10955-013-0822-9.

[236] EVANS, D. J., AND SEARLES, D. J. Fluctuation theorems. *Adv. Phys. 51* (2002), 1529. DOI: 10.1080/00018730210155133.

[237] MAES, C. On the origin and use of fluctuation relations for entropy. *Sém. Poincaré 2* (2003), 29. Online at http://www.bourbaphy.fr/maes.pdf.

[238] MAES, C. Nonequilibrium entropies. *Phys. Scr. 86* (2012), 058509. DOI: 10.1088/0031-8949/86/05/058509.

[239] RITORT, F. Work fluctuations and transient violations of the second law: perspectives in theory and experiments. *Sém. Poincaré 2* (2003), 63. Online at http://www.bourbaphy.fr/ritort.pdf.

[240] BUSTAMANTE, C., LIPHARDT, J., AND RITORT, F. The nonequilibrium thermodynamics of small systems. *Phys. Today 58* (2005), 43. DOI: 10.1063/1.2012462.

[241] GASPARD, P. Hamiltonian dynamics, nanosystems, and nonequilibrium statistical mechanics. *Physica A 369* (2006), 201. DOI: 10.1016/j.physa.2006.04.010.

[242] KURCHAN, J. Non-equilibrium work relations. *J. Stat. Mech.* (2007), P07005. DOI: 10.1088/1742-5468/2007/07/P07005.

[243] HARRIS, R. J., AND SCHÜTZ, G. M. Fluctuation theorems for stochastic dynamics. *J. Stat. Mech.* (2007), P07020. DOI: 10.1088/1742-5468/2007/07/P07020.

[244] MAES, C., NETOČNÝ, K., AND WYNANTS, B. On and beyond entropy production: the case of Markov jump processes. *Markov Processes Relat. Fields 14* (2008), 445. Online at http://arxiv.org/abs/0709.4327.

[245] SEIFERT, U. Stochastic thermodynamics: principles and perspectives. *Eur. Phys. J. B 64* (2008), 423. DOI: 10.1140/epjb/e2008-00001-9.

[246] PROST, J., JOANNY, J.-F., AND PARRONDO, J. M. R. Generalized fluctuation-dissipation theorem for steady-state systems. *Phys. Rev. Lett. 103* (2009), 090601. DOI: 10.1103/PhysRevLett.103.090601.

[247] VAN DEN BROECK, C. The many faces of the second law. *J. Stat. Mech.* (2010), P10009. DOI: 10.1088/1742-5468/2010/10/P10009.

[248] Campisi, M., and Hänggi, P. Fluctuation, dissipation and the arrow of time. *Entropy 13* (2011), 2024. DOI: 10.3390/e13122024.

[249] Klages, R., Just, W., and Jarzynski, C., Eds. *Nonequilibrium Statistical Physics of Small Systems.* Reviews of Nonlinear Dynamics and Complexity. Wiley-VCH, Weinheim, Germany, 2013. ISBN 978-3-527-41094-1.

[250] Holubec, V. *Non-equilibrium Energy Transformation Processes.* Springer Theses. Springer, New York, 2014. ISBN 978-3-319-07090-2, DOI: 10.1007/978-3-319-07091-9.

[251] Esposito, M., Harbola, U., and Mukamel, S. Nonequilibrium fluctuations, fluctuation theorems, and counting statistics in quantum systems. *Rev. Mod. Phys. 81* (2009), 1665. DOI: 10.1103/RevModPhys.81.1665.

[252] Campisi, M., Hänggi, P., and Talkner, P. Colloquium: Quantum fluctuation relations: foundations and applications. *Rev. Mod. Phys. 83* (2011), 771. DOI: 10.1103/RevModPhys.83.771.

[253] Ritort, F. Work and heat fluctuations in two-state systems: a trajectory thermodynamics formalism. *J. Stat. Mech.* (2004), P10016. DOI: 10.1088/1742-5468/2004/10/P10016.

[254] Imparato, A., and Peliti, L. Work-probability distribution in systems driven out of equilibrium. *Phys. Rev. E 72* (2005), 046114. DOI: 10.1103/PhysRevE.72.046114.

[255] Chvosta, P., Reineker, P., and Schulz, M. Probability distribution of work done on a two-level dystem during a nonequilibrium isothermal process. *Phys. Rev. E 75* (2007), 041124. DOI: 10.1103/PhysRevE.75.041124.

[256] Šubrt, E., and Chvosta, P. Exact analysis of work fluctuations in two-level systems. *J. Stat. Mech.* (2007), P09019. DOI: 10.1088/1742-5468/2007/09/P09019.

[257] Chvosta, P., Einax, M., Holubec, V., Ryabov, A., and Maass, P. Energetics and performance of a microscopic heat engine based on exact calculations of work and heat distributions. *J. Stat. Mech.* (2010), P03002. DOI: 10.1088/1742-5468/2010/03/P03002.

[258] Mazonka, O., and Jarzynski, C. Exactly solvable model illustrating far-from-equilibrium predictions. *ArXiv:cond-mat/9912121* (1999). Online at http://arxiv.org/abs/cond-mat/9912121.

[259] Imparato, A., Peliti, L., Pesce, G., Rusciano, G., and Sasso, A. Work and heat probability distribution of an optically driven Brownian particle: theory and experiments. *Phys. Rev. E 76* (2007), 050101. DOI: 10.1103/PhysRevE.76.050101.

[260] Baule, A., and Cohen, E. G. D. Fluctuation properties of an effective nonlinear system subject to Poisson noise. *Phys. Rev. E 79* (2009), 030103. DOI: 10.1103/PhysRevE.79.030103.

[261] Baule, A., and Cohen, E. G. D. Steady-state work fluctuations of a dragged particle under external and thermal noise. *Phys. Rev. E 80* (2009), 011111. DOI: 10.1103/PhysRevE.80.011110.

[262] VAN ZON, R., AND COHEN, E. G. D. Extension of the fluctuation theorem. *Phys. Rev. Lett. 91* (2003), 110601. DOI: 10.1103/PhysRevLett.91.110601.

[263] VAN ZON, R., CILIBERTO, S., AND COHEN, E. G. D. Power and heat fluctuation theorems for electric circuits. *Phys. Rev. Lett. 92* (2004), 130601. DOI: 10.1103/PhysRevLett.92.130601.

[264] VAN ZON, R., AND COHEN, E. G. D. Stationary and transient work-fluctuation theorems for a dragged Brownian particle. *Phys. Rev. E 67* (2003), 046102. DOI: 10.1103/PhysRevE.67.046102.

[265] VAN ZON, R., AND COHEN, E. G. D. Extended heat-fluctuation theorems for a system with deterministic and stochastic forces. *Phys. Rev. E 69* (2004), 056121. DOI: 10.1103/PhysRevE.69.056121.

[266] COHEN, E. G. D. Properties of nonequilibrium steady states: a path integral approach. *J. Stat. Mech.* (2008), P07014. DOI: 10.1088/1742-5468/2008/07/P07014.

[267] TANIGUCHI, T., AND COHEN, E. G. D. Onsager-Machlup theory for nonequilibrium steady states and fluctuation theorems. *J. Stat. Phys. 126* (2007), 1. DOI: 10.1007/s10955-006-9252-2.

[268] TANIGUCHI, T., AND COHEN, E. G. D. Inertial effects in nonequilibrium work fluctuations by a path integral approach. *J. Stat. Phys. 130* (2008), 1. DOI: 10.1007/s10955-007-9398-6.

[269] TANIGUCHI, T., AND COHEN, E. G. D. Nonequilibrium steady state thermodynamics and fluctuations for stochastic systems. *J. Stat. Phys. 130* (2008), 633. DOI: 10.1007/s10955-007-9471-1.

[270] SINGH, N. Onsager-Machlup theory and work fluctuation theorem for a harmonically driven Brownian particle. *J. Stat. Phys. 131* (2008), 405. DOI: 10.1007/s10955-008-9503-5.

[271] JIMÉNEZ-AQUINO, J. I., AND VELASCO, R. M. Power fluctuation theorem for a Brownian harmonic oscillator. *Phys. Rev. E 87* (2013), 022112. DOI: 10.1103/PhysRevE.87.022112.

[272] JIMÉNEZ-AQUINO, J. I., AND VELASCO, R. M. Power-fluctuation theorem for a Brownian oscillator in a thermal bath. *J. Phys. A: Math. Theor. 46* (2013), 325001. DOI: 10.1088/1751-8113/46/32/325001.

[273] SPECK, T., AND SEIFERT, U. Dissipated work in driven harmonic diffusive systems: general solution and application to stretching Rouse polymers. *Eur. Phys. J. B 43* (2005), 521. DOI: 10.1140/epjb/e2005-00086-6.

[274] SPECK, T. Work distribution for the driven harmonic oscillator with time-dependent strength: exact solution and slow driving. *J. Phys. A: Math. Theor. 44* (2011), 305001. DOI: 10.1088/1751-8113/44/30/305001.

[275] MINH, D. D. L., AND ADIB, A. B. Path integral analysis of Jarzynski's equality: analytical results. *Phys. Rev. E 79* (2009), 021122. DOI: 10.1103/PhysRevE.79.021122.

[276] DEZA, R. R., IZÚS, G. G., AND WIO, H. S. Fluctuation theorems from non-equilibrium Onsager-Machlup theory for a Brownian particle in a time-dependent harmonic potential. *Cent. Eur. J. Phys. 7* (2009), 472. DOI: 10.2478/s11534-009-0038-4.

[277] KWON, C., NOH, J. D., AND PARK, H. Work fluctuations in a time-dependent harmonic potential: Rigorous results beyond the overdamped limit. *Phys. Rev. E 88* (2013), 062102. DOI: 10.1103/PhysRevE.88.062102.

[278] LO, C. F. Exact propagator of the Fokker-Planck equation with logarithmic factors in diffusion and drift terms. *Phys. Lett. A 319* (2003), 110. DOI: 10.1016/j.physleta.2003.10.005.

[279] GIAMPAOLI, J. A., STRIER, D. E., BATISTA, C., DRAZER, G., AND WIO, H. S. Exact expression for the diffusion propagator in a family of time-dependent anharmonic potentials. *Phys. Rev. E 60* (1999), 2540. DOI: 10.1103/PhysRevE.60.2540.

[280] WEI, J., AND NORMAN, E. Lie algebraic solution of linear differential equations. *J. Math. Phys. 4* (1963), 575. DOI: 10.1063/1.1703993.

[281] WILCOX, R. M. Exponential operators and parameter differentiation in quantum physics. *J. Math. Phys. 8* (1967), 962. DOI: 10.1063/1.1705306.

[282] WOLF, F. Lie algebraic solutions of linear Fokker-Planck equations. *J. Math. Phys. 29* (1988), 305. DOI: 10.1063/1.528067.

[283] KARLIN, S., AND TAYLOR, H. M. *A First Course in Stochastic Processes*. Academic Press, New York, 1975. ISBN 0-12-398552-8.

[284] KARLIN, S., AND TAYLOR, H. M. *A Second Course in Stochastic Processes*. Academic Press, New York, 1981. ISBN 0-12-398650-8.

[285] LUTZ, E., AND RENZONI, F. Beyond Boltzmann–Gibbs statistical mechanics in optical lattices. *Nat. Phys. 9* (2013), 615. DOI: 10.1038/nphys2751.

[286] BRAY, A. J. Random walks in logarithmic and power-law potentials, nonuniversal persistence, and vortex dynamics in the two-dimensional XY model. *Phys. Rev. E 62* (2000), 103. DOI: 10.1103/PhysRevE.62.103.

[287] HIRSCHBERG, O., MUKAMEL, D., AND SCHÜTZ, G. M. Approach to equilibrium of diffusion in a logarithmic potential. *Phys. Rev. E 84* (2011), 041111. DOI: 10.1103/PhysRevE.84.041111.

[288] HIRSCHBERG, O., MUKAMEL, D., AND SCHÜTZ, G. M. Diffusion in a logarithmic potential: scaling and selection in the approach to equilibrium. *J. Stat. Mech.* (2011), P02001. DOI: 10.1088/1742-5468/2012/02/P02001.

[289] DECHANT, A., LUTZ, E., KESSLER, D. A., AND BARKAI, E. Fluctuations of time averages for langevin dynamics in a binding force field . *Phys. Rev. Lett. 107* (2011), 240603. DOI: 10.1103/PhysRevLett.107.240603.

[290] KESSLER, D. A., AND BARKAI, E. Infinite covariant density for diffusion in logarithmic potentials and optical lattices. *Phys. Rev. Lett. 105* (2010), 120602. DOI: 10.1103/PhysRevLett.105.120602.

[291] KESSLER, D. A., AND BARKAI, E. Theory of fractional Lévy kinetics for cold atoms diffusing in optical lattices. *Phys. Rev. Lett. 108* (2012), 230602. DOI: 10.1103/PhysRevLett.108.230602.

[292] DECHANT, A., LUTZ, E., KESSLER, D. A., AND BARKAI, E. Superaging correlation function and ergodicity breaking for Brownian motion in logarithmic potentials. *Phys. Rev. E 85* (2012), 051124. DOI: 10.1103/PhysRevE.85.051124.

[293] DOETSCH, G. *Introduction to the Theory and Application of The Laplace Transformation.* Springer-Verlag, Berlin, 1974. ISBN 3-540-06407-9.

[294] WYBOURNE, B. G. *Classical Groups for Physicists*, 2 ed. John Wiley & Sons, New York, 1974. ISBN 0-471-96505-7.

[295] STRIER, D. E., DRAZER, G., AND WIO, H. S. An analytical study of stochastic resonance in a monostable non-harmonic system. *Physica A 283* (2000), 255. DOI: 10.1016/S0378-4371(00)00163-1.

[296] POLYANIN, A. D., AND ZAITSEV, V. F. *Handbook of Exact Solutions for Ordinary Differential Equations*, 2 ed. Chapman & Hall/CRC, Boca Raton, 2003. ISBN 1-58488-297-2.

[297] BATEMAN, H., AND ERDÉLYI, A. *Tables of Integral Transforms*, vol. 1. McGraw-Hill Book Company, INC., New York, 1954. ISBN 07-019549-8.

[298] ERDÉLYI, A., Ed. *Higher Transcendental Functions*, vol. 2. Robert E. Krieger Publishing Company, INC., Malabar, Florida, 1955. ISBN 0-89874-069-X (v. II).

[299] KLOEDEN, P. E., AND PLATEN, E. *Numerical Solution of Stochastic Differential Equations.* Springer-Verlag, Berlin, 1999. ISBN 3-540-57074-8.

[300] COHEN, A. E. Control of nanoparticles with arbitrary two-dimensional force fields. *Phys. Rev. Lett. 94* (2005), 118102. DOI: 10.1103/PhysRevLett.94.118102.

[301] BLICKLE, V., AND BECHINGER, C. Realization of a micrometre-sized stochastic heat engine. *Nature Physics 8* (2012), 143. DOI: 10.1038/nphys2163.

[302] NICKELSEN, D., AND ENGEL, A. Asymptotic work distributions in driven bistable systems. *Phys. Scr. 86* (2012), 058503. DOI: 10.1088/0031-8949/86/05/058503.

[303] DE HAAN, L., AND FERREIRA, A. *Extreme Value Theory.* Springer, New York, 2006. ISBN-13 978-0-387-23946-0.

[304] ABRAMOWITZ, M., AND STEGUN, I. A., Eds. *Handbook of Mathematical Functions with Formulas, Graphs, and Mathematical Tables*, 10 ed. National Bureau of Standards, Washington, 1972.

[305] SLOANE, N. J. A. The on-line encyclopedia of integer sequences. Online at https://oeis.org/.